Mathematical formulations of water mixing for reactive transport through heterogeneous media

Joaquim Soler Sagarra

Mathematical formulations of water mixing for reactive transport through heterogeneous media

Author:

Joaquim Soler Sagarra

Supervisor:

Dr. Jesús Carrera Ramírez

Dedicat a aquells militants de la solidaritat que de manera altruista i anònima busquen canviar un gran sistema injust a partir d'accions i connexions a petita escala

Abstract

The study of transport of reacting solute through aquifers is relevant in many engineering fields. Reactive transport (RT) is complex because it consists of two phenomena, solute transport and chemical reactions, both of which are affected by heterogeneity. Because of this complexity, RT is solved by using numerical methods obtained from mathematical formulations. This thesis seeks to improve these mathematical formulations for RT and, specifically, to (a) provide a formulation that recognizes the heterogeneity of transport and chemistry at different scales and (b) improve the algorithms to solve RT.

The thesis proposes using water exchange to describe mixing, which controls fast chemical reactions. This choice leads to a family of formulations. The Water Mixing Approach (WMA) is initially proposed as an efficient formulation equivalent to the Advection Dispersion equation (ADE). Multi-Rate Water Mixing (MRWM) is employed to account explicitly for chemical heterogeneity. Finally, the Multi-Advective Water Mixing Approach (MAWMA) allows distinguishing between dispersion, driven by hydraulic heterogeneity, and mixing, driven by both hydraulic heterogeneity and diffusion. In all these formulations, the entire transport phenomenon may be modeled as water processes. This implies that solute concentration becomes an attribute of water, exclusively relevant for chemical phenomena that become decoupled from transport. The accuracy of these formulations is tested in several cases.

Resum

L'estudi de transport de soluts reactius en aqüífers és rellevant en molts camps de l'enginyeria. Aquest transport reactiu (TR) és complex perquè és una conseqüència de dos fenòmens (transport de solut i reaccions químiques) i ambdós afectats per l'heterogeneïtat. Donada la seva complexitat, el TR es resol mitjançant models numèrics obtinguts a partir de formulacions matemàtiques. La present tesis busca millorar aquestes formulacions matemàtiques pel TR i, específicament (a) donar una formulació que reconegui la heterogeneïtat del transport i la química implicada a diferents escales i (b) millorar els algoritmes per resoldre el TR.

La tesis proposa utilitzar intercanvi d'aigües per descriure la mescla de soluts, la qual controla les reaccions químiques ràpides. La proposta condueix a una família de formulacions. La *Water Mixing Approach* (WMA) es proposa inicialment com una formulació eficient i equivalent a l'Equació d'Advecció i Dispersion (ADE). La formulació *Multi-Rate Water Mixing* (MRWM) s'utilitza per representar explícitament l'heterogeneïtat química. Finalment, la formulació *Multi-Advective Water Mixing Approach* (MAWMA), permet distingir la mescal (controlada per l'heterogenitat hidràulica i la difusió) de la dispersió (controlada únicament per l'heterogenitat hidràulica). En totes aquestes formulacions, el fenomen de transport es pot modelar exclusivament com a processos de transport d'aigua. Per tant, la concentració de solut esdevé un atribut de l'aigua i afecta únicament al fenomen químic, que és completament desacoblat del fenomen de transport. Comprovem en repetides ocasions la precisió d'aquestes formulacions.

Resumen

El estudio de transporte de solutos reactivos en acuíferos es importante en muchos campos de la ingeniería. El transporte reactivo (TR) es complejo porque resulta de dos fenómenos, transporte de soluto y reacciones químicas, afectados por heterogeneidad. Dada la complejidad del TR, su solución requiere modelos numéricos obtenidos a partir de formulaciones matemáticas. La presente tesis busca mejorar estas formulaciones para el TR y específicamente: (a) dar una formulación que reconozca la heterogeneidad química y del transporte a diversas escalas y (b) mejorar los algoritmos para resolver el TR.

La tesis propone emplear el intercambio de aguas para definir la mezcla, lo que da lugar a una familia de formulaciones. La *Formulación de mezcla de aguas* (WMA) se propone inicialmente como una forma eficiente y equivalente de la Ecuación de Advección y Dispersión. La formulación *de mezcla de aguas Multi-Ritmo* (MRWM) se utiliza para representar explícitamente la heterogeneidad química. Finalmente, la formulación *de mezcla de aguas Multi- Advectiva* (MAWMA), distingue la mezcla de la dispersión. En todas estas formulaciones, el fenómeno de transporte se puede modelar únicamente mediante procesos de transporte de agua. Por lo tanto, la concentración de soluto se convierte exclusivamente en un atributo del agua, que afecta los fenómenos químicos, que quedan desacoplados del fenómeno de transporte. Comprobamos en repetidas ocasiones la precisión de estas formulaciones.

Acknowledgements

I would like to express my deep gratitude to all who gave me their support along these years.

Primer vull agrair al meu director, Jesús Carrera, tota la confiança que ha dipositat en mi i la gran inversió de coneixements que ha fet al llarg d'aquets anys. Sense la seva aposta, no hagués començat aquesta aventura en la que m'ha guiat, donant-me l'autonomia suficient per créixer.

En segundo lugar, quiero agradecer a toda la gente del GHS con la que he compartido esta experiencia, me llevo cosas positivas de todos y cada uno de ellos. Especialmente la gente del CSIC y del despacho fondo-izquierdo. Han sido un gran soporte, con un ambiente de trabajo privilegiado y grandes compañeros de comidas, cafés, cenas, cervezas y risas.

També vull agrair a tots els grans amics fora de la feina que m'han acompanyat durant aquest temps i que també són una gran part d'aquesta tesis: els Cavalls que sempre hi ha sigut (i que no faltin mai), als de la carrera d'EG que són massa, als Tius, als dels esmorzars a la plaça de camins que sé que sempre hi seran, als del màster i l'Oriol Martorell que m'han confirmat que un món millor és possible, a tota la gran família del bàsquet, als castellers, a la gent de la Vila de Gràcia i als que m'he pogut oblidar.

Finalment, també vull agrair a la gran família que tinc: pares, tiets, cosins... que m'han fet com soc. I a tu, que sempre hi has sigut per donar-me grans moments.

iv

Table of Contents

List of Figures

List of Tables

Chapter 1

Introduction

The study of groundwater phenomena is of environmental interest and involves different sciences, such as physics, thermodynamics, chemistry, politics, sociology or economics, among others. In particular, the transport of reactive solutes through geologic media is needed for engineering applications such as aquifer de-contamination (Jurado et al., 2014), artificial recharge (Valhondo et al., 2015), geologic nuclear waste disposal and carbon sequestration (Auli Niemi et al., 2016). Partial Differential Equations (PDE) are used to describe mathematically reactive transport (RT) problems, which leads to complex and non-linear behaviour. Analytical solutions have been presented for particular problems (Donado et al. 2009; Cirpka and Valocchi 2007; De Simoni et al. 2005), but numerical methods must be used in general. Moreover, iterative algorithms such as Sequential Iteration Approach (SIA) and Direct Substitution Approach (DSA) must be used due to the non-linearity.

RT consists of two different phenomena: solute transport and chemical reactions. In turn, two types of chemical reactions can be distinguished considering the reaction rate. On the one hand, kinetic reactions are slow and controlled by the residence time of the solute. On the other hand, equilibrium reactions are fast and controlled by mixing (De Simoni et al., 2005). Both types of reactions require an accurate definition of transport. Transport is also required in many natural and engineered processes including animal

foraging patterns (Viswanathan et al., 1996), freely diffusing molecules in tissue (Yu et al., 2009), tracer diffusion in suspensions of swimming microorganisms (Leptos et al., 2009), biased transport in complex networks (Nicolaides et al. 2010), disease spreading through river networks (Rinaldo et al., 2012), medical applications in microfluidic devices (Whitesides, 2006) and urban traffic (Kerner, 1998).

Solute transport in homogeneous media is well characterized by the advection-dispersion equation (ADE). However, this is not the case when solutes are transported by groundwater because natural materials are highly heterogeneous (Le Borgne et al. 2008; Gjetvaj et al. 2015; Willmann et al. 2008), which leads to a commonly observed non-equilibrium (Alcolea et al. 2008; Vogel et al. 2006). This is termed anomalous transport (i.e., non-Fickian transport), which is critical when chemical reactions take place (Battiato et al. 2009; Sadhukhan et al. 2014; Scheibe et al. 2015; Soler-Sagarra et al. 2016; Tartakovsky et al. 2009; Luquot et al. 2016). Anomalous transport occurs at various scales from pore (Bijeljic et al. 2011; Kang et al. 2014; Seymour et al. 2004) to column (Hatano et al. 1998; Heidari et al. 2014) and field scale (Becker et al. 2000; Garabedian and LeBlanc 1991; Kang et al. 2015; Mckenna et al. 2001). Anomalous transport is evidenced by tailing in concentration breakthrough curves (Valocchi 1985; Carrera 1993). The classic ADE is no longer valid in heterogeneous media because it does not distinguish between dispersion (solute spreading, driven by velocity heterogeneity) and mixing (solute dilution, occurring by diffusion, but also driven by dispersion).

Dispersion is caused by spatial fluctuations in velocity. It is characterized by solute spreading (i.e., the variance of the spatial distribution of concentration)and its value is scale dependent (L.W. Gelhar et al., 1985). This reflects that every scale has different heterogeneity. Deterministic information on both the structure of the soil and their parameters is essential to bound the growth of dispersion with scale. However, it must be dealt with unknown heterogeneity at some scales. In such cases, the velocity evolution is best defined as Markovian in space (Le Borgne et al. 2008b; De Anna et al. 2013; Holzner et al. 2015; Kang et al. 2014). It can therefore be characterized with a Transition Matrix M^{vs} which expresses the probability to change the velocity state v given constant steps in space phase s (De Anna et al. 2013; Kang et al. 2011, 2014,

2015). The above suggests adopting velocity as a new dimension of the state variable such as space and time. This new dimension must be taken into account in a phase space formulation such as the one proposed by Kang et al. 2017. However, this formulation does not consider mixing.

Mixing is caused by reflects Brownian displacements of solute particles within the flowing fluid. It is characterized by solute dilution (i.e., the variance of concentration). Therefore mixing should be Markovian in time despite the fact that the fluid velocity evolution is Markovian in space. Unlike dispersion, mixing is a direct cause of chemical reactions in fluids (Cirpka and Valocchi 2007; Rezaei et al. 2005; De Simoni et al. 2005, 2007; Tartakovsky et al. 2008). Mixing is also important when applied to porous media (Kapoor and Kitanidis 1998; Kitanidis 1994; Kleinfelter et al. 2005). Locally, mixing is defined in terms of concentration gradients, which helps in defining the rate of fast chemical reactions (De Simoni et al., 2005). Nevertheless, conventional transport formulations tend to equate mixing and dispersion and do not account for the fact that mixing occurs because of the Brownian motion of each particle (Einstein, 1905).

There are some links between dispersion and mixing despite the fact that they are different processes (Peter K. Kitanidis, 1988, 1994). Solute spreading increases the concentration contrast, which enhances mixing (Le Borgne et al. 2010; Chiogna et al. 2011; Rolle et al. 2009; Tartakovsky et al. 2008). In particular, processes such as stretching and folding have been identified (De Anna et al. 2013; Jiménez-Martínez et al. 2015; Le Borgne et al. 2015). This leads to non-Fickian behaviour at early times (Berkowitz et al. 2006; Le Borgne et al. 2008a; Le Borgne and Gouze 2008; Neuman and Tartakovsky 2009; Zhang et al. 2009). Fickian behaviour at late times are explained by the spreading rate (Tanguy Le Borgne et al., 2010a).

Numerous alternatives to ADE have been proposed to address anomalous transport (Frippiat & Holeyman, 2008). Examples of continuum scale non-local in time methods include CTRW (Berkowitz and Scher 1997; Bijeljic et al. 2011; Le Borgne et al. 2008a; Le Borgne et al. 2008b; Dentz et al. 2004; Dentz et al. 2015; Edery et al. 2014; Geiger et al. 2010; Kang et al. 2011; Wang and Cardenas 2014), fADE (Benson et al., SCST (Becker & Shapiro, 2003) or MRMT (Babey et al. 2015; Carrera et al. 1998; De Dreuzy et al. 2013; Fernandez-Garcia and Sanchez-Vila 2015; Haggerty and Gorelick 1995; Soler-Sagarra et al. 2016). It has been demonstrated that these methods methods do not

1. Introduction

reproduce mixing appropetly (Jean Raynald De Dreuzy & Carrera, 2016). Given that the chemical reaction occurs at pore scale (Steefel et al., 2005), other alternative methods that have been proposed include Lattice Boltzmann equation (Acharya et al. 2007; Benzi et al. 1992; Chen and Doolen 1998; Kang et al. 2006; Willingham et al. 2008), Smoothed Particle Hydrodynamics (Liu & Liu, 2010; a. M. Tartakovsky et al., 2009, 2015; Alexandre M. Tartakovsky et al., 2007) or pore network models (Blunt, 2001; Blunt et al., 2002; Li, et al., 2006; Meile and Tuncay, 2006; Raoof et al., 2010; Raoof and Hassanizadeh, 2012; Varloteaux, 2013). However, dealing with field scale problems demands a continuum formulation that represents properly mixing and dispersion. Hybrid methods have been proposed to overcome this scale duality (Battiato et al. 2011; Leemput et al. 2007; Tartakovsky et al. 2008) but they are complex because coupling the continuum and pore scale domain is required. A new formulation is therefore necessary. The suitable equation for anomalous transport must take into consideration advection, dispersion and mixing (de Dreuzy et al. 2012; De Dreuzy et al. 2016). This distinction between dispersion and mixing must be assessed carefully.

The aim of this thesis is to present an efficient formulation for RT. Specific objectives are to:

1. improve the algorithms to solve reactive transport,
2. recognize the heterogeneity of transport and chemistry at different scales. and
3. separate explicitly dispersion and mixing.

The thesis consists of four parts.

In the first part (second chapter), a formulation to solve RT in porous media is presented. We term this formulation the Water Mixing Approach (WMA). The essence of this formulation is to represent transport through the mixing of water instead of individual solute concentrations. This concept simplifies calculations of water, which facilitates decoupling chemical and transport calculations because (1) concentration is reduced to just an attribute of water used for chemical calculations, and (2) transport is restricted to the computation of water mixing ratios, which can be used for any transport solution method. The WMA has been implemented into a transport solver with a streamline-oriented grid with constant travel time between sequential cells (isochronal grid), which is free of numerical dispersion. . The accuracy and efficiency (low CPU

cost) of the WMA are illustrated by comparison with the Direct Substitution Approach (DSA), on two RT cases (an analytical solution of a binary system and a calcite dissolution problem).

The second part (third chapter, based on Soler-Sagarra et al. (2016)) focuses on the simulation of the geochemical micro localization at pore scale. To this end, WMA is extended to Multi-Rate Mass Transfer formulation (mobile-immobile zones). The method is termed Multi-Rate Water Mixing (MRWM). MRWM is employed to simulate laboratory experiments of CO_2-rich brine transport through carbonate rich samples. Pore scale chemical heterogeneity is reproduced by varying the mineral assemblages and residence time of immobile regions. Unlike conventional formulations, MRWM reproduces the geochemical localization observed in reality (i.e., the occurrence of two different pH micro environments, none of which would be consistent with local equilibrium). The resulting method is very practical since it can reproduce a broad range of pore scale processes in a Darcy scale model.

A phase space formulation is proposed in the third part (fourth chapter) to simulate transport through heterogeneous media. The essence of this formulation is to consider velocity as a new dimension such as time or space. The formulation is based on the WMA and is termed the Multi-Advective Water Mixing Approach (MAWMA). This formulation includes a new mixing term between velocity classes. It is tested on Taylor's stratified flow case by using the Water Parcel method (WP), which is obtained by discretizing MAWMA in space, time and velocity. Results show high accuracy in both dispersion and mixing. Moreover, the mixing process exhibits Markovianity in space even though it is modeled with time steps.

The MAWMA formulation is tested for highly heterogeneous domains in the last part (fifth chapter). In these cases WP needs two velocity transition matrices (probabilities of water transitions between two velocity classes): one for advection (Markovian in space) and one for mixing (Markovian in time). This chapter shows how the water transition matrix of mixing is obtained and demonstrates that it is constant in time. Moreover, the WP method is compared with a classic Random Walk method (RW) in a highly heterogeneous domain. Results show that WP overestimates mixing at late times as do the classic methods since mixing is a sub-velocity phase process (the WP method must

be extended to take into account incomplete mixing within velocity classes), but represents satisfactorily the separation between dispersion and mixing.

Chapter 2

Water Mixing Approach (WMA) for reactive transport modeling

2.1.   Introduction

The study of geochemical processes in porous media is critical in many engineering fields (e.g., clean-up of contaminated aquifers, geological storage of CO_2, nuclear waste storage, mining or other geoenvironmental problems). In all of these, solute transport mechanisms such as advection and dispersion need to be coupled to chemical reactions (e.g., complexation, adsorption, biodegradation or precipitation), leading to reactive transport (RT). Fully coupled RT is needed to assess the rate of chemical reactions, their location, or the conditions under which they occur (Rezaei et al., 2005). Although analytical solutions exist for particular conditions and problems (Donado et al. 2009; Haberman 1998; Cirpka and Valocchi 2007; De Simoni et al. 2005), numerical methods are needed in most cases.

Numerical solution of reactive transport involves coupling transport PDEs for each species to algebraic equations representing chemical reactions (basically mass action law for fast reactions and kinetic laws for slow reactions), which leads to a nonlinear set of equations. Nonlinearity often causes RT to become complex and non-trivial and

requires iterative solution methods. Both Picard (e.g., the Sequential Iteration Approach, SIA or Operator splitting approach), and Newton-Raphson methods (e.g., the Direct Substitution Approach, DSA or Global implicit) have been used to solve RT problems (reviews of RT are given by Steefel and MacQuarrie, 1996, Steefel, 2019; or Liu et al., 2019). It should be noted, that SIA and DSA become identical when explicit schemes are used. Examples of model codes that use SIA include those of Nardi et al. (2014); Parkhurst and Appelo (1999); Parkhurst et al. (2010); Samper et al. (2003); Šimůnek et al. (2008); Xu et al. (2011); Yeh and Li (2004). Examples of model codes that use DSA include those of Mayer et al. (1999); Mills et al. (2005); Pruess (2005); Saaltink et al. (2004); Steefel and Yabusaki (1996). See Steefel et al. (2015) for a review. Figure 2. 1a and 2. 1b provide the calculation flow algorithm of SIA and DSA, respectively.

Actually, the key to accurate reactive transport is proper simulation of (1) mixing, which control the rate of fast reactions (Rezaei et al. 2005; De Simoni et al. 2005; Sanchez-Vila et al. 2007), and (2) residence times, which control the rate of slow reactions. The latter is well reproduced by most simulation methods. Therefore, the challenge is to develop an approach that reproduces mixing properly.

In this paper, we propose a reactive transport methodology to simplify and effectively decouple transport from chemical calculations by formulating reactive transport as a reactive mixing calculation of waters at every time step. Therefore, we term it Water Mixing Approach (WMA).
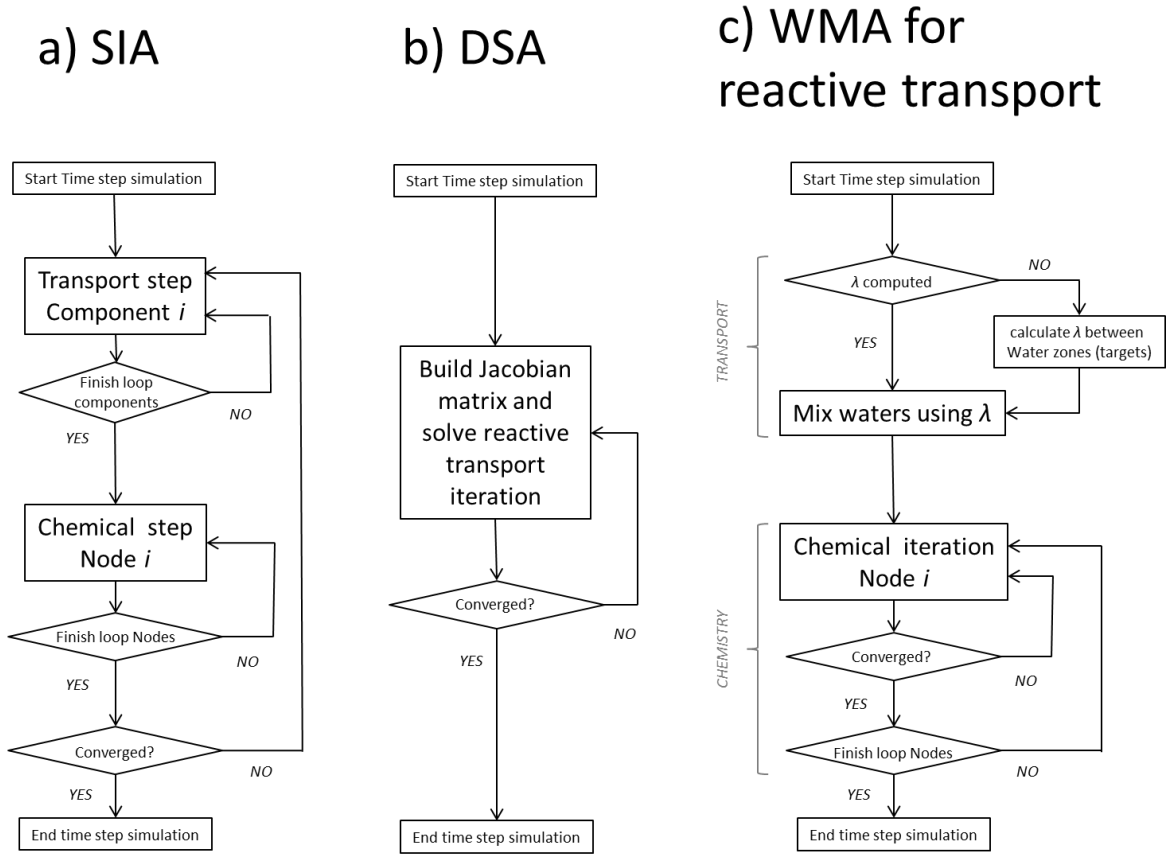
Figure 2. 1: Algorithm flow to solve reactive transport time step simulation using: *a)* SIA, *b)* DSA and *c)* applied WMA formulation to reactive transport

2.2.   Governing equations

2.2.1.   The ADE as a Water Mixing Equation

The standard formulation for solute reactive transport relies on representing transport through the Advection Dispersion equation (ADE), which expresses the mass balance of each aqueous species (Saaltink et al. 1998; Yeh and Tripathi 1989) as

$$\phi \frac{\partial c}{\partial t} = \nabla \cdot (\boldsymbol{D} \nabla c) - \boldsymbol{q} \cdot \nabla c + b(c_e - c) + f_Q \tag{2.1}$$

where c $[M/L^3]$ is concentration, ϕ $[-]$ is porosity, t $[T]$ is time, $\boldsymbol{D}[L^2/T]$ is the hydrodynamic dispersion tensor, $\boldsymbol{q}[L^3/L^2/T]$ is the Darcy flux, b represent sink/sources

of water with concentration c_e(when $b > 0$) or directly the resident concentration c (when $b < 0$) and f_Q [M/L^3/T] includes the contributions of chemical reactions to the mass balance of the species. This equation applies to aqueous species. The full reactive problem needs to be complemented with the mass balance of immobile species (minerals and sorbed species), the mass action law for equilibrium reactions, and appropriate expressions for kinetic reactions (See, e.g., Bethke 1996, Parkhurst and Appelo, 1999 or Saaltink et al., 1998 for details).

The ADE expresses that the rate at which concentration change (left hand side of Eq.(2. 1)) results from dispersion, advection, chemical reactions, and sinks and sources. Insight on dispersion can be gained from perturbation approaches, typical of stochastic formulations. In these formulations, variables are split as the sum of an (ensemble) mean plus a zero-mean perturbation (i.e., $c = \bar{c} + c'$, $q = \bar{q} + q'$). Assuming that the ADE is valid at some microscopic scale, the "hydromechanical" dispersive flux becomes $\overline{q'c'}$, and the total ("hydrodynamic") dispersive flux is

$$J_D = \overline{q'c'} - D_m \nabla c \qquad (2. 2)$$

where D_m is the molecular diffusion coefficient. Eq. (2. 2) expresses that the solute is spread by molecular diffusion and by velocity fluctuations with respect to the mean. Gelhar and Axness (1983) demonstrated that this dispersive flux can be approximated by a fickian term ($D\nabla c$) for large scale transport, but the choice of a fickian form for dispersion is much older (Bear, 1972). Dispersion represents that, when the plume advances, the high permeability portions of the porous medium (i.e., where q is larger than the mean) will likely be invaded by the (upstream) water (i.e., where c is larger than the mean), whereas the low q portions will remain with downstream water. That is, dispersion represents exchange between the upstream and downstream waters. Since the difference in upstream and downstream concentrations can be approximated by ∇c times a characteristic exchange distance (L_D), the fickian form emerges naturally. However, it might have been equally natural to keep the water exchange formulation, that is:

$$J_D = \overline{q'c'} - D_m \nabla c \simeq -D \nabla c = \overline{q_D c} \qquad (2. 3)$$

where $\boldsymbol{q}_D$ is the water flux that exchanges around the mean flux (similar to $\boldsymbol{q}'$, but accounting also for molecular diffusion) and we have chosen to write c, instead of c', in the last term to emphasize that it is the whole water parcel (not only the concentration perturbation) what is exchanging around the mean flux. The water exchange instead of net flux of solute is why no concentration gradient appears in Eq. (2. 3) (see Figure 2. 2).

ADE $\quad F_c\left[\text{MOL}/\text{t}\right] = D\nabla c = D\dfrac{(c_j - c_i)}{L_D}$ $\quad$ **WMA** $\quad \overline{q_D c} = F_w c_j - F_w c_i = \dfrac{D}{L_D}c_j - \dfrac{D}{L_D}c_i$

$$F_w\left[V_w/\text{t}\right]$$
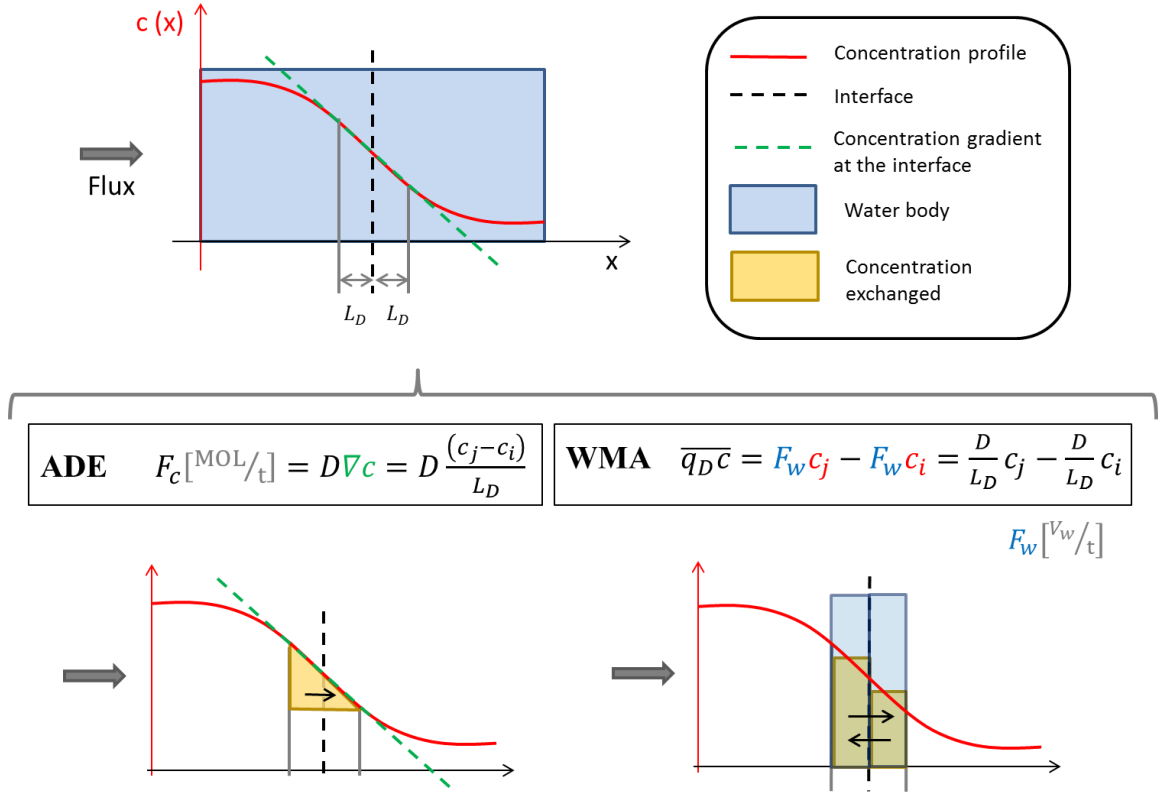
Figure 2. 2: Graphical scheme of dispersion process in ADE and WMA formulations. L_D [M] is the length scale of the dispersion process

In the following we will adopt a WMA form of the ADE, by assuming (2. 3) to be valid, so that (2. 1) can be written as:

$$\phi\frac{\partial c}{\partial t} = -\nabla \cdot (\overline{q_D c}) - \boldsymbol{q} \cdot \nabla c + b(c_e - c) + f_Q \tag{2. 4}$$

Several remarks can be made regarding this equation. First, when $\boldsymbol{q}_D c$ represents Fickian dispersion term, then Eq. (2. 4) is just another form of the ADE. But other forms of dispersion may be adopted and Eq. (2. 4) would still be valid. We write it here in this

way both for generality and, especially, to highlight that mixing can be viewed as occurring in response to water flux fluctuations. The latter is convenient for reactive transport, but they are identical provided that $D_L = q_{DL}L_{DL}$ and $D_T = q_{DT}L_{DT}$, where subscripts L and T stand for longitudinal and transverse, respectively (in fact, we will assume that D_L and D_T are known to define the water exchange rates). Therefore, Eq. (2. 4) represents a possibly crude approximation of reality because, at the microscopic scale, $\overline{q'c'}$ spreads solutes but does not produce mixing, but equating mixing and spreading is a feature of the ADE. If all species have the same dispersion coefficient,

Eq. (2. 4) can be extended to transport of a concentrations vector $\vec{c} = \langle c_1, c_2, \dots, c_{ns} \rangle$ where ns is the number of species. In this case, Eq. (2. 4) could be seen as a water transport equation. However, it might be argued that mixing (if viewed as dissipation of concentration gradients) is species dependent in at least two cases: (1) when diffusion is acknowledged to be species dependent, or (2) when advection is slowed down by fast adsorption. In the first case, it is possible to correct Eq. (2. 4) for the species dependent molecular diffusion (and we will show how to do it in Section 2.2.1). However, species dependent diffusivity implies also a species dependent dispersion (Chiogna et al. 2010), for which a proper formulation is lacking. While the issue may be important for neutral compounds, it is usually disregarded for ionic species on the basis that the resulting electrical imbalance tends to compensate the relative displacements of one species with respect to another (but this remains to be proven). Adsorption is strictly a chemical reaction and, as such, its role is included in the reaction rates term. The fact that the reaction rate is proportional to $\partial c / \partial t$ causes the velocity of concentration fronts to depend on the retardation coefficient, but this effect is properly represented in Eq. (2. 4), although it may complicate numerical solution.

2.2.2. Generic numerical formulation.

The ADE and WMA can be solved with a broad range of numerical methods (Finite Element Method, Finite Volumes or Finite Differences among others), but all of them lead to equations of the form (e.g.,Huyakorn 1983):

$$\phi_i V_i \frac{c_i^{k+1} - c_i^k}{\Delta t} = \sum_{j \neq i}^{N_{conn}} F_{ij}(c_j - c_i) + b_i V_i (c_{ei} - c_i) + V_i f_{Qi} \tag{2.5}$$

where k identifies the time step and typically, V_i represents the volume associated to numerical target (i.e., nodes, cell or elements) i, Δt is the time increment, N_{conn} is the number of all targets j connected to i (i.e.: $F_{ij} \neq 0$). Note that the first term on the right-hand side of Eq. (2.5) represents the contributions associated to water exchanges (including both advective and dispersive exchanges) from targets. The second term represents mass input from inflowing water. Note also that we have left purposefully undefined the time at which concentrations are evaluated in the right-hand side of Eq. (2.5). In traditional numerical formulations, this time can be k, $k+1$, or any time in between, which leads to explicit, fully implicit or time centered schemes, respectively.

Regardless of the time integration scheme, transport is linear, so that concentrations at time step $k+1$ can be written as a linear combination of those at time step k, plus the possibly non-linear reactions term, which reads:

$$c_i^{k+1} = \sum_j^{N_{conn}+1} \lambda_{ij} c_j^k + \frac{f_{Qi}}{\phi_i} \Delta t \tag{2.6}$$

where the sum now includes not only targets connected to i, but also target i and external waters. Note that $\sum_j \lambda_{ij} = 1$, to ensure that when all c_j^k are equal and in the absence of reactions, c_i^{k+1} is equal to the same value. Therefore, Eq. (2.6) can be viewed as a reactive mixing equation (e.g., Pelizard et al., 2017) and it is natural to call λ_{ij} a mixing ratio, although it represents not only mixing but also advection (it is simply the fraction of water in target i that started in target j at the beginning of the time step).

While this equation can represent any transport formulation, its terms are easiest to obtain for explicit integration schemes (otherwise inversion of the full system matrix or subblocks is required). In such case, Eq. (2.6) can be obtained by dividing Eq. (2.5) by the volume of parcel i (water content associated to the numerical target i, i.e., $\phi_i V_i$) and multplying by the time step Δt. Therefore, $\lambda_{ij} = \Delta t\, F_{ij}/\phi_i V_i$ for connected parcels or $\lambda_{ij} = \Delta t\, b_i/\phi_i$ for external waters. Note that mixing ratio is expressed as a fraction of

the parcel volume i. The latter differs from the use of mixing ratios of end members proposed by (De Simoni et al. 2007; Cirpka and Valocchi 2007; Ginn et al. 2017).

Some observations can now be made about Eq. (2. 6). First, c can be extended to a vector of only concentrations of aqueous species with the result that it can be regarded as a definition of a water zone. Thus, Eq. (2. 6) indicates that solute transport can be reproduced as a consequence of mixing between connected waters and/or external sources waters. In other words, Eq. (2. 6) could be understood as a fluid mass balance that takes into account water diffusion (Harris and Woolf 1980; Spyrou 2009), which has no effect on water flux phenomenon but can reproduce the solute diffusion. This is important because it reduces the number of transport equations from ns (the number of aqueous species) to 1:

$$W_i^{k+1} = \sum_{j}^{N_{conn}+1} \lambda_{ij} W_j^k \qquad (2.7)$$

where W_i is the water parcel definition (or water solution) of cell i. Moreover, the equation is very simple. Now concentrations are considered just attributes of W (like Temperature, viscosity or density). This way, chemistry is separated from transport because transport is defined entirely by the water mixing ratio term λ. Thus, the WMA only iterates at chemical step (unlike DSA or SIA) because concentration becomes solely a chemical variable (see Figure 2. 1). Chemical effects are produced by f_{Qi} which is calculated as described in section 2.2.3.

The use of water as a transport of solute has already been applied by (Konikow, 2010; Winston et al., 2018), although it was not formulated as an equation.

2.2.3. Chemical Calculations

The evaluation of the chemical sink/source term, f_{Qi}, or directly, the computation of concentrations can be viewed as the mass balance resulting from reactive mixing of waters connected to parcel i, with mixing ratios λ_{ij}, given by

$$\begin{bmatrix} c_{ai}^{k+1} \\ c_{imi}^{k+1} \end{bmatrix} = \begin{bmatrix} \sum_{j}^{N_{conn}+1} \lambda_{ij} c_{aj}^{k} \\ c_{imi}^{k} \end{bmatrix} + S_{ei}^{t} r_{ei} \frac{\Delta t}{\phi_i} + S_{ki}^{t} r_{ki} \frac{\Delta t}{\phi_i} + \begin{bmatrix} f_i^c \\ 0 \end{bmatrix} \qquad (2.8)$$

where the top row represents the mass balance of aqueous (mobile) species (vector of concentrations c_{ai} at parcel i) and the bottom row represents the mass balance of immobile species (vector of concentrations c_{imi}), S_{ei} and S_{ki} are the stoichiometric matrices for equilibrium and kinetic reactions, which depends on i because the number and types of reactions may change depending on the minerals and sorption surfaces available (Rubin, 1983), r_{ei} and r_{ki} are the vectors of equilibrium and kinetic reaction rates, respectively, and f_i^c is the vector of correction terms for species dependent dispersion. These equations need to be complemented with the mass action law for equilibrium reactions and with kinetic rate laws for kinetic reactions.

Note that, except for the separation between mobile and immobile species and the inclusion of the correction term, f_i^c, Eq. (2.8) is a conventional set of reactive mixing equations (similar to, e.g., Eq. (5.57) of Parkhurst and Appelo, 1999, or Eq. (8) of Pelizardi et al. 2017). Numerous methods are available to solve this type of equations (Fang et al. 2003; Friedly and Rubin 1992; Kräutle and Knabner 2005, 2007; Molins et al. 2004; Saaltink et al. 1998; De Simoni et al. 2005; Yeh and Tripathi 1989). Here, we multiply the concentration vector by a full-ranked components matrix U (Steefel, MacQuarrie 1996; Lichtner 1985) to eliminate the rates of equilibrium reactions and by a matrix E (Saaltink et al. 1998) to eliminate constant activity species. Saaltink et al. 1998 discussed six of such formulations to reduce the number of chemical equations. Any of the six formulations would be valid for WMA. We use their fifth formulation.

$$\begin{bmatrix} E_i U_{ai} c_{ai}^{k+1} \\ E_i U_{si} c_{si}^{k+1} \end{bmatrix} = \begin{bmatrix} \sum_{j}^{N_{conn}+1} \lambda_{ij} u_{aj}^{k} \\ u_{si}^{k} \end{bmatrix} + \sum_{j} E_i U_i S_{kin}^{t} r_{kin}(c_j^k) \frac{\Delta t}{\phi_i} + \begin{bmatrix} E_i U_{ai} f_i^c \\ 0 \end{bmatrix} \qquad (2.9)$$

where U_a and U_s are submatrices of components matrix U referring to aqueous and sorbed species, respectively, and where u_a and u_s are the aqueous and sorbed component concentrations ($u_a = U_a c_a$, $u_s = U_s c_s$). Note that if there are no kinetic and no adsorption reactions, r_{kin} and u_s disappear and component u_a may be found by solving the system as a conservative solute problem. Concentrations of the next time

15

step ($c_{a,i}{}^{k+1}$ and $c_{s,i}{}^{k+1}$) can be solved from Eq. (2. 9) and the mass action laws for the equilibrium reactions. Note that the right-hand side of Eq. (2. 9) is calculated entirely from the concentrations of the previous time step. However, other time schemes can also be used. Calculation of $c_{a,i}{}^{k+1}$ and $c_{s,i}{}^{k+1}$ constitutes the only non-linear part of the proposed method, and is therefore the costliest part of the calculations with respect to CPU time. However, Eq. (2. 9) can be solved for each parcel independently, thereby reducing the size of the non-linear system to the number of chemical components. The concentration of the minerals can also be calculated by formulating a mass balance similar to Eq. (2. 9) but without eliminating the minerals. Solving Eq. (2. 9) is a standard chemical speciation calculation and any speciation code may be used.

2.2.4.   Isochronal formulation for WMA.

For the sake of generality, section 2.2.1 formulates ADE as water mixing terms (i.e. WMA) in Eulerian form. Then, a general discretization valid for any numerical method was presented in section 2.2.2 . However, standard ADE models tend to overpredict solute mixing (Ginn et al. 1995; Kitanidis 1988, 1994; MacQuarrie and Sudicky 1990; Molz and Widdowson 1988) in part because modellers adopting Eulerian transport formulations are forced to either use large dispersion coefficients (which affects mixing ratios in Eq. (2. 6)) or to accept numerical dispersion. The latter can be explained because Eq. (2. 6) includes advection, so that that the "mixing ratios" for parcels downstream of i will tend to be negative, which is appropriate to represent advection, but not for mixing calculations (pointing that mixing is a dissipative process, while advection is not). These problems can be overcome by adopting Eulerian-Lagrangian formulations (e.g., Bell and Binning, 2004 ; Cirpka et al., 1999b; Batlle et al., 2002; Ramasomanana et al., 2012; Zhang et al., 2007), which allows modelling advection dominated problems. In these formulations, the time variation of concentration in a flowing parcel of water is written with the material derivative $Dc/Dt = \partial c/\partial t + (q/\phi) \cdot \nabla c$. Using this definition in Eq. (2. 4) leads to

$$\phi \frac{Dc}{Dt} = -\nabla \cdot (\overline{\boldsymbol{q_D}c}) + r(c_e - c) + f_Q \tag{2.10}$$

Written this way, the equation expresses that flowing water concentration changes only due to mixing and reactions, thus highlighting that advection does not produce mixing and therefore does not produce change in the concentrations of flowing water. The material derivative can be approximated as

$$\frac{Dc}{Dt} = \frac{c_i^{k+1} - c_{i-}^k}{\Delta t} \tag{2.11}$$

where $i-$ refers to the location in the previous time step of the center of the water parcel that ended in parcel i at time $k+1$. Note that Eqs. (2.5), (2.6) and (2.7) may still be valid, except that (1) now the sum is extended over the concentrations that were at locations $i-$ at the end of the previous time step, and (2) only dispersive processes are included within F_{ij}, which ensures that λ_{ij} are positive (a sufficient condition of stability for all conventional numerical methods).

To facilitate numerical evaluation of the material derivative and water mixing fluxes, we adopt a streamline oriented grid (Cirpka et al 1999a; Frind 1982; Crane and Blunt 1999; Thiele et al. 1997; Di Donato et al. 2003; Yabusaki et al. 1998; Herrera et al. 2010). This choice reduces significantly numerical dispersion (Cirpka et al. 1999a) and facilitates the use of finite volumes methods. Still, some smoothing may remain because concentrations at locations $i-$ need to be interpolated from the surrounding parcels.

To eliminate interpolation errors, we define isochronal grids by ensuring that location $i-$ must coincide with a cell center (see Figure 2.3). That is, a downstream position j exists such that

$$x_j = x_{i-} = x_i - \boldsymbol{v}\Delta t \tag{2.12}$$

where $\boldsymbol{v}$ is the velocity $(\boldsymbol{q}/\phi)$ upstream of cell i.
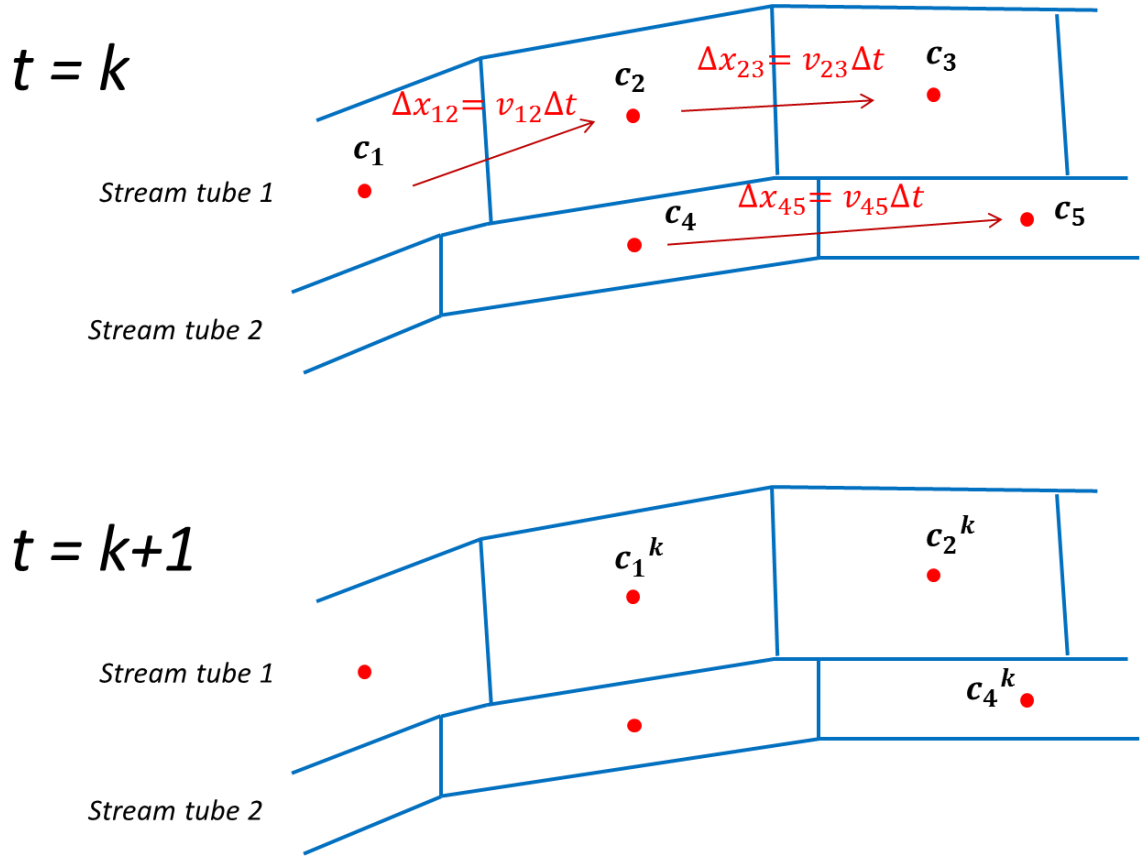
Figure 2. 3: Advection within a dual stream-tube in the proposed isochronal grid

Eq. (2. 12) implies that the initial mesh must be recalculated if either time step simulation or flow (velocity) change. Appendix A shows the building procedure of the proposed isochronal grid. This grid also facilitates the computation of the mixing ratios λ_{ij}. Transport terms are calculated from concentrations of the previous time step in explicit schemes. Explicit schemes are fast, but they are subject to stability criteria that require dispersion coefficients to be small. Therefore, mixing ratios equal zero except for the following cases:

$$\lambda_{ij} = \frac{D_L w_{ij} \Delta t}{\phi_i V_i L_{ij}} \text{ if } i \text{ and } j \text{ are adjacent along a streamline} \tag{2. 13a}$$

$$\lambda_{ij} = \frac{D_T w_{ij} \Delta t}{\phi_i V_i L_{ij}} \text{ if } i \text{ and } j \text{ } belong \text{ to } adjacent\ stramlines \tag{2. 13b}$$

$$\lambda_{ij} = \frac{r_i \Delta t}{\phi_i} \text{ if } j \text{ represents an external inflow} \tag{2. 13c}$$

$$\lambda_{ii} = 1 - \sum_{j \neq i}^{N_{adj}} \lambda_{ij} \tag{2. 13d}$$

where w_{ij} is the width of the interface between cells i and j, L_{ij} is the distance between cell centers in (2. 13a) or the mean distance between streamlines in (2. 13b), and D_L and D_T are the longitudinal and transverse, respectively, dispersion coefficients. Note that, for λ_{ii} to be positive, Eq. (2. 13d) requires $\sum_{j \neq i} \lambda_{ij} < 1$, which is a stability condition for any explicit method. Otherwise, the parcel volume entering the cell would be larger than that in the cell.

The obtained formulation can be viewed as a generalization of the mixing-cells approach of Campana (1975), which was extended to reactive transport by Appelo and Willemsen (1987), and is now widely used in 1-D as part of PHREEQC (Parkhurst and Appelo 1999). However, one can use it in 2D problems (see Eq. (2. 13b)).

It must be stressed that these mixing ratios are identical for all species provided that the dispersion coefficients are. We obtain the following expression

$$c_i^{k+1} = \sum_{j-}^{N_{adj}+1} \lambda_{ij} c_{j-}^k + \frac{f_{Qi}}{\phi_i} \Delta t \tag{2. 14}$$

where N_{adj} is the number of all parcels j adjacent to i. If dispersion coefficients are species dependent, the transport equation can be corrected as follows

$$c_i^{k+1} = \sum_{j-}^{N_{adj}+1} \lambda_{ij} c_{j-}^k + \frac{f_{Qi}}{\phi_i} \Delta t + f_i^c \tag{2. 15}$$

Where $f_i^c = \sum_{j-} \lambda_{ij}^c c_{j-}^k$ is a species dependent correction, with λ_{ij}^c given by Eq. (2. 13), except that D's in (2. 13a) and (2. 13b) are substituted by $(D - D^c)$, where D^c is the dispersion coefficient of each species. As discussed in section 2.2.1, this correction should be small for ionic species.

2.3. Applications

We test here the accuracy and efficiency of the WMA by comparison to both analytical solutions (section 2.3.1) and computational results from the literature (section 2.3.2). While the WMA could be implemented in any transport simulator, we test it on the formulation presented in section 2.2.4 in all cases. An explicit scheme is used. We employed the chemical library CHEPROO in both WMA and DSA models. CHEPROO is an object oriented code for geochemical calculations (S. A. Bea et al., 2009).

2.3.1. Half injection domain

This test aims at verifying that the WMA performs well in cases of transverse dispersion and equilibrium reactions, which are particularly relevant for the amount of mixing and reaction rate (see e.g., Werth et al. 2006; De Simoni et al. 2005). We consider the steady-state analytical solution of De Simoni et al. (2007) for reactive transport, based on the analytical solution of Haberman (1998) for conservative transport. Flow occurs in a 2D homogeneous domain with velocity aligned along the x axis. Two end member waters enter the domain at the inflow boundary ($x = 0$), creating a transverse mixing zone. Longitudinal dispersion is neglected. We consider a binary chemical system consisting of two species, Ca^{2+} and SO_4^{2-}, in equilibrium with gypsum. The physical problem is defined in Table 2. 1. The analytical solution for aqueous component concentration, considering the end members with u values of 1 and 0, is the follow

$$u_a(x,y) = \frac{1}{2}\left(1 - erf\left[\frac{\eta}{2}\right]\right) \qquad (2.16)$$

Where $\eta = \sqrt{Pe}\, y/x$ is a similarity variable, representing a normalized transverse coordinate with dependency of x and y space coordinates and Peclet number $Pe=v\cdot x/D_T$. v is the velocity. $erf[\cdot]$ is the error function. The analytical expression of reaction rate is giving as

$$r(x,y) = \phi\,\frac{v}{x}\frac{\partial^2 c_{Ca^{2+}}}{\partial u^2}\left(\frac{du}{d\eta}\right)^2 \qquad (2.17)$$

Where $du/d\eta = -1/(2\sqrt{\pi})\,exp[-\eta^2/4]$ and $\partial^2 c_{Ca^{2+}}/\partial u^2 = 2K/(u^2+4K)^{3/2}$. K is the equilibrium constant. Although the analytical solution is steady state, WMA is solved as a transient problem.

Table 2. 1: Solute transport parameters of half injection domain

Transport		Chemistry			
q (m/d)	0.142857	K = 10^-2 (Temperature 25 ^{0}C)			
		Injection water 1 (kg/m³)		**Injection water 2** (kg/m³)	
Δx (m)	0.25				
Δy (m)	0.25	$c_{Ca^{2+}}$	9.902·10^{-3}	$c_{Ca^{2+}}$	0.1
ϕ	0.3	$c_{SO_4^{2-}}$	1.009902	$c_{SO_4^{2-}}$	0.1
Δt (d)	0.525	u_a	1	u_a	0
α_t (m)	0.02				
P_e	12.5				

Figure 2. 4 shows the cross sections along the *y* axis of (a) reaction rates and (b) *u* component at three different *x* values. Analytical and numerical solutions appear to be very similar. Nevertheless, errors are slightly larger close to the injection boundary where concentration gradients are highest. This may be attributed to the poor reproduction of concentration gradient at this stage, which may violates the criterion of 5 elements across a front suggested by Kinzelbach (1986). Close to the injection boundary, the size of the transverse front is too small with respect to element size.
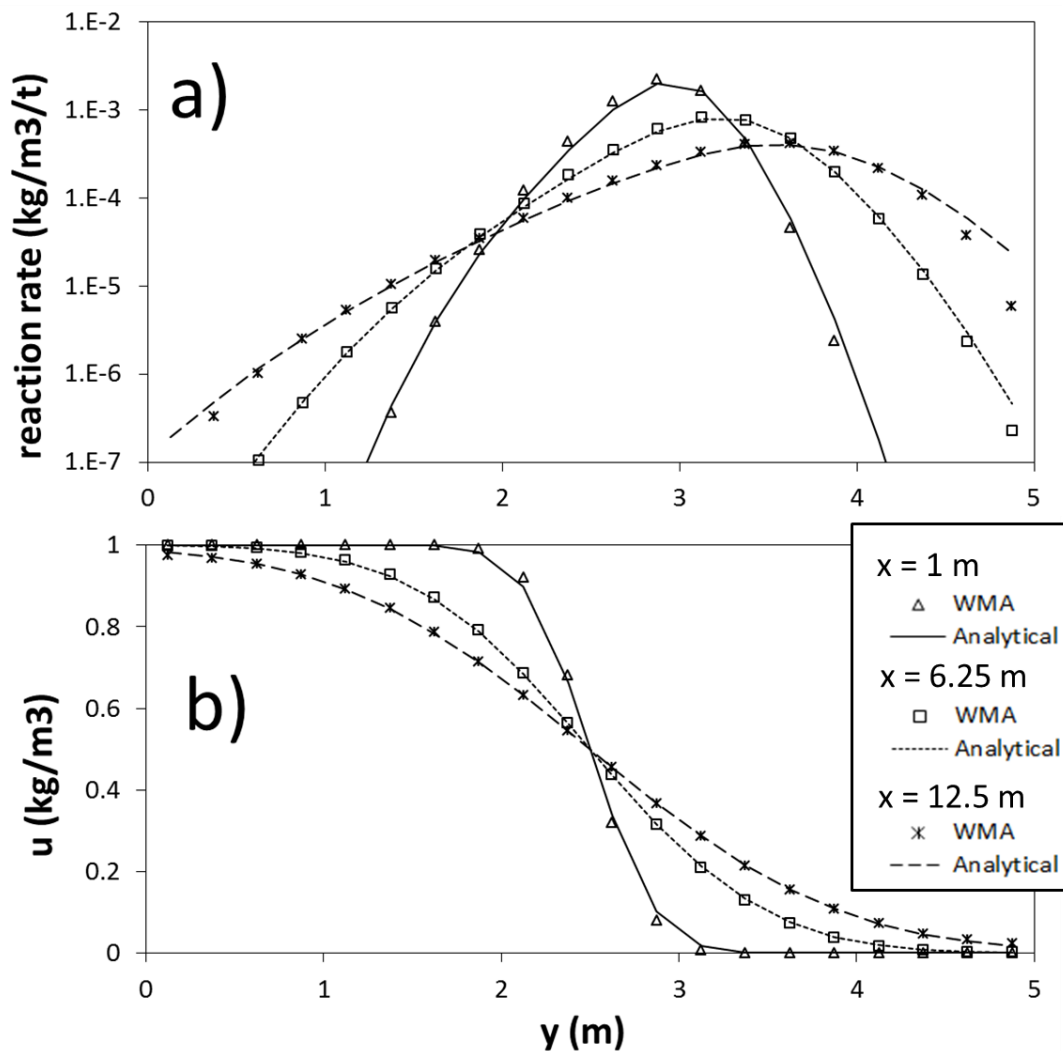
Figure 2. 4: Profiles at different *x* positions of reaction rate and component concentration of numerical and analytical solutions for the half injection domain.

Because no concentration gradient is defined in mixing term of Eq. (2. 4) neither in Eq. (2. 6), the WMA formulation supplies a complementary explanation. The

conservative form of Eq. (2. 14) tells us that the error comes from either the mixing rations λ_{ij} or the previous step concentration distribution c_{j-}^{k}. It is easy to check that λ is constant at any time step because all the terms of Eq. (2. 13b) are also constants. That is, only a small portion of solute near the interface does actually exchange. Therefore, approximating it by the mean parcel concentration is poor close to the injection boundary, when concentration varies sharply within the cell. In short, a proper discretization is needed for an accurate solution. The discretization is sufficient when concentrations are smooth. Despite the previous discussion, the results are very acceptable even near the injection boundary.

2.3.2.   The CAL case

Accuracy and efficiency of WMA for reactive transport performance are tested in this section by comparison with the DSA method. DSA method has been preferred because it is more robust than SIA. We tests the chemical system of Saaltink et al. (2001) termed CAL, which consists of the injection of calcite subsaturated water in a domain with initial saturated water and the consequent dissolution of calcite. Both, equilibrium and kinetic cases are tested. Transport and chemical details are shown in Table 2. 2.

The transport part of the DSA method is performed by TRACONF code (Carrera et al. 1993). Both compared codes use the same chemical library, CHEPROO (S. A. Bea et al., 2009). Therefore, the differences between the two methods are due to the treatment of transport. TRACONF transport formulation has two main differences from the formulation defined in section 2.2.4 First, time integration of TRACONF transport is calculated with implicit scheme which involves concentrations at the next time step. Although this implies the use of full system matrix, it is free of time instabilities, unlike faster explicit schemes. Second, an Eulerian formulation (Eq. (2. 1)) is applied instead of mixed Eulerian-Lagrangian formulation (Eq. (2. 10)). Eulerian solution approaches need to meet spatial stability criteria. To avoid complications with stability, the stability criteria are met in all tested models.

Table 2. 2: Physical and chemical parameters of the CAL case in both equilibrium and kinetic reactions. Equilibrium constant is taken from the program EQ3NR (Wolery, 1992)

CAL case			
Transport	**Chemistry**		
q (m/yr) 2	Mineral Calcite	Rate Constant ($mol \cdot m^{-2} s^{-1}$)	$4.64 \cdot 10^{-7}$
ϕ 0.1	**Initial conc. Of primary species (log mol l^{-1})**	**Injection conc. Of primary species (log mol l^{-1})**	
1D problem	H^+ -7.978	H^+ -5.496	
L (m) HCO_3^-	HCO_3^- HCO_3^-	HCO_3^- -5.421	
α (m) Ca^{2+}	Ca^{2+} Ca^{2+}	Ca^{2+} -4.398	
2D problem	**Kinetic case**	Initial reactive surface (m^{-1})	$6.8 \cdot 10^{-5}$
L$_x$ (m) 280			
L$_y$ (m) 100			
α_x (m) 1.2			
α_y (m) 1.2			

First, we compare the CPU time as a function of the number of numerical targets. We perform a 2D simulation (see Table 2. 2). A calculation proposed by Saaltink et al. (2001) is used to predict the CPU time for more refined grids. We assumed that the CPU time consumed by DSA is the sum of that of the chemical calculations, the LU decomposition and the construction of the Jacobian matrix expressed by subscripts *chem*, *dec* and *jac*, respectively. Then the CPU^{DSA} time can be calculated as

$$CPU^{DSA} = CPU_{chem}^{DSA} + CPU_{dec}^{DSA} + CPU_{jac}^{DSA}$$

(2. 18)

$$CPU_{chem}^{DSA} = k_{chem}^{DSA} N_{nod}$$

(2. 19)

$$CPU_{jac}^{DSA} = k_{jac}^{DSA} N_{nod} N_{con}$$

(2. 20)

$$CPU_{dec}^{DSA} = k_{dec}^{DSA}(N_{ban})^2 N_{nod} = k_{dec}^{DSA} m (N_{nod})^2 \tag{2.21}$$

Where N_{nod} is the number of nodes and N_{ban} is the semi-bandwith. As we work with rectangular grids (because the medium is homogeneous), N_{ban} is proportional to the square root of N_{nod} times m (m being the ratio between the number of rows and columns). k are constants that only depend on the test case. N_{con} is the maximum number of nodes connected to a particular node including itself (which equals 7 for regular grids of triangular finite elements).

Since we use an explicit scheme for the WMA transport part, the module does not need to solve a system of equations. Almost all CPU time is consumed by the calculation of the chemistry. However, unlike DSA, the spatial discretization affects the time discretization because of the isochronal mesh (see Figure 2. 3). To calculate the CPU time we assumed the number of chemical systems to be solved to be proportional to the number of nodes and the number of time steps. Therefore, the consumption of CPU time can be expressed as:

$$CPU^{WMA} = CPU_{chem}^{WMA} = k_{chem}^{WMA} N_{nod} N_{\Delta t} \tag{2.22}$$

Where $N_{\Delta t}$ is the number of time steps, which is proportional to the number of columns (Figure 2. 3). This, together with the definition of m, leads to:

$$CPU^{WMA} = k_{chem}^{WMA}(N_{nod})^{1.5} \tag{2.23}$$

The results are plotted in Figure 2. 5. As can be observed, the measured CPU time is consistent with the calculated CPU time for DSA cases. Kinetic case is slightly costlier though equal convergence criteria are employed. Regarding WMA, calculations using equation (2. 23) do not fit well the measured CPU time. The measurements fit better an exponent of 1.2 instead of 1.5. This can be attributed to the fact that less iterations are employed to solve chemical systems with finer grids. In both cases the differences between WMA and DSA become important when large numbers of nodes are employed. It may therefore be concluded that the WMA outperforms the DSA in both equilibrium and kinetic problems.
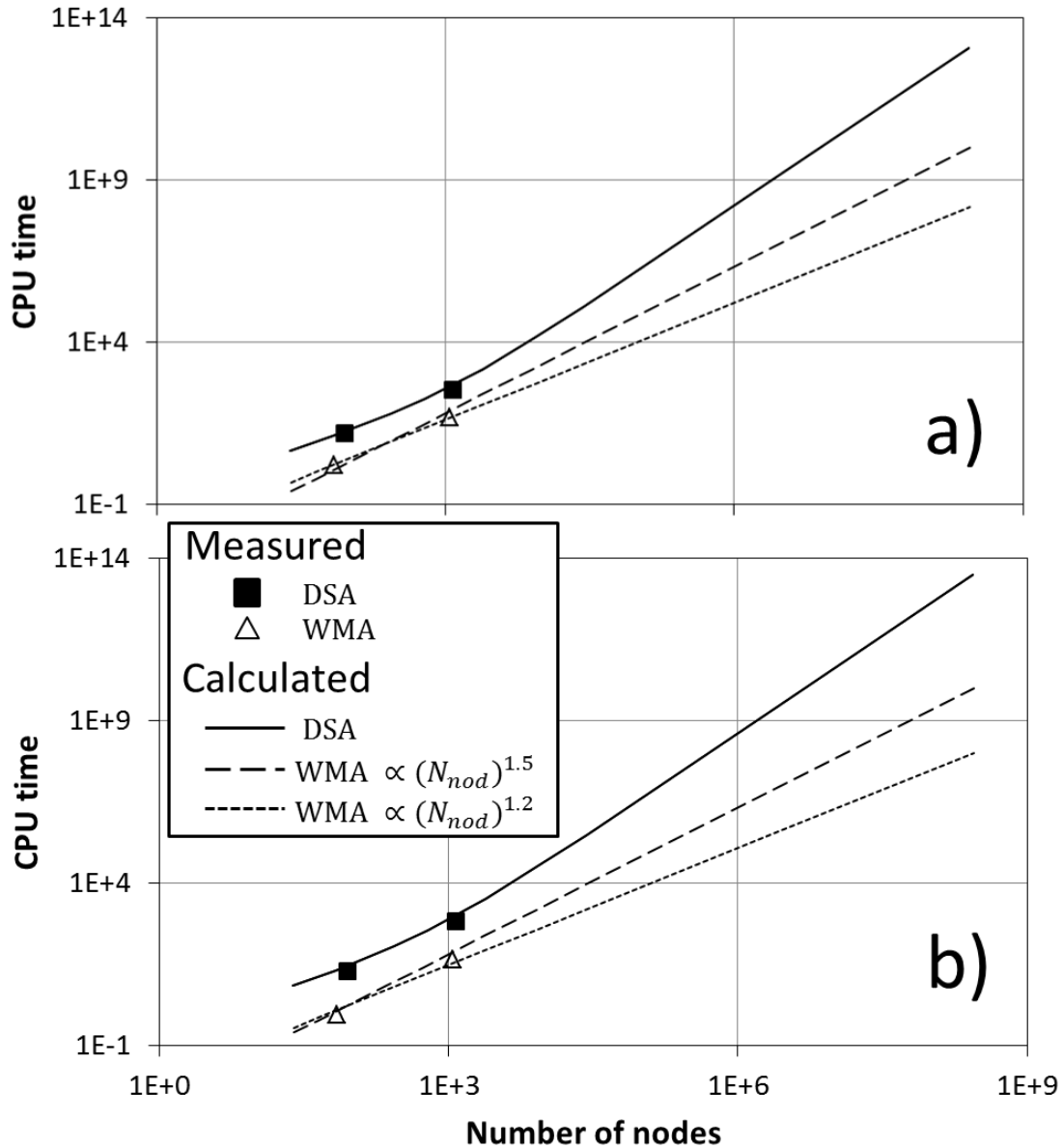
Figure 2. 5: Measured and calculated CPU times as a function of the total number of nodes for both WMA and DSA for (a) equilibrium CAL case and (b) kinetic CAL case.

Second, the absence of numerical dispersion as evidenced in section 2.2.4 should be confirmed. To this end, 1D simulations were performed (see Table 2. 2) using the previous WMA and DSA codes. Three different time steps were used for both methods (3 months, 1.5 month and 22 days). Because of the mesh definition (see Figure 2. 3), the WMA needs 20, 40 and 80 parcels, respectively whereas the DSA mesh is composed by 101 nodes in all models. Results are plotted in Figure 2. 6. Note that results of the DSA

using an implicit scheme depend on the time step indicating numerical dispersion. On the other hand, the WMA isochronal method presents no numerical dispersion even when the isochronal grid employs a smaller number of nodes.

DSA is also performed and plotted with Crank-Nicholson time integration in Figure 2. 6a. Crank-Nicholson provides a second order error, unlike the first order error of explicit and implicit scheme. Theoretically, this should be without numerical dispersion. Indeed, it gives almost identical results to the WMA.
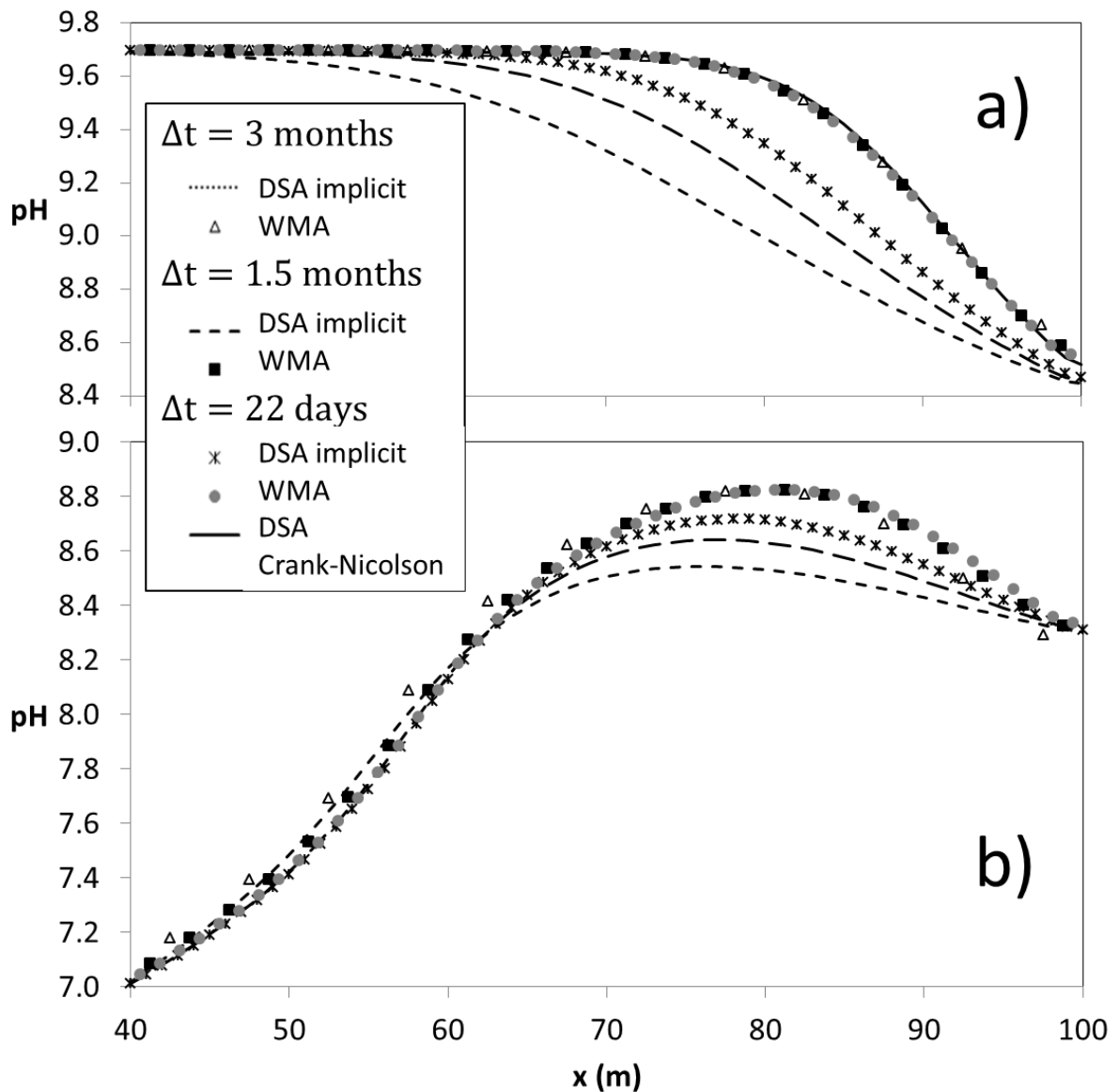
Figure 2. 6: Spatial distribution of pH at 1 pore volume (5 years) for WMA using isochronal mesh, DSA in implicit scheme and DSA in Crank-Nicolson scheme using 3 different time steps for (a) equilibrium CAL case and (b) kinetic CAL case.

2.4.   Conclusions

We have presented a new reactive transport formulation and modeling method based on water mixing which we term the Water Mixing Approach (WMA). The basic idea behind the approach is to restrict the coupling between chemistry and transport only to the terms that matter: residence time (relevant for kinetic reactions) and mixing (relevant for fast reactions). These are strictly transport concepts. The resulting reactive transport problem is restricted to the computation of a sequence of reactive mixing calculations, which is simpler and more efficient than traditional reactive transport methods. Effectively, the method implies modelling the transport of water volumes instead of components or species. This decouples transport from chemistry.

Two cases have tested the satisfactory accuracy and computational efficiency of WMA. The approach can be employed in any existing transport approach, although the proper definition and computation of mixing ratios is an important issue. This is why the WMA method has been tested using a streamline oriented isochronal grid, which allows for numerical simulations free of numerical dispersion even for coarse grids. In particular, mixing ratios definition should be especially relevant for transport formulations in heterogeneous media. In this article we have discussed only cases with uniform flow. Nevertheless, the results suggest that the WMA will also perform well for 2D or 3D heterogeneous cases with non-uniform flow. This is shown by the fact that the WMA becomes increasingly more competitive to the Eulerian methods of DSA for grids of higher dimension and larger number of targets.

Chapter 3

Simulation of chemical reaction localization using a multi-porosity reactive transport approach[*]

3.1.   Introduction

Reactive transport deals with geochemical processes that occur in porous media due to the physical transport of reacting chemical species. It plays a major role in many civil and/or environmental issues such as cleanup of contaminated aquifers, nuclear waste storage, mining and geological storage of CO_2. Reactive transport may be very complex and non-trivial. As a result, numerical models are an indispensable tool for understanding and predicting these processes. One problem encountered is the high level of heterogeneity, which can be both chemical and hydrodynamic. Reactive transport models typically assume local equilibrium with fast dissolution kinetic minerals. Even so, non-equilibrium is commonly observed and is attributed to this heterogeneity (Alcolea et al., 2008; Vogel et al., 2006). For instance, breakthrough curves typically display tailing at late times (Valocchi 1985; Carrera 1993). This non-

---

[*] This chapter is based on the paper by Soler-Sagarra et al. (2016)

equilibrium may be due to diffusion into immobile regions, kinetic sorption or heterogeneity. This implies that reactive transport should be formulated as non-local in time which means that the concentration at a given point depends on its concentration history. A large number of formulations (Carrera et al., 1998; Dentz and Berkowitz, 2003; Haggerty and Gorelick, 1995; Silva et al., 2009; Sudicky, 1989), simulation approaches (Ray et al., 1997; Salamon et al., 2006; Suresh Kumar, 2008; Tsang, 1995; Willmann et al., 2008; Zhang et al., 2006; Zhang et al., 2007) and analytical solutions (Toride et al., 1993) have been proposed to deal with non-local in time transport (see Dentz et al., 2011a, for a review).

In parallel with Darcy scale models, a number of researchers have overcome this non-locality by formulating transport at pore scale because chemical processes occur at pore scale (Steefel et al., 2005) . One such formulation is the Lattice Boltzmann equation, which replaces the velocities of individual particles by a distribution function of velocities in which the population of particles moves (Benzi et al., 1992; Chen and Doolen, 1998; Kang et al., 2006; Acharya et al., 2007; Willingham et al., 2008). Another formulation is Smoothed Particle Hydrodynamics, which is based on the idea that a continuous field can be represented by a superposition of smooth bell-shaped functions centered on a set of points whereas the gradient of the field is given by the same superposition of the gradients of the smoothing function (Liu and Liu, 2010; Tartakovsky et al., 2007, 2009, 2015). A third option consists of simulating the pore network to explicitly simulate the pore volumes and connecting necks (Blunt, 2001; Blunt et al., 2002; Li, et al., 2006; Meile and Tuncay, 2006; Raoof et al., 2010; Raoof and Hassanizadeh, 2012; Varloteaux, 2013). These formulations are very accurate in reproducing local physics, but are computationally demanding for large scale models or when many chemical species and reactions are involved. Moreover, the upscaling of the results to field scale has not yet been resolved.

Other researchers prefer continuous models at larger than pore scales to gain in computational cost and model simplicity. The classic approach consists on representing heterogeneity by a dispersion tensor, but it fails to quantify solute mixing accurately (Ginn et al., 1995; Kitanidis, 1988; MacQuarrie and Sudicky, 1990; Molz and Widdowson, 1988; Dreuzy et al., 2012), which is critical for reactive transport as reaction rates are driven by mixing (De Simoni et al., 2007). There are a number of approaches to quantify mixing rates more accurately. The most widely used are the

Multi-Rate Mass Transfer (MRMT) and Continuous Time Random Walk (CTRW). MRMT is a non-local in time continuous formulation that simulates mass transfer between a mobile and multiple immobile regions by diffusive or first-order mass transfer terms (Benson and Meerschaert, 2009; Carrera et al., 1998; Donado et al., 2009; Fernandez-Garcia and Sanchez-Vila, 2015; Geiger et al., 2013; Gouze et al., 2008; Haggerty and Gorelick, 1995; Haggerty et al., 2000; Roth and Jury, 1993; Wang et al., 2005; Willmann et al., 2010; Zhang et al., 2007). Models similar to MRMT exist for diffusion from a fracture into the matrix of the rock (Cvetkovic et al., 1999; Gerke and van Genuchten, 1996; Grisak and Pickens, 1980; Małoszewski and Zuber, 1985; Moreno and Neretnieks, 1993; Shapiro, 2001). CTRW is a class of Random Walk methods in which not only particle displacements, but also time steps are modeled as a stochastic process (Montroll and Weiss, 1965; Berkowitz and Scher, 1998; Metzler and Klafter, 2000; Barkai and Cheng, 2003; Cortis, 2004; Dentz et al., 2004; Berkowitz et al., 2006). Its validity has been proven using pore network models (Bijeljic and Blunt, 2006). CTRW has been applied to reactive transport using particles explicitly, which is computationally demanding. But, in practice, CTRW and MRMT are equivalent (Dentz and Berkowitz, 2003; Neuman and Tartakovsky, 2009; Silva et al., 2009).

The latter methods have been used to study the effect of hydrodynamic heterogeneity on reactive transport. Most of these studies used simple chemical systems of one or more chemical reactions (e.g., Donado et al., 2009; Willmann et al., 2010). Other studies have focused on more complex chemical systems (Ayora et al., 1998; Steefel and Lichtner, 1998). Research has been carried out on specific surface area heterogeneity (Cvetkovic and Gotovac, 2014) and on network fracture heterogeneities (Cheng et al., 2003; Frampton and Cvetkovic, 2007, Painter et al., 2008). The effect of chemical heterogeneity was addressed by Dentz el al. (2011b), but on an abstract system that did not allow acknowledging explicitly that porous media consist of multiple mineral phases, which create their own local conditions and precipitation/dissolution reactions. We use the term geochemical localization to describe the creation of local micro environments favoring reactions that would not occur in media that are fully mixed at the Representative Elementary Volume (REV) scale. We argue that geochemical localization is driven by mineral heterogeneity at the pore scale and may cause reaction heterogeneity at such scale. Geochemical localization has been observed by Luquot et al. (2016), who performed percolation experiments under *in situ*

temperature, pressure and salinity conditions to predict the different chemical reactions which can occur during the migration of CO_2-rich brine at the Heletz site (A. Niemi et al., 2012; Auli Niemi et al., 2016). These authors verified their experimental results using the CrunchFlow code (Steefel, 2009) that regards dispersion as the only mixing process. They obtained good matches between the experimental and numerical results for the main dissolved and precipitated minerals with fast reaction kinetics (carbonates and gypsum). Nevertheless, secondary mineral reactions were not predicted accurately (e.g., K-feldspar dissolution and clay precipitation). They concluded that these secondary reactions, which may play an important role in the change of hydrodynamic properties, occur at scales smaller than the REV and cannot be taken into account in conventional reactive transport models that are based on the Advection-Dispersion Equation (ADE).

We conjecture that geochemical localization can be reproduced using multi-porosity formulations, such as MRMT, provided that geochemical heterogeneity is included in the model. The objective of this work is to test such conjecture and to gain further insight into the effect of mineralogical and hydrodynamic heterogeneity. To this end, the MRMT based method was used, varying the mineral composition of mobile and immobile zones (see Figure 3. 1). A simplified chemical system based on Luquot et al. (2016), was employed. The mathematical formulation of reactive transport used in the MRMT approach is described in section 3.2. In section 3.3, we discuss the numerical solution of these equations, which basically consists of extending the Water Mixing Approach (WMA) of chapter 2 to MRMT, obtaining the proposed Multi-Rate Water Mixing (MRWM). Models definitions and their results are presented in section 3.43.4. Finally, section 3.5 is dedicated to discussion and conclusions.
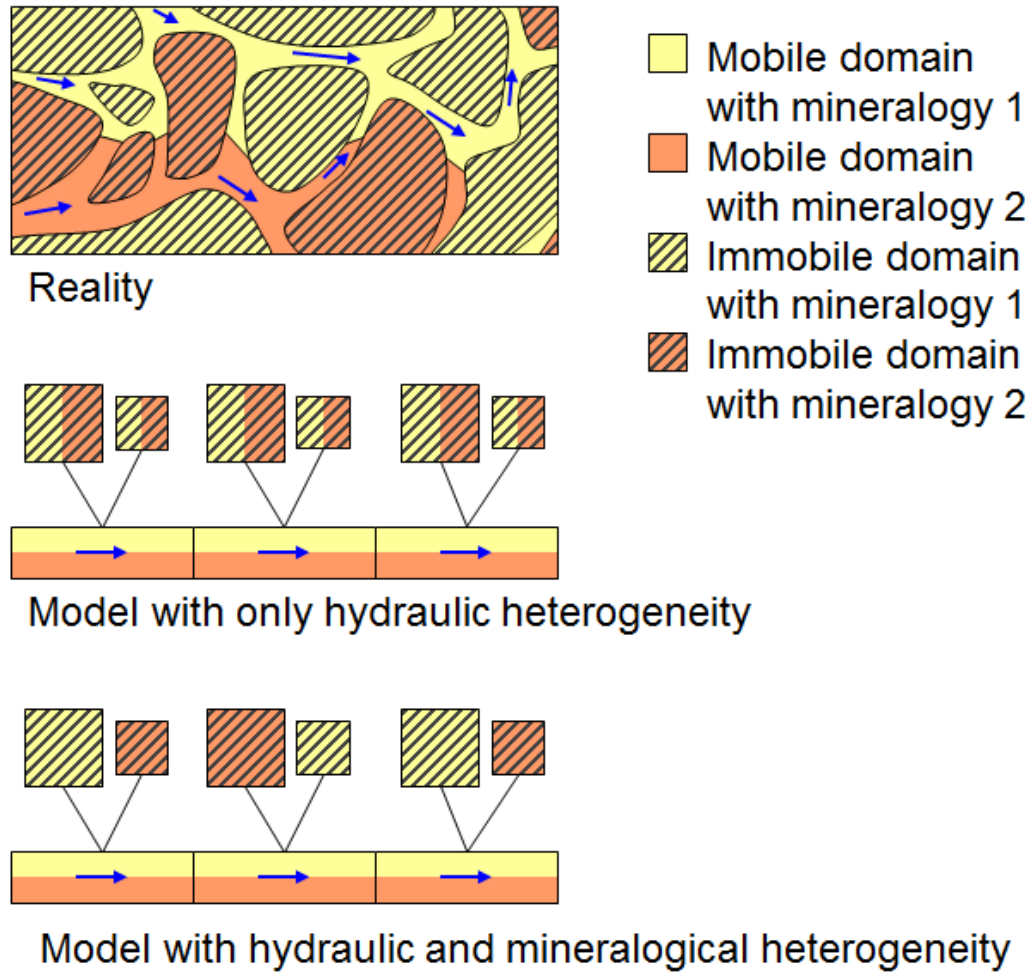
Figure 3. 1: Schematic spatial mineralogy distribution. The top image displays the 'real' distribution. The central image shows a classical MRMT distribution without considering mineralogical localization. The bottom image shows the distribution of the mineral phases in several immobile zones connected to a mobile node.

3.2.   Governing equations

The standard formulation for reactive transport is based on applying the ADE to all chemical species with sink/source terms to represent reactions (i.e., sinks for reactants and sources for reaction products). This leads to a complex set of N_s ADE (N_s is the number of species), which uses the vector concentrations c $[M/L^3]$ as state variable, and N_r constraints (mass action laws for equilibrium reactions and rate laws for kinetic reactions) for the chemical reactions. Instead, here the WMA formulation is extended to MRMT by adding the mixing of mobile and immobile zones. This reduces the number

33

of transport equations. As a consequence, The Multi-Rate Water Mixing (MRWM) formulation is obtained. The system may be simplified by the use of components. These are obtained by multiplying the concentration vector by a full-ranked kernel matrix U, dimensions $(N_s\text{-}N_e)\cdot N_s$, where N_e is the number of equilibrium reactions so that equilibrium reaction rates are eliminated (Lichtner, 1985; Steefel and MacQuarrie, 1996). The advantage is twofold: equilibrium reaction rates are eliminated from the system and the dimension of the problem is reduced from N_s+N_r to $N_s\text{-}N_e$. Therefore, the reactive ADE is usually formulated as mass balances of components. A variety of approaches are available to define the components (Fang et al., 2003; Friedly and Rubin, 1992; Kräutle and Knabner, 2005, 2007; Molins et al., 2004; Saaltink et al., 1998; De Simoni et al. 2005; Yeh and Tripathi, 1989). Here, we use the method of Saaltink et al. (1998), which complements the aqueous reactions component matrix with a matrix E to eliminate rapid dissolution/precipitation reactions, further reducing the number of unknowns and equations.

We used the above formulation in a MRMT framework (Donado et al., 2009; Willmann et al., 2010) but the framework was specially designed to allocate different chemical systems in each immobile zone. Therefore, the system of equations contains not only mass balances (transport equations) but also different chemical system in the mobile and immobile zones. The set of equations to be resolved may be written in compact form as:

$$\phi_m \frac{\partial \boldsymbol{u_{am}}}{\partial t} = \nabla \cdot (\overline{\boldsymbol{q_D u_{am}}}) - \boldsymbol{q} \cdot \nabla \boldsymbol{u_{am}} - \sum_{j=1}^{Nim} \alpha_j \big(\boldsymbol{u_{am}} - \boldsymbol{u_{aim,j}} \big) + \boldsymbol{f} + \boldsymbol{f_{chem,m}} \qquad (3.\,1)$$

$$\phi_{im,j} \frac{\partial \boldsymbol{u_{aim,j}}}{\partial t} = \alpha_j \big(\boldsymbol{u_{am}} - \boldsymbol{u_{aim,j}} \big) + \boldsymbol{f_{chem,im,j}} \qquad j = 1, \dots, N_{im} \qquad (3.\,2)$$

$$\log \boldsymbol{c_2} = \boldsymbol{S_a} (\log \boldsymbol{c_1} + \log \boldsymbol{\gamma_1}) - \log \boldsymbol{\gamma_2} - \log \boldsymbol{k_a} \qquad (3.\,3)$$

$$\log \boldsymbol{c_s} = \boldsymbol{S_s} (\log \boldsymbol{c_1} + \log \boldsymbol{\gamma_1}) - \log \boldsymbol{\gamma_s} - \log \boldsymbol{k_s} \qquad (3.\,4)$$

$$0 = \boldsymbol{S_{min}} (\log \boldsymbol{c_1} + \log \boldsymbol{\gamma_1}) - \log \boldsymbol{k_{min}} \qquad (3.\,5)$$

$$\boldsymbol{c_a} = \begin{pmatrix} \boldsymbol{c_1} \\ \boldsymbol{c_2} \end{pmatrix} \qquad (3.\,6)$$

$$\boldsymbol{u_a} = \boldsymbol{E U_a c_a} \qquad (3.\,7)$$

$$u_s = EU_s c_s \qquad (3.8)$$

$$f_{chem,l} = EUS_k^t r_k(u_a, u_s) - \phi_l \frac{\partial u_s}{\partial t} \qquad l = m, im \qquad (3.9)$$

In these equations, subscript a, s and min stand for aqueous, sorbed and mineral concentrations and components, respectively, and m and im refer to mobile and immobile zones, respectively. Equation (3. 1) defines the transport equation in mobile domains but the third term in the right-hand side represents a linear mass exchange between mobile and immobile zones. In this equation, vector u [M/L^3] contains component concentrations defined by equations (3. 7) and (3. 8), ϕ [-] is porosity, t [T] time, q[L^3/L^2/T] Darcy flux, f [M/L^3/T] is a non-chemical sink/source term, q_D[L^3/L^2/T] is the water flux that exchanges due to dispersion in the mobile zone, f_{chem} [M/L^3/T] is a sink/source term for kinetic and sorption reactions and α_j [T^{-1}] is a first-order mass transfer rate coefficient. Equation (3. 2) defines the specific mass balance in the jth immobile region as a linear exchange with the mobile domain. N_{im} is the number of immobile zones connected to a mobile. Note that the sum of equations (3. 1) and (3. 2) expresses the total mass balance in both mobile and immobile zones. Equations (3. 3), (3. 4) and (3. 5) describe the mass action laws for equilibrium reactions in the aqueous, surface (sorption and cation exchange) and mineral phases, respectively. The vector of aqueous species concentrations (c_a) is split into two vectors c_1 and c_2 of primary and secondary concentrations (equation (3. 6)) such that c_2 can be expressed as an explicit function of c_1 by means of equations (3. 3). Vector γ has the same subscripts as c and contains the activity coefficients. S_k and r_k in (3. 9) are the stoichiometric matrix and the vector of reaction rates for kinetic reactions, respectively. Note that in the absence of kinetic reactions and adsorption, component u_{am} can be resolved as a conservative transport problem.

In these equations, the set of chemical reaction occurring at any point and defined by the stoichiometric matrices S are space dependent. That is, different chemical systems can be defined in different portions of the domain to represent large scale heterogeneity or in different immobile zones to represent sub-REV (pore scale) chemical heterogeneity. Therefore the definition of components will also be space dependent. A potential source of conflict may arise from adjacent cells with different chemical systems and thus different components. To circumvent them, we adopt the rule

"dressing code defined by the host", meaning that the mass balance of a cell, which can include contributions from adjacent cells, is defined for the components of the chemical system of that cell. This way, components are defined at every point with the local chemical system.

3.3. Numerical Formulation

We use here an isochronal grid (Appendix A) to model the mobile domain of MRWM. That is, travel time between nodes equals the time step, which facilitates simulating advection by simply displacing concentrations from one cell to the next one downstream. Dispersion is simulated by mixing water of a cell with that of adjacent cells. The method is well suited to advection dominated problems. In this way we can express the aqueous concentration of a component at a mobile cell i as a function of concentrations of adjacent cells at a previous time step:

$$\boldsymbol{u}_{am,i}^{k+1} = \boldsymbol{u}_{am,i-}^{k} + \sum_{n=1}^{Nm} \lambda_{in}(\boldsymbol{u}_{am,n}^{k} - \boldsymbol{u}_{am,i-}^{k}) + \sum_{j=1}^{Nim} \lambda_{ij}(\boldsymbol{u}_{aim,j}^{k} - \boldsymbol{u}_{am,i-}^{k}) + \boldsymbol{R}_i \quad (3.10)$$

where subscript $i-$ indicates the position of ith cell at time step k, i.e. the upstream cell if an isochronal grid is used, λ_{in} is the mixing ratio, i.e. the proportion of n cell water that mixes with i cell water during the time step, Nm and Nim are the number of mobile and immobile cells connected to cell i, respectively, and $\boldsymbol{R}_i$ is the vector of contributions from kinetic and sorption reactions to aqueous components. For the sake of simplicity, the non-chemical sink/source term is represented by one of the mixing terms n. Therefore λ [-] can have different expressions depending on whether they represent the mixing fraction with adjacent mobile cells, the source term and exchange with the immobile zone, respectively.

$$\lambda_{in} = D_{in} \frac{A_{in} \cdot \Delta t}{L_{in} \cdot \phi_{m,i} \cdot V_i} \tag{3.11}$$

$$\lambda_{in} = \frac{Q_i}{\phi_{m,i} \cdot V_i} \Delta t \tag{3.12}$$

$$\lambda_{ij} = \frac{\alpha_{ij}}{\phi_{m,i}} \Delta t \tag{3.13}$$

where Δt is the time step, D_{in} $[L^2/T]$ is the dispersion coefficient at the i-n interface, i.e. longitudinal dispersion in the flow direction or transverse dispersion, with area A_{in}

$[L^2]$, at a distance L_{in} $[L]$, V_i is the water volume of the cell, and Q_i is the flow rate of sources into cell i. R_i $[M/L^3/T]$ in equation (3. 10) is given by

$$R_i = u_{sm,i}^k - u_{sm,i}^{k+1} + \frac{EUS_k^t r_k(u_{am,i}^k)}{\phi_{m,i}} \Delta t \qquad (3.\ 14)$$

Advection is defined through $u_{am,i-}^k$. Using an isochronal one-dimensional mesh allows us to write

$$u_{am,i-}^k = u_{am,i-1}^k \qquad (3.\ 15)$$

Substituting (3. 15) into (3. 10) yields:

$$u_{am,i}^{k+1} = \lambda_{ii} u_{am,i-1}^k + \sum_{\substack{n=1 \\ n \neq i}}^{Nm-1} \lambda_{in} u_{am,n-1}^k + \sum_{j=1}^{Nim} \lambda_{ij} u_{aim,j}^k + R_i \qquad (3.\ 16)$$

Note that the mixing ratio λ_{ii} $[-]$ is simply the fraction of water that is not exchanged with adjacent cells:

$$\lambda_{ii} = 1 - \sum_{\substack{n=1 \\ n \neq i}}^{Nm-1} \lambda_{jn} - \sum_{j=1}^{Nim} \lambda_{ij} \qquad (3.\ 17)$$

A full numerical analysis of the solution method falls beyond the scope of this paper. Let us simply state here that the method is consistent, but stability is conditional and requires $\lambda_{ii} > 0$, which limits the maximum time step to be used. If this condition is met and an isochronal mesh is used, convergence is second-order for conservative transport. Speciation would have to be done once the components were calculated. In practice, however, speciation is done simultaneously with mixing calculations equation (3. 10), because species concentrations are necessary for evaluating R_i, by means of equation 14. This calculation is also explicit and we assume that it will also be conditionally stable, but we have not been able to derive an easy to apply stability condition. Therefore, we have made sensitivity analysis to the time step size. In the results presented here, the solution was not sensitive to the time step. The algorithm is described in Figure 2. 1a and is linked to chemical library CHEPROO, which is an Object Oriented code for geochemical calculations (Bea et al., 2009).

For the sake of simplicity, porosity changes caused by mineral precipitation/dissolution were neglected. Hence, flux may be regarded as steady state. Otherwise, the isochronal mesh would have to be recalculated at each time step and

several parameters (such as permeability and mass transfer rate) should be recalculated for each new element causing numerical errors.

3.4.   Application models

3.4.1.   Model descriptions and parameters

The MRWM method was applied to a simplification of the G5 laboratory experiment performed by Luquot et al. (2016). The G5 experiment involved injecting CO_2 rich brine into a sandstone sample from Heletz at a low flow rate. In order to study the localization of chemical reactions, we built four numerical models (Figure 3. 2) by varying the hydrodynamic and/or chemical heterogeneity. However, parameters such as inflow rate, porosity, domain bulk volume or total surface area of every mineral (except WMA-2) remained constant for all models.
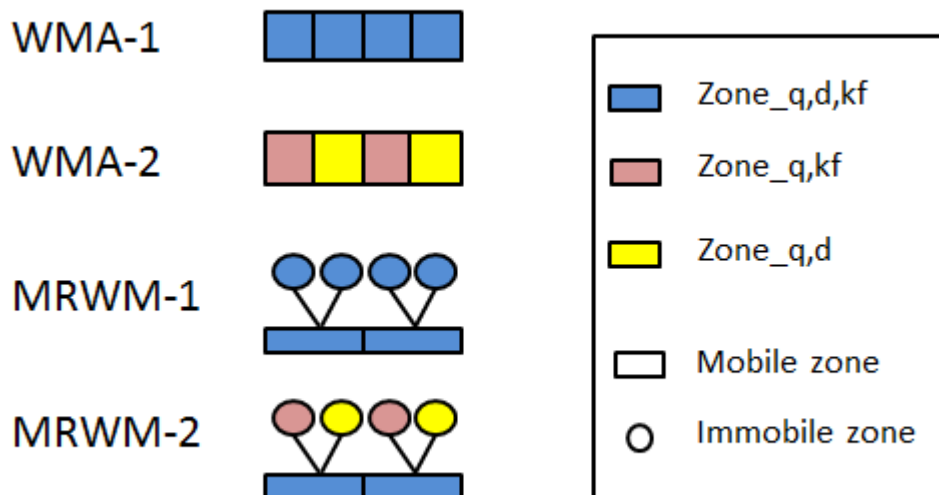
Figure 3. 2: Conceptual sketch of the different simulations. WMA and MRWM schemes are represented with 4 and 2 mobile nodes scheme, respectively. WMA numerical models use 150 mobile nodes whereas MRWM models use 75 mobile nodes.

We used a one-dimensional domain discretized by an isochronal mesh (i.e., transit time per cell equal to the time step). The first two models (WMA 1 and WMA 2) consisted of 150 mobile cells, each with a volume of $3.85 \cdot 10^{-9}$ m^3. The other two models (MRWM 1 and MRWM 2) had the same total volume as the WMA models but only half of this volume was defined as mobile. The MRWM mobile cells (75) have the same volume as the WMA cells ($3.85 \cdot 10^{-9}$ m^3). Therefore, the time step is the same for all the models because so are the flow rate, cell volume and mobile porosity. The fact that water flows only through half of the domain (the other half is immobile) causes velocity to be twice as high (hence, MRWM cells have lengths twice that of WMA cells and the number of mobile MRWM cells is half that of WMA cells).

Each mobile cell was connected to 2 immobile cells of $1.925 \cdot 10^{-9}$ m^3 in the MRWM models. Hydrodynamic parameters are summarized in Table 3. 1. The time step was set to 0.905 seconds with a total simulated time of 5 hours. According to equation (3. 11) this gives a mixing ratio of 0.1 between the mobile cells. With a transfer coefficient (α) of $2.07876 \cdot 10^{-5}$ s^{-1}, the water mixing ratio between mobile and immobile cells becomes $9.9 \cdot 10^{-5}$, 1010 times lower value than for exchange between mobile cells.

Table 3. 1: Physical hydrodynamic parameters used in the models. First column refers to those used in all models. First row of the second column refer to WMA models and third row to MRWM models, respectively.

All models		Specific models WMA 1, WMA 2	
Initial porosity (ϕ_m)	0.19	Mobile nodes	150
Input flow (Q)	$8.33 \cdot 10^{-10}$ m^3 s^{-1}	Specific models MRWM 1, MRWM 2	
Domain length	$1.5 \cdot 10^{-2}$ m	Mobile nodes	75
Time increment (Δt)	0.904762 s	Immobile cell volume	$1.9 \cdot 10^{-9}$ m^3
Mix. ratio mob. cells (λ_{in})	0.1	Initial immobile porosity (ϕ_{im})	0.19
Mobile cell volume	$3.8 \cdot 10^{-9}$ m^3	Mixing ratio mobile-immobile cells (λ_{ij})	$9.9 \cdot 10^{-5}$

Model mineralogical compositions are motivated by those of Luquot et al. (2016), only simpler to facilitate interpretation (see Table 3. 2). The only carbonate phase is dolomite. The model considers two minerals with fast reaction kinetics (dolomite and gypsum) as well as three slowly reacting minerals (quartz, K-feldspar and kaolinite). Total porosity (18.8%), rate laws for reacting minerals (Table 3. 3) and effective

reactive surface areas were taken equal to those of Luquot et al. (2016) for experiment G5. The initial surface areas of secondary minerals (gypsum and kaolinite) were set to 1 m^2/m^3 to initiate the precipitation. Gypsum was assumed initially present in small concentrations.

Table 3. 2: Brine composition of the Heletz field and those used here as well as the saturation index for the different minerals used in experiment G5 (Luquot et al., 2016).

Brine compositions (mol/kg$_w$)

Heletz brine eq. Gypsum		Brine composition used here	
Element	Concentration	Concentration pore water	Concentration injected solution
Ca	$6,88 \cdot 10^{-2}$	$6,88 \cdot 10^{-2}$	$6,88 \cdot 10^{-2}$
Cr	$1,29 \cdot 10^{-6}$	-	-
Cu	$2,79 \cdot 10^{-5}$	-	-
Fe	$2,17 \cdot 10^{-5}$	-	-
K	$1,08 \cdot 10^{-2}$	$1,08 \cdot 10^{-2}$	$1,08 \cdot 10^{-2}$
Mg	$2,13 \cdot 10^{-2}$	$2,13 \cdot 10^{-2}$	$2,13 \cdot 10^{-2}$
Mn	$1,05 \cdot 10^{-6}$	-	-
Na	$7,68 \cdot 10^{-1}$	$7,88 \cdot 10^{-1}$	$7,88 \cdot 10^{-1}$
Ni	$3,03 \cdot 10^{-7}$	-	-
S	$3,21 \cdot 10^{-2}$	$2,48 \cdot 10^{-2}$	$2,48 \cdot 10^{-2}$
Si	$4,70 \cdot 10^{-5}$	$4,70 \cdot 10^{-5}$	$4,70 \cdot 10^{-5}$
Sr	$1,13 \cdot 10^{-4}$	-	-
Cl	$7,99 \cdot 10^{-1}$	$8,99 \cdot 10^{-1}$	$8,99 \cdot 10^{-1}$
Al	$3,46 \cdot 10^{-7}$	$3,46 \cdot 10^{-7}$	$3,46 \cdot 10^{-7}$
C	$3,28 \cdot 10^{-4}$	$3,28 \cdot 10^{-4}$	$1,10 \cdot 10^{-1}$
pH	7,30	7,30	2,33

Saturation index

Mineral	log(IAP/K)	log(IAP/K)
Quartz	-0,85	-0,81
Dolomite	0,00	-11,94
K-Feldspar	-1,33	-12,54
Kaolinite	-0,05	-12,69
Gypsum	0,00	0,00

The brine composition is shown in Table 3. 3. The composition of the injected solution is the same as that of the initial solution, after adding 0.11 mol of CO_2 per kg of

water (equilibrium with CO_2 at 18 bar). This lowers pH and renders the solution unsaturated with respect to the main minerals.

Table 3. 3: Simplified mineral composition of the Heletz sandstone and parameters used in numerical models. Values of E_a are taken from Palandri and Kharaka 2004. Illite, ankerite and pyrite are not considered here.

Mineral compositions and reactive parameters

Heletz mineral								
Mineral	wt.%	wt.% *, ¥			Reactive surface area (m^2/m^3)	$k_{m,25}$ (mol m^{-2} s^{-1})	n H$^+$	E_a (kcal mol^{-1})
		Zone_q,d,kf	Zone_q,d	Zone_q,kf				
Quartz	60.06 ± 2.13	67,28	75,19	59,39	4300	3,98 E-14	-0,3	21,72
K-Feldspar	17.44 ± 2.05	20,25	0	40,49	4500	8,71 E-11	0,5	12,36
Dolomite	8.87 ± 0.23	12,35	24,69	0	150	6,46 E-4	0,5	8,63
Kaolinite	2.24 ± 1.31	0			1	4,90 E-12	0,77	15,75
Gypsum	2.30 ± 0.84	0,12			1	1,62 E-3	-	0
Illite	5.62 ± 0.93	*) the zero values indicate the potential precipitated minerals taken into account in the model.						
Ankerite	2.95 ± 0.11							
Pyrite	0.52 ± 0.11	¥) q, d and kf are respectively used for quartz, dolomite and K-Feldspar.						

Forty-nine aqueous species were considered in the simulations. All the equilibrium constants (log K at 60 °C), including those for the mineral reactions, and stoichiometric coefficients were taken from the EQ3/6 database (Wolery et al., 1990). Activity coefficients were calculated using the extended Debye-Hückel formulation (b-dot model) with the parameters listed in the database.

3.4.2.   WMA – 1: model with homogeneous mineral zones

The WMA-1 model represents a homogeneous mineral distribution along the core sample with transport dominated by advection. It has the same configuration as the one used by Luquot et al. (2016). The resulting dissolution and precipitation processes are in agreement with those of Luquot et al. (2016) despite our simplified chemical system. The total volume of dissolved and precipitated minerals at the end of the simulation is presented in Table 3. 4. We predict high dolomite dissolution near the sample inlet, which diminishes near the outlet (Figure 3. 3b). As a result, pH increases (Figure 3. 3a). The rate of dolomite dissolution falls at 3 mm from the inlet due to the dependence of

dolomite dissolution kinetics on pH (Table 3. 3). Gypsum precipitates near the inlet, peaking also at some 3 mm from the inlet, due to the build-up of Ca driven by dolomite dissolution (Figure 3. 3d). The dissolution of K-feldspar is not displayed in Figure 3. 3 because it is similar to that of dolomite in shape, albeit with lower rates, because of a similar dependence on pH.
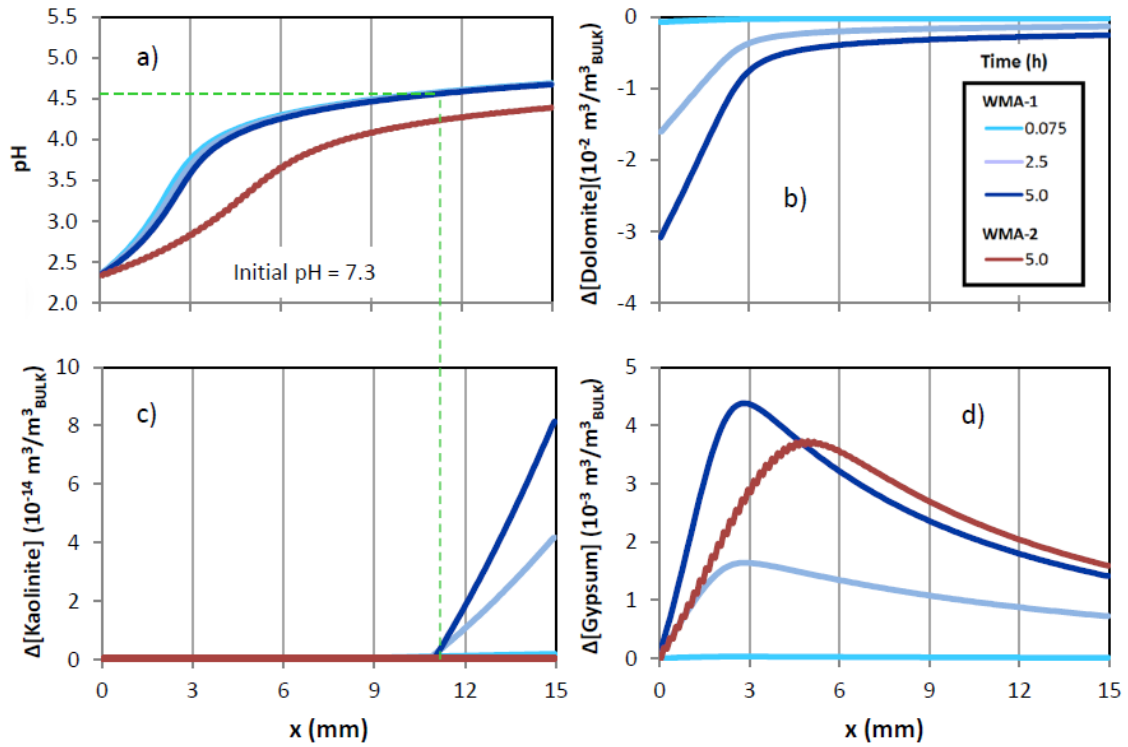
Figure 3. 3: Variation along the sample length for different time steps (0.075 h, 2.5 h and 5h) of (a) pH, (b) dolomite (c) kaolinite, and (d) gypsum concentration changes for simulation WMA-1. The dashed green line shows the minimum pH at which Kaolinite precipitation occurs. For comparison, the final time step of WMA-2 variation concentration of pH, gypsum and kaolinite are shown. The Representative Elementary Volume (REV) bulk volume is $3.85 \cdot 10^{-9} \, m^3$

Table 3. 4: Total volume of dissolved and precipitated minerals for the four simulations.

Total dissolved and precipitated mineral (m³)					
Model	Quartz	Dolomite	K-Feldspar	Kaolinite	Gypsum
WMA-1	$-3.05 \cdot 10^{-14}$	$-3.65 \cdot 10^{-9}$	$-5.10 \cdot 10^{-14}$	$5.96 \cdot 10^{-21}$	$1.49 \cdot 10^{-9}$
WMA-2	$-2.30 \cdot 10^{-14}$	$-2.89 \cdot 10^{-9}$	$-4.13 \cdot 10^{-14}$	0	$1.41 \cdot 10^{-9}$
MRWM-1	$-4.35 \cdot 10^{-14}$	$-2.93 \cdot 10^{-9}$	$-4.41 \cdot 10^{-14}$	$1.50 \cdot 10^{-18}$	$9.50 \cdot 10^{-10}$
Mobile	$-1.14 \cdot 10^{-14}$	$-2.84 \cdot 10^{-9}$	$-4.00 \cdot 10^{-14}$	0	$9.23 \cdot 10^{-10}$
Immobile	$-3.21 \cdot 10^{-14}$	$-9.23 \cdot 10^{-11}$	$-4.13 \cdot 10^{-15}$	$1.50 \cdot 10^{-18}$	$2.72 \cdot 10^{-11}$

MRWM-2	$-3.49 \cdot 10^{-14}$	$-2.91 \cdot 10^{-9}$	$-7.48 \cdot 10^{-14}$	$4.28 \cdot 10^{-19}$	$9.48 \cdot 10^{-10}$
Mobile	$-1.13 \cdot 10^{-14}$	$-2.86 \cdot 10^{-9}$	$-4.03 \cdot 10^{-14}$	0	$9.23 \cdot 10^{-10}$
Immobile q,kf	$-5.31 \cdot 10^{-15}$	0	$-3.45 \cdot 10^{-14}$	$1.76 \cdot 10^{-21}$	$1.14 \cdot 10^{-11}$
Immobile q,d	$-1.83 \cdot 10^{-14}$	$-4.80 \cdot 10^{-11}$	0	$4.26 \cdot 10^{-19}$	$1.36 \cdot 10^{-11}$

Kaolinite precipitates are transient. Some kaolinite precipitates during very early times ahead of the pH front, which is slightly delayed by dolomite dissolution, promoted by the arrival of K-feldspar dissolution products. However, this kaolinite dissolves subsequently (Figure 3. 4) upon the drop in pH. In fact, most of the time, the experiment runs under quasi-steady state conditions, with an slight increase in pH over time, as dolomite dissolution causes a small reduction in specific area and, thus, in reaction rate. As a result, only a small, but growing, amount of kaolinite remains at the last 3 mm of the sample (Figure 3. 3c), where pH stays above 4.6 throughout the simulation (Figure 3. 3a). Kaolinite precipitation is often driven by K-feldspar dissolution (Carroll et al., 2013; Fu et al., 2009; Luquot et al., 2012; Tutolo et al., 2015). However, it can also be affected by the total alkalinity of the solution leading to an oversaturation with respect to kaolinite, as shown in Figure 3. 3. The dashed green line indicates the pH necessary to precipitate kaolinite. Despite the foregoing, the volume of precipitated Kaolinite is negligible.
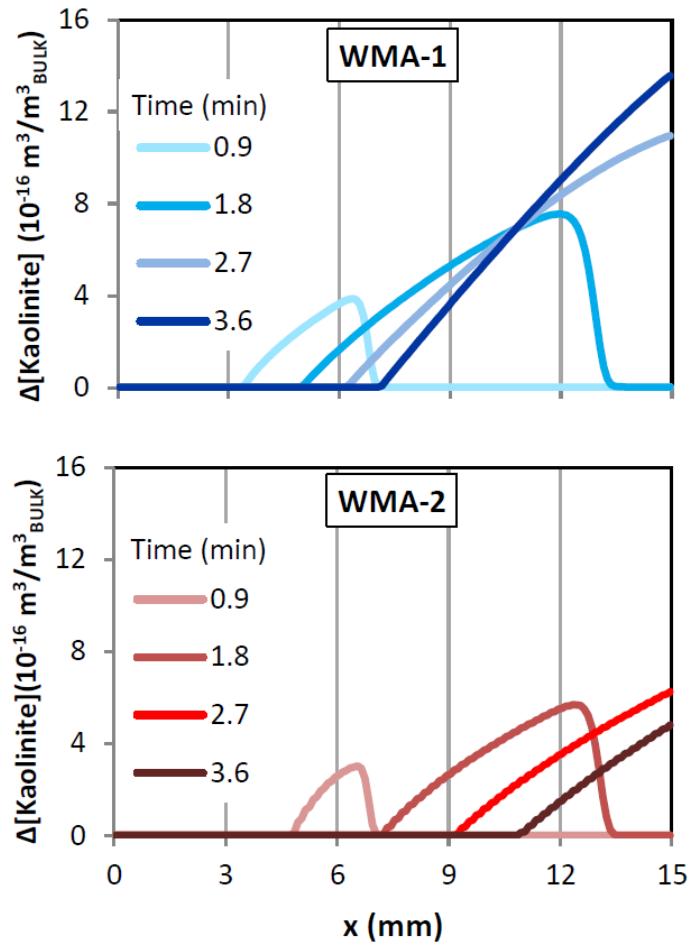
Figure 3. 4: Comparison of kaolinite concentration variation along the sample length for different early time steps for simulations WMA-1 and WMA-2. The Representative Elementary Volume (REV) bulk volume is $3.85 \cdot 10^{-9} \, m^3$

3.4.3.   WMA - 2: model with heterogeneous mineral zones

The WMA -2 model uses the same average mineralogy and transport conditions as the model WMA-1. However, the initial mineralogy is different because heterogeneity is acknowledged. Odd cells are only composed of quartz and K-feldspar. All even cells contain quartz and dolomite. Simulations were performed both with the same total mineral surfaces as in WMA-1 (i.e., multiplying by two the specific surfaces of dolomite and K-feldspar in the corresponding cells) and with the same specific mineral surfaces. Results for the first case are not shown because they are virtually identical to those of WMA-1, which implies that mineral localization along the mobile flow path

does not affect much the results, at least in this kinetics controlled case. There, in the following, we restrict the discussion to the case in which specific surfaces are identical to those of WMA-1, which can be viewed as an analysis of the sensitivity of model results to mineral surfaces.

Like the WMA-1 model, pH increases downstream as a result of dolomite dissolution (Figure 3. 3a). However, acid water penetrates deeper in the WMA-2 model and the change in the pH slope occurs at 6mm instead of 3mm. This is attributed to the slowdown in mineral distribution which implies that only half of the domain counteracts the input acidity. Dolomite and K-feldspar dissolution is slower than in the WMA-1 model (Table 3. 4) despite the fact the model contains the same amount of mineral. Mineral distribution thus plays a role in the reaction. The reaction is transport-limited since the total amount of dolomite and K-feldspar remains identical.

No precipitation of kaolinite is predicted in the total mass balance in Table 3. 4, because pH stays below 4.6 throughout the simulation (Figure 3. 3a). Nevertheless, as observed for WMA-1, kaolinite precipitates at early times ahead of the pH front (Figure 3. 4).

In the case of WMA-2 the fronts move faster with the result that no kaolinite remains after the simulated time of 5 hours. Given that gypsum precipitation depends on dolomite dissolution, its peak is found further from the inlet than in the case of WMA-1 (Figure 3. 3d). In addition, this peak is lower and more dispersed.

3.4.4. MRWM - 1: model with homogeneous mineral immobile zones

Mobile and immobile zones, and their mineralogy are homogeneously distributed in the model MRWM-1, identical to those of WMA-1 (see Figure 3. 2).

As the volume of the mobile zone is smaller than in the previous models, the pore water velocity is higher. This leads to a deeper penetration of the acid water (Figure 3. 5), similar to that of model WMA-2. Dissolution of dolomite and K-feldspar in addition to gypsum precipitation occurs mainly in the mobile zone (Table 3. 4). The pH remains relatively high in the immobile cells (around 5.3, Figure 3. 5) due to the limited exchange of acidity with the mobile zone. An autonomous equilibrium is established in

immobile zones between the protons diffusing into the immobile zone and their consumption by dolomite dissolution. This moderate pH, together with the diffusion of Al and Si create favorable conditions for kaolinite precipitation in the immobile zone (see Figure 3. 5). In summary, limiting the diffusion of acidity is sufficient to promote chemical localization and favor the precipitation of kaolinite despite the fact that flowing water is too acid to sustain kaolinite precipitates.
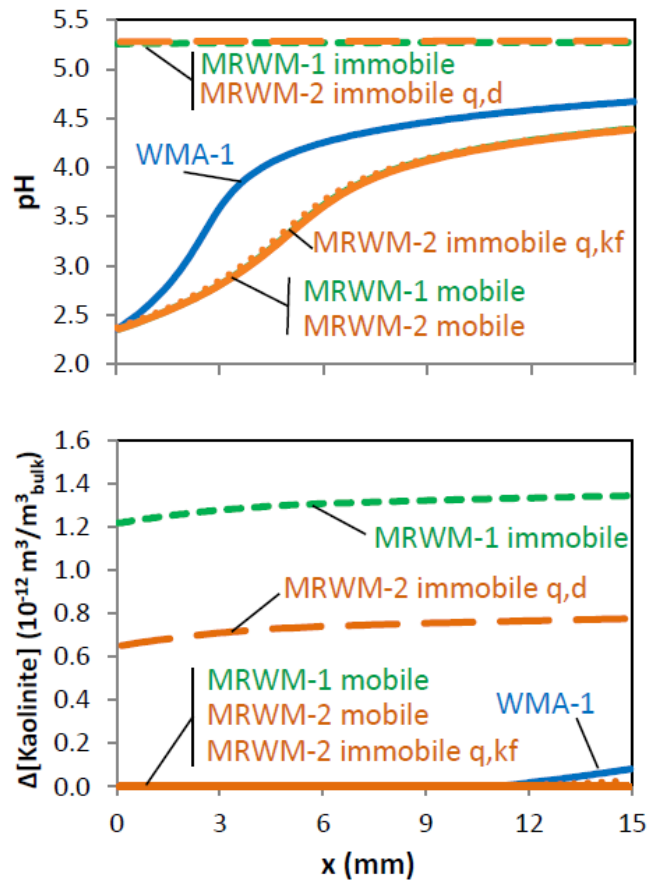
Figure 3. 5: pH and kaolinite concentration variation along the sample length at final time steps for simulations WMA-1 (blue), MRWM-1 (green) and MRWM-2 (orange). Mobile zones are represented by continuum lines. Immobile zones are depicted by dashed or dotted lines. The Representative Elementary Volume (REV) bulk volume for WMA-1 is $3.85 \cdot 10^{-9}$ m^3. The REV bulk volume for MRWM models is $7.7 \cdot 10^{-9}$ m^3 and includes one mobile node and two connected immobile nodes.

3.4.5. MRWM - 2: model with heterogeneous mineral distribution in immobile zones

Model MRWM-2 also contains mobile and immobile zones, but the mineralogy is heterogeneously distributed in the immobile zones using the same definition as in the model WMA-2. The results in the mobile zones are similar to those in MRWM-1 (Table 3. 4 and Figure 3. 5). However, because of the mineralogical heterogeneity of the immobile zones, precipitation/dissolution is also different in each immobile zone. Obviously, dolomite dissolution occurs only in the immobile *zone_q,d* (see Table 3. 3 and Figure 3. 2). K-feldspar dissolves only in *zone_q,kf*. The distribution of pH in the immobile *zone_q,d* is similar to that of MRWM-1 (Figure 3. 5) because a similar autonomous equilibrium is reached between diffusion of protons and theirs consumption by dolomite dissolution. This causes kaolinite to precipitate, albeit in a smaller amount (Table 3. 4) because K-feldspar is not present in this zone, so that Al and Si need to diffuse from the mobile zone. Ironically, in the immobile zone_*q,kf*, which contains K-feldspar, source of Al and Si for kaolinite, this mineral does not precipitate because pH is in slaved equilibrium with the mobile zone and remains low. These results are supported by the experiments of Luquot at al. (2016), who observed that kaolinite tends to precipitate preferentially around dissolved carbonate crystals.

The above discussion supports the conjecture that motivated this work. Geochemical localization (i.e., the occurrence of reactions that would not occur in well mixed media) requires both mineralogical localization and transport limitation. In our case, it controls whether, where, and how much kaolinite precipitates (Table 3. 4). Kaolinite precipitation occurs mainly in immobile zones where dolomite is dissolved and pH remains moderately high. We call the precipitation of Kaolinite slaved, because it results from the diffusion of reactants that were produced elsewhere and occurs solely because local conditions are favorable. As a result, it will come closer to equilibrium and, we conjecture, produce more crystalline precipitates than "autonomous" reactions.

The case of gypsum allows us to illustrate further the concept of autonomous and slaved reactions. Gypsum precipitates both in immobile *zone_q,d* and *zone_q,kf*. The difference between these two immobile zones is observed only on the inflow side of the

domain (Figure 3. 6). Less gypsum is obtained in *zone_q,kf* (Table 3. 4) because it results from Ca and SO$_4$ diffusing from the mobile zone. Therefore, gypsum precipitation in *zone_q,kf* can be regarded as a chemically "slaved" process, whereas gypsum precipitation *zone_q,d* should be regarded as "autonomous" since the amount of precipitated mineral is controlled by the local dissolution of dolomite.
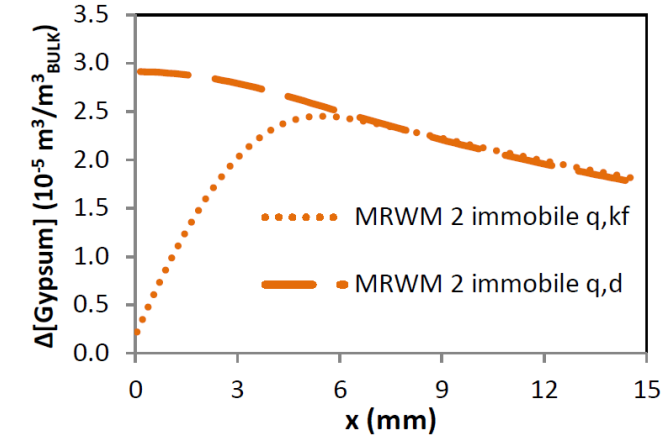
Figure 3. 6: Comparison of gypsum concentration variations along the sample length at final time steps in immobile *zones_q,kf* (pointed) and *zones_q,d* (dashed) for simulations MRWM-2. The Representative Elementary Volume (REV) bulk is $7.7 \cdot 10^{-9}$ m^3 and includes 1 mobile node and two connected immobile nodes.

3.4.6.   Sensitivity to immobile zone parameters

The immobile volume and exchange mass coefficients of models MRWM-1 and MRWM-2 have been chosen somewhat arbitrarily. The discussion of results of these two models makes it clear that the impact of multi-rate model parameters on the reactions is non-trivial, as it is controlled by several simultaneous processes. On the one hand, kinetically limited reactions are controlled by residence time ($\phi_{im,j}/\alpha_j$), but also by the flux of reactants, which is proportional to α_j, and whether their concentrations are the result of an autonomous or a slaved process.

The rate of slaved reactions can be easily derived from Eq. (3. 2) by assuming that the slaved reaction is governed by first order kinetics (i.e., $f_{chem,j} = \mu \cdot u_{aim,j}$, where $u_{aim,j}$ is the concentration of the species or component controlling the reaction rate).

This yields $r = \mu\alpha_j/(\alpha_j + \mu) \cdot u_{am}$, assuming that the reaction of the controlling species or component in the mobile domain, u_{am}, is (quasi) stationary. This implies that [1] the reaction rate is independent of the fraction of immobile region ($\phi_{im,j}$) or residence time, but [2] it will depends equally on both the local reaction rate constant and the exchange rate. The reaction grows with both α_j and μ and is controlled by the smallest of them. That is, the reaction rate is small when either of them is small and large when both are large.

The situation is more complex in the case of autonomous reactions. Figure 3. 7 illustrates the effect of reducing the mixing fraction between mobile and immobile zones (λ_{ij}), which is equivalent to reducing α_j. On the one hand, kaolinite precipitation increases because of the resulting high pH, even though a smaller amount of K-feldspar is dissolved. This reflects that the supply of Si and Al due to K-feldspar dissolution is sufficient to feed kaolinite precipitation, which was limited by pH. On the other hand, gypsum precipitation is reduced, which reflects a reduced supply of Ca and/or SO_4, both limited by the reduced exchange rate.
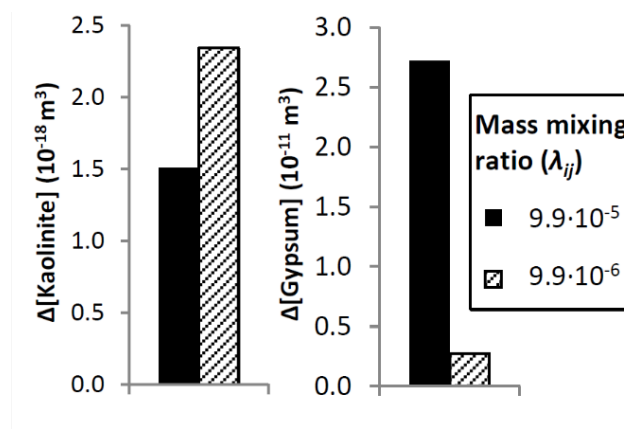
Figure 3. 7: Comparison of total volume variation of gypsum and kaolinite in immobile zones at final time steps for simulation MRWM-1 applied to different water mass ratio exchanged between mobile and immobile zones.

3.5.   Discussion and conclusions

We developed a multi-continuum formulation model (MRWM), which was applied to simulate geochemical localization. This model aims at reproducing the effect of pore scale heterogeneity by creating localized micro environments favoring reactions that

would not occur in the traditional ADE reactive transport models where local homogenization and full mixing are assumed. To this end, we used the MRMT approach with diverse mineral compositions for different cells. Transport was calculated by the WMA of chapter 7, which was extended to account for immobile zones and chemical localization.

We applied this method to four models inspired by dissolved CO_2 flow-through experiments performed on sandstone samples from Heletz (Luquot et al., 2016). Model results confirm the original conjecture that coupling chemical and hydrodynamic heterogeneities exerts a significant influence on reactive transport processes. Specifically, including immobile zones containing dolomite allows us to simulate kaolinite precipitation, which would not occur if concentrations were homogenized. These results indicate that kaolinite precipitation is pH controlled and precipitated only close to carbonate dissolution or at least a pH buffer as observed by Luquot et al. (2016). In summary, localization and how it is represented in the model controls whether, where, and how much kaolinite precipitates.

The MRWM model requires three additional parameters for each immobile domain: porosity, exchange rate and mineralogy. We found that the spatial distribution of dissolution and precipitation processes is sensitive to all of them. As a result, the behaviour of the model is complex and hard to anticipate. In an attempt to facilitate the explanation of model results and parametrization, we distinguish between "slaved" and "autonomous" reactions. Autonomous reactions occur between reactants produced locally. For example, gypsum precipitation in a dolomite zone is an autonomous reaction because it is driven by dolomite dissolution in this zone. Actual rates are the result of interactions between the two kinetic laws (e.g., dolomite dissolution and gypsum precipitation) with the mobile-immobile exchange rate and the immobile porosity. As a result, these reaction rates are hard to predict. Slaved reactions occur between reactants produced elsewhere that diffuse into (away from) the precipitation (dissolution) site, where conditions are favourable. An example of these is the precipitation of kaolinite in a dolomite immobile domain controlled by the local high pH even though SiO_2 and Al result from dissolution of K-feldspar in other zones. The behaviour of these reactions appears to be more predictable than that of autonomous reactions because the reaction rate is controlled monotonically by both the exchange and the local kinetics rates. However, things may be more complex than they look, because

local conditions for slaved reactants may be controlled by autonomous reactions. For example, kaolinite precipitation is controlled by pH, which is the result of an autonomous reaction (dolomite dissolution).

It may therefore be concluded that, although the MRWM model is very powerful in reproducing the effect of pore scale chemical processes in Darcy scale models, reliable parameterization is difficult and further research is warranted before application.

Chapter 4

Modeling mixing in high heterogeneous media: the role of water discretization in phase space formulation

4.1. Introduction

Solute transport in homogeneous media is well reproduced by the advection-dispersion equation (ADE). However, this is not the case in real aquifers because of the heterogeneity of the soil (Le Borgne et al. 2008; Gjetvaj et al. 2015; Willmann et al. 2008), which leads to a commonly observed non-equilibrium (Alcolea et al., 2008; Vogel et al., 2006). Observed transports is termed anomalous (i.e., non-Fickian anomalous transport is evidenced by tailing in concentration breakthrough curves (Valocchi 1985; Carrera 1993). But beyond failing, accurate representation of anomalous transport is critical when chemical reactions take place (Battiato et al. 2009; Sadhukhan et al. 2014; Scheibe et al. 2015; Soler-Sagarra et al. 2016; Tartakovsky et al.

2009). For instance, the classic ADE is no longer valid in heterogeneous media because it does not distinguish between dispersion (solute spreading) and mixing (diffusion of the solute). ADE employs Fick's law (Fick, 1855) to characterize both processes by using concentration gradients. As an alternative, the Water Mixing Approach (WMA) has been proposed in chapter 2, which uses water exchange instead. In contrast to dispersion, mixing is a direct cause of chemical reactions in fluids (Cirpka and Valocchi 2007; Rezaei et al. 2005; De Simoni et al. 2005, 2007; Tartakovsky et al. 2008). A new formulation is therefore needed. The new equation for anomalous transport must reproduce advection, dispersion and mixing (de Dreuzy et al. 2012; De Dreuzy et al. 2016).

A large number of Particle based methods have been proposed as alternatives to ADE (Benson et al. 2009; Bijeljic et al. 2006; Le Borgne et al. 2008a; Delay et al. 2005; Fernàndez-Garcia et al. 2011; Lester et al. 2014; Painter et al. 2005 and Russian et al. 2016). Particle, methods have shown that velocity transitions can be viewed as a correlated random process. This process is markovian when transitions are made not after a fixed time step, but after particles have (reverse) covered a fixed spatial distance (Le Borgne et al. 2008b). The fact that velocities may change after a fixed spatial step is consistent with a fixed heterogeneity structure. We conjecture that this is a good basis for alternative transport formulations. Although all the discussions above are relevant. They have yielded a new view on transport. Yet, none of them considers mixing.

The difficulty in representing mixing lies in its close relationship with spreading. Velocity variation produce stretching of lamelas, which enhances mixing by increasing the contact area between different waters. The fact that velocity variations occur at all scales and that they control mixing suggest using velocity as a new dimension of the state variable (like time and space), which leads to a phase space formulation. The success of Markovian formulation further suggests representing velocity variability as a Markov process. Markovian processes are typically represented by means of a Transition Matrix M^{vs}, which here expresses the probability of a particle to change the velocity state v given constant steps in space phase s (De Anna et al., 2013; P. K. Kang et al., 2011, 2014, 2017; P. K. Kang, Borgne, et al., 2015). Transitions may occur either because of heterogeneity along a flow line, which does not produce mixing, or because of water particles diffusion across flow tubes, which is the mixing mechanism

associated to plume stretching. A proper representation of mixing should distinguish these two types of transitions.

In this chapter, we propose a phase space formulation for transport that acknowledges velocity transitions both by heterogeneity along the flowlines and by diffusion. The formulation based on the WMA. We present a numerical method based on the equation and tested with Taylor's laminar flow case.

4.2. Governing equations

Kang et al. (2017) proposed a phase space formulation for heterogeneous domains to find an alternative to ADE. Phase space formulations express state variables not only as dependent on time and space, but also on velocity. The formulation was originally presented for pore-scale models using particle probability p. However, it can be easily extended to Darcy scale. We express it in terms of concentrations, $c=c(x,v,t)$ $[M/L^3]$ by using basic definitions to write $p = c\phi/M$, where ϕ $[-]$ is porosity and M is the total solute mass. With these definitions, Kang et al. (2017) can be rewritten as

$$\phi\frac{\partial c}{\partial t} = -\phi v \cdot \nabla c - \phi\frac{v}{\bar{l}}c + \int_{v'} \phi g^{vs}(v|v')\frac{v}{\bar{l}}c'dv' + r \qquad (4.1)$$

where t $[T]$ is time, v $[L/T]$ is velocity, $\bar{l}[L]$ is the characteristic length, g^{vs} $[T/L]$ is the transition probability density of jumping from v' to v after a $\bar{l}$ space step, $c'=c(x,v',t)$ and r $[M/L^3/T]$ is the sink/source term. Thus, the formulation implies a non-unique concentration value at fixed time and space. Eq. (4. 1) expresses dispersion naturally by acknowledging velocity variability. The second and third terms of the right-hand side (RHS) define the solute transition to velocity states, but they do not distinguish between diffusion transitions (purple arrow in Figure 4. 1) and advection transitions (green arrow in Figure 4. 1). This is inappropriate since it does not allow treating mixing and dispersion as separate processes. To overcome this limitation, we propose to (a) restrict transitions caused by heterogeneity to advection transitions (i.e., changes in velocity

along streamlines, like defined by green arrow in Figure 4. 1), and (b) simulate diffusion separately.

We use the WMA formulation proposed in chapter 2 to define the mixing process. Originally, the WMA expresses ADE as a mixing of different waters, rather than solutes, which is convenient for reactive transport. The WMA is formulated as follows

$$\phi \frac{\partial c}{\partial t} = -\phi v \cdot \nabla c - \nabla \cdot (\overline{q_D c}) + r \qquad (4.\,2)$$

where the term $\overline{q_D c}$ represent solute exchange driven by water dispersion and mixing. That is q_D $[L^3/L^2/T]$ represents water flux exchange with respect to the mean water flux, which is accounted for in the advection term. Here, we propose to restrict this concept to molecular diffusion. This may sound confusing since diffusion is commonly associated to solute, rather than water. In reality, water is exchanged by diffusion at a rate comparable to that of solutes (Harris and Woolf, 1980). Furthermore, without entering into this debate, the formulation of Eq. (4. 2) is equivalent to Fickian diffusion, which employs concentration gradient, if $q_D = \phi D_w/L_D$, where $D_w [L^2/T]$ and L_D $[L]$ are water molecular diffusion coefficient and the characteristic diffusion scale, respectively.

The new formulation is obtained by restricting Eq. (4. 1) to advective transitions and Eq. (4. 2) as to diffusion term

$$\phi \frac{\partial c}{\partial t} = -\phi v \cdot \nabla c - \phi \frac{v}{\overline{l}} c + \int_{v'} \phi g^{vs}(v|v') \frac{v}{\overline{l}} c' dv' + \nabla \cdot (\overline{q_D c}) + r \qquad (4.\,3)$$

Eq. (4. 3) is not a complete formulation yet. Velocity transitions occur due to advection and diffusion (Figure 4. 1). Since we are still restricting g^{vs} to characterize velocity transitions along streamlines, we need a new transition term for velocity changes driven by diffusion (purple arrow in Figure 4. 1). Advection changes characterized by g^{vs} are Markovian in space (Le Borgne et al. 2008b), but diffusion driven exchanges should be Markovian in time. The two transitions must be described independently. Diffusion transitions require adding two terms to (4. 3), which yields

$$\phi \frac{\partial c}{\partial t} = -\phi v \cdot \nabla c - \phi \frac{v}{\bar{l}} c + \int_{v'} \phi g^{vs}(v|v') \frac{v}{\bar{l}} c dv' + \nabla \cdot (\overline{q_D c})$$

(4. 4)

$$+ \int_{v'} \phi f^{vt}(v|v') c' dv' - \int_{v'} \phi f^{vt}(v'|v) c dv' + r$$

where $f^{vt}(v|v')$ *[T/L/T]* is the probability density of exchange between velocity states *v* per unit time. The fourth term on the RHS define the diffusion process in space domain (orange arrow in Figure 4. 1), while the fifth and sixth expresses the diffusive mass balance in velocity domain (purple arrow in Figure 4. 1). Assuming that f^{vt} is solute independent, this equation is consistent with the WMA: define the diffusion of water instead of solute. This is why we termed the formulation Multi-Advective Water Mixing Approach (MAWMA). Note that we consider the requirements highlighted by De Dreuzy and Carrera (2016): adequate separation of advection, diffusion and dispersion.
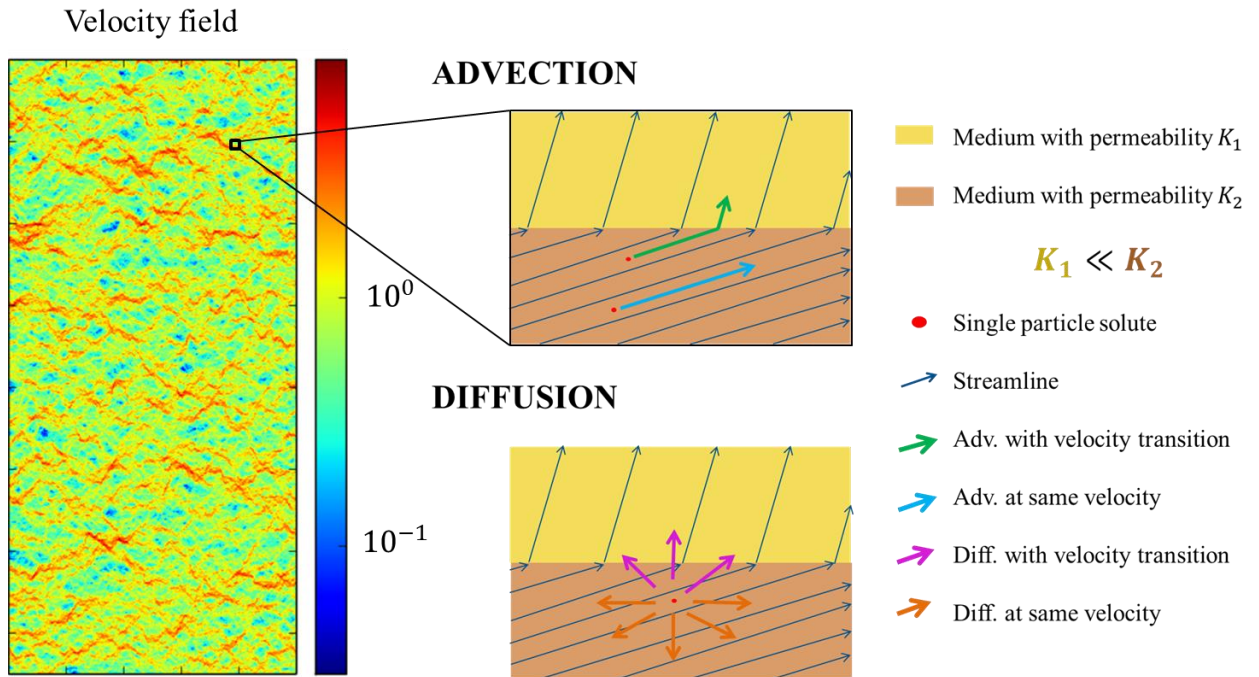
Figure 4. 1: Scheme of particle transport processes through continuum heterogeneous domain. The left image is a computed velocity field. The right-top image displays the advection path of two particles. The right-bottom image shows the diffusion possibilities of a single particle.

4.3. MAWMA formulation applied to WP method

Assessing the validity of the MAWMA, Eq. (4. 4), could be arduous. Given that the novel processes presented are the fifth and sixth terms on the RHS, we make three simplifications:

a) A stratified parallel flow may be considered. This implies that no velocity transition occurs due to advection, which leads to neglecting the second and third terms on the RHS of the Eq. (4. 4). We further assume that all strata carry the same flow rate (i.e., high velocity strata are narrower than low velocity strata) to simplify space and velocity discretization (Figure 4. 2b)

b) Diffusion is only considered transversal to the main flow direction. Adding this to the stratified flow leads to velocity changes because of diffusion (Bolster et al., 2011; Dentz and Carrera, 2007; Taylor, 1953). The fourth term of the RHS may therefore be ignored. Transverse mixing has been proven to be of paramount importance when chemical reactions are involved (Werth, et al. 2006)

c) A Lagrangian formulation is adopted for advection by using material derivative $d \cdot /dt$ since it provides a better definition of mixing (Batlle et al. 2002; Bell and Binning 2004; Cirpka et al. 1999; Ramasomanana et al. 2012; Zhang et al. 2007).

These three simplifications allow us to rewrite Eq. (4. 4) as

$$\phi \frac{dc}{dt} = \int_{v'} \phi f^{vt}(v|v')c'dv' - \int_{v'} \phi f^{vt}(v'|v)cdv' + r \qquad (4. 5)$$

Time, space and velocity should be discretized and integrated in Eq. (4. 5). We now describe the Water Parcel (WP) method used to solve this equation. Other methods might also be used.

The spatial domain is discretized in parcels (see Figure 4. 2c) with the same water volume as the isochronal structured water (IW) method using the WMA formulation (see Figure 4. 2b). This discretization covers the domain, in the sense that water parcels represent actual water and the sum of their volumes should be equal to the total water within the spatial domain. The concentration is only considered an attribute of each parcial and is homogeneous within each parcel. The later implies that the shape function used for space integration associated to the parcel is equal to 1 if (x,v) belong in the parcel domain, and 0 otherwise. Each water parcel is associated to a centroid that determines its position in both x axis and velocity state. Therefore the shape function associated is also mobile. Centroids are injected and displaced through the domain like a single solute particle.
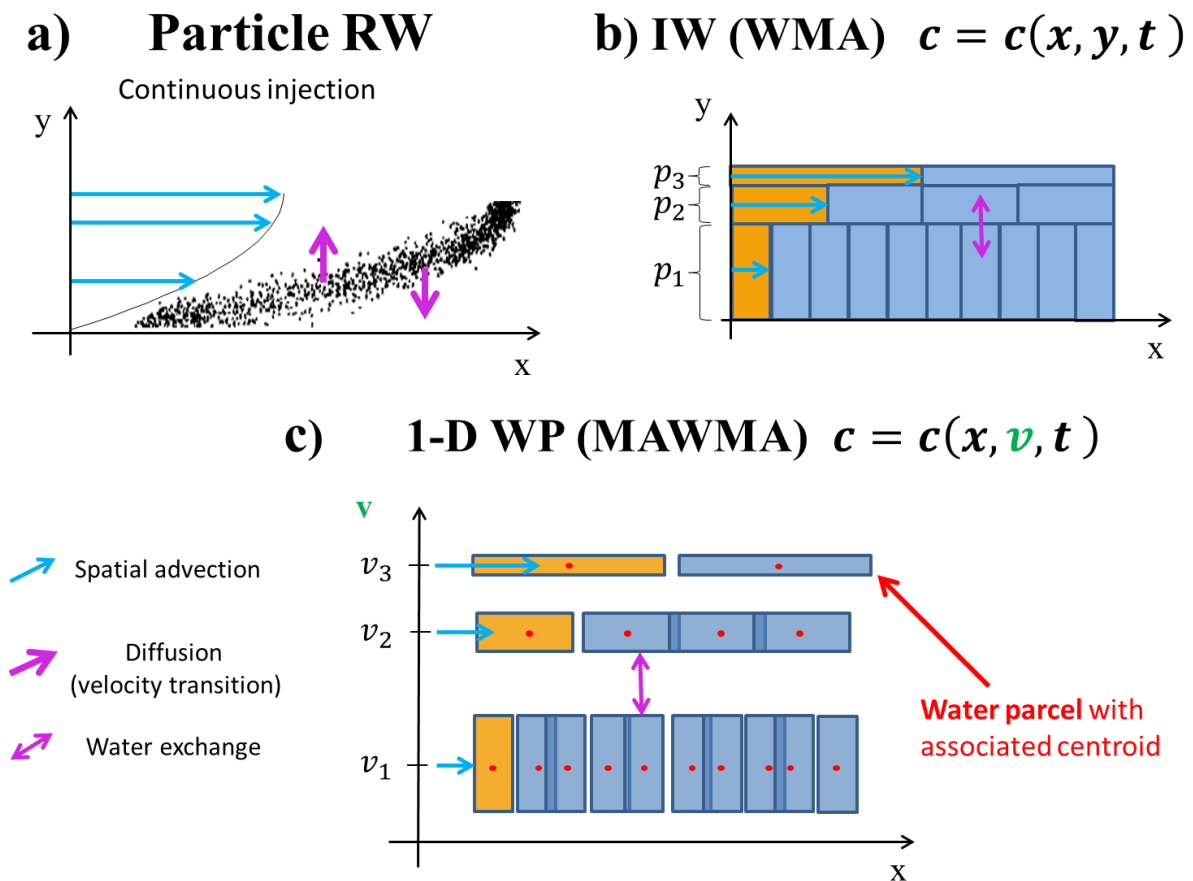
Figure 4. 2: Scheme of heterogeneous stratified models using three velocity classes: (a) Random Walk Particle (b) Isochronal Water method using Water Mixing Approach formulation and (c) Water Parcels method using Multi-Advective Water Mixing Approach formulation

The velocity state of each parcel is assigned randomly after injection, which is conditioned and leads to an unstructured mesh unlike IW (see Figure 4. 2b and 4. 2c). We integrate along the *y* coordinate for simplicity and for demonstration purposes. That is, we perform a dimension reduction, so that concentration in Eq. (4. 5) depends solely on *x* and *v*. As shown in Figure 4. 2, this simplification might look trivial as it suggests that we are substituting the *y* coordinate by *v*. Note, however, that we assume that we do not know the vertical structure of velocity, but only its velocity distribution and transition probabilities. Figure 4. 2c shows parcel shape dependence on velocity state. As suggested by the tub-lines (see Figure 4. 2b), the longitudinal axis of our water parcels is proportional to their velocities, while their width is inversely proportional (see Figure 4. 2c). Another explanation is that the distance travelled *Δx* is proportional to the velocity *v* at the same time step *Δt*. As a consequence, the water parcels with low velocity tend to cram longitudinally (i.e., number of low velocity water parcels per unit length is inverse proportional to velocity). This ensures an adequate representation of the entire distribution of velocities.

Velocity may be discretized adopting Eulerian or Lagrangian distribution. The Eulerian distribution yields the probability density function (pdf) of velocity sampled randomly in space. Discretizing Eulerian pdf determines the velocity classes with the same volume in the domain at a given moment. The Lagrangian distribution yields the distribution of fluxes (i.e., the pdf of velocity along a streamline sampled at equal spatial intervals). The Lagrangian pdf equals the Eulerian pdf weighted by the velocity (Dentz et al. 2016). Discretizing Lagrangian pdf determines velocities with the same flux (i.e., same injection probability, see Figure 4. 2c). Therefore, we use the Lagrangian distribution to discretize the velocity dimension in equally probable flux intervals.

The simulation proceeds by integrating Eq. (4. 5) by time steps. The question therefore is how to reproduce mixing between the parcels (i.e., the first two terms in the RHS). We use the finite volume method. The discretized form of (4. 5) for every parcel i in velocity class l is

$$V_{w_i} \frac{c_i^{k+1} - c_i^k}{\Delta t} = \sum_{m \neq l}^{N_v} \sum_{j}^{N_{mi}} a_{ij} F_{lm}^{vt} c_j^k - \sum_{m \neq l}^{N_v} \sum_{j}^{N_{mi}} a_{ji} F_{ml}^{vt} c_i^k , \qquad i \in I_l \qquad (4.\ 6)$$

where V_w $[L^3]$ is the volume water in parcel, $\Delta t[T]$ is the time step, N_v is the number of discretized velocity classes, N_{mi} is the number of parcels of velocity class m connected with parcel i. F_{lm}^{vt} is the volume of water exchanged between velocity classes l and m per unit time. k is time steps number and I_l is the domain associated to the velocity class l. Finally, a_{ij} is the fraction of this flux that will be exchanged between parcels i and j. per unit time a_{ij} could be either equi-distributed or weighted contact-area. Here, a weighted contact-area is assumed. As in WMA, this is an exchange process, which implies that $F_{lm}^{vt} = F_{ml}^{vt}$ and $a_{ij}=a_{ji}$. The expression of a concentration in time step $k+1$ can be obtained.

$$c_i^{k+1} = c_i^k - \Delta t \sum_{\substack{m \neq l}}^{N_v} \sum_{j}^{N_{mi}} a_{ij} F_{lm}^{vt} c_i^k + \Delta t \sum_{\substack{m \neq l}}^{N_v} \sum_{j}^{N_{mi}} a_{ji} F_{ml}^{vt} c_j^k, \qquad i \in I_l \qquad (4.7)$$

Some new terms may now be defined: (a) $\lambda_{lm} = \Delta t \cdot F_{lm}^{vt} / V_{w_l}$ is the water mass mixing ratio (chapter 7) but applied to exchanges of velocity class. λ_{lm} is term at the lm-th position of the water transition matrix $\boldsymbol{M^{vt}}$. Note that the matrix is Markovian in time applied to velocity phase. This matrix differs from the classic transition matrix $\boldsymbol{M^{vs}}$ (De Anna et al., 2013; P. K. Kang et al., 2011, 2014, 2017; P. K. Kang, Borgne, et al., 2015; Le Borgne et al., 2008a) because Markovianity is applied in time t instead of space s. $\boldsymbol{M^{vt}}$ is obtained like $\boldsymbol{M^{vs}}$, but accounting only diffusive transitions during a fixed Δt; (b) the self-water mixing ratio of the l velocity must satisfy $\lambda_{ll} = 1 - \sum_{\substack{m \neq l}}^{N_v} \lambda_{lm}$ with the result that $\sum_{m}^{Nv} \lambda_{lm} = 1$. If the velocity discretization is Eulerian (equi-probable classes), this matrix must also satisfy $\sum_{l}^{Nv} \lambda_{lm} = 1$; (c) the water mixing ratio between ith and jth parcels may be defined as $\lambda_{ij} = a_{ij}\lambda_{lm}$

$$c_i^{k+1} = \lambda_{ii} c_i^k + \sum_{\substack{m \neq l}}^{N_v} \sum_{j}^{N_{mi}} \lambda_{ij} c_j^k \qquad (4.8)$$

The use of λ implies that mixing does not depend on the concentration gradient, as in WMA. As a result, concentration is just an attribute (such as temperature), which is transferred with the water fraction. Note that the mixing of parcels depends on their velocity class. However, the unstructured mesh does not ensure mass conservation in

the mixing process such as $\lambda_{ij} = \lambda_{ji}$, which diminishes exchanges of water volume. This is why a post-process by defining $\lambda_{ij} = \lambda_{ji} = max\{\lambda_{ij}, \lambda_{ji}\}$ is necessary.

Although chemical reactions are not the main objective of this work, they are the ultimate goal of our research. By using the water mass mixing ratio formulation, the link with chemical processes is immediate (chapter 7).

4.4.   Applications

To compute mixing and dispersion of equation (4. 5), a stratified case is needed (Taylor, 1953). We considered the velocity distribution v in parallel planes

$$v = (3/2)v_{mean}(1 - (1 - y/a)^2) \tag{4. 9}$$

where v_{mean} is the mean velocity of the distribution, y is the vertical position and a is the half distance between the planes. Owing to the horizontal symmetry of the case, we only modeled the half domain y = {0,a} (Figure 4. 2). We focused on the time evolution, especially at times earlier than the dispersion time scale τ_D, which denotes the typical time for the macrodispersive spreading of the solute.

$$\tau_D = \frac{a^2}{D_w} \tag{4. 10}$$

We opted for Lagrangian velocity discretization since low velocities are more probable than high velocities (Gotovac et al. 2009), which contrasts sharply with Eulerian equi-probable discretization. Moreover, we considered a continuum injection of solute instead of an instantaneous injection used by other authors (Bolster et al., 2011; Dentz and Carrera, 2007).

The WP model was compared with IW and Particle Random Walk (RW) models (Figure 4. 2). Note that the concentration associated with parcels (WP and IW) is analogous to particle solute. The WP was simulated using the KRATOS framework

62

(Dadvand et al. 2010). As regards the particle random walk model, a flux weight injection was used at every time step. The RW simulations were performed as proposed by Dentz and Carrera (2007). The concentration was obtained by projecting the particles in the IW mesh cells. The simulation details are shown in Table 4. 1.

Table 4. 1: Transport problem parameters and simulation details

Transport Problem					
v_{mean}	1 m/s	D_w	0.5 m^2/s	$c_{initial}$	0 mol/(m$_{water}$)^3
a	1 m	ϕ	0.5	$c_{injection}$	1 mol/(m$_{water}$)^3
Simulation					
		Δt	4·10^{-3} s		
WP		IW		RW	
N_v	30	N_v	10	$c_{unitari}$	$\dfrac{10^3 \text{ particles}}{2 \cdot 10^{-4} \text{ (m}_{water})^3}$
V_w parcel	3.3·10^{-5} (m$_{water}$)^3	V_w parcel	2·10^{-4} (m$_{water}$)^3		

4.4.1. Statistical parameters

Both, mixing and spreading must be tested. Mixing was calibrated by the Dissipation Rate (Pope, 2000). The classic scalar dissipation rate uses the local concentration gradient. However, a simpler and more robust and stable quantification has been proposed by Le Borgne et al. (2010). We extend in here (Appendix B) the one continuous injection

$$\chi(t) = \int_\Gamma c\phi v\left(c_{inj} - {c}/{2}\right)d\Gamma - \frac{1}{2}\int_\Omega \phi \frac{\partial(c^2)}{\partial t}d\Omega \qquad (4.11)$$

where Ω is the simulation domain, Γ is its boundary and c_{inj} is the injection concentration. The results of the three models are plotted in Figure 4. 3a. Only a slight mismatch is observed at the earliest times. The oscillations of the particle model may be attributed to the fact that concentrations are calculated from the particle positions (Figure 4. 1a) in the IW mesh (Figure 4. 1b). The WP model presents lower values at the earliest times, indicating more mixing. This is due to the max post-process described

above. Despite these lower values, the same overall behavior is displayed by all the models.
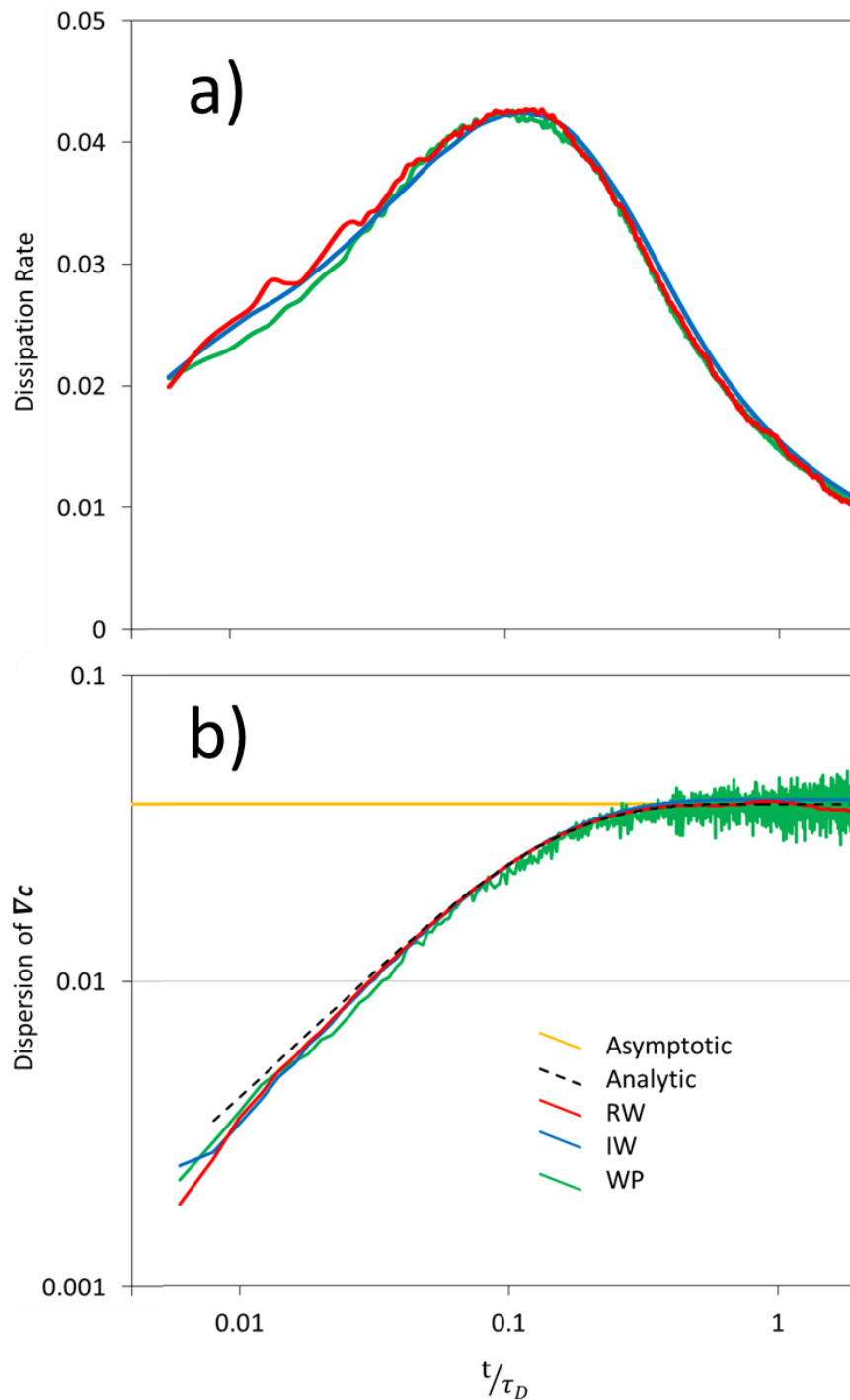
Figure 4. 3: (a) Scalar Dissipation rate and (b) apparent Dispersion of concentration gradient for continuum injection. Dashed black line and yellow line display the analytical solution of the apparent dispersion (Haber and Mauris, 1988) and the asymptotic dispersion (Aris, 1956), respectively

In instantaneous injection, the scalar dissipation rate typically displays a diminishing monotonous behavior (Bolster et al., 2011; Le Borgne et al., 2010b). However, an initial increase is observed in continuum injection, resulting in a bell shape which peaks at $0.1\tau_D$. This is due to the combination of only transverse diffusion and vertical interface. Thus, two regimes were distinguished. The earlier regime displays an increasing scalar dissipation rate, which suggests that mixing is enhanced because the contact area is increased in the longitudinal direction. This stretching phenomenon has already been observed in instantaneous injection (Le Borgne et al. 2013, 2014 and 2015). However, it is the continuous injection what causes the dissipation rate to increase in the later regime, dissipation rate decreases. Mixing diminishes because concentration contrast becomes smoother and a relaxed state is achieved.

As for dispersion, this would have a linear behavior if computed in the standard way, (which is termed apparent dispersion by Dentz and Carrera 2007) because of the continuous injection employed. Thus, the classic definition of dispersion is no longer valid in this case. However, an equivalent definition is obtained from the concentration gradient distribution instead of the concentration distribution. We integrate vertically the concentration to obtain its correlation with the x coordinate. The concentration gradient of this distribution is computed to obtain its (apparent) dispersion D_{acg}

$$D_{acg}(t) = \frac{1}{2}\frac{\partial(\sigma_{\nabla c}{}^2)}{\partial t} \tag{4.12}$$

where $\sigma_{\nabla c}{}^2$ is the variance of the concentration gradient. The definition of D_{acg} helps us to study the interface evolution. The analytical solution of the temporal dispersion evolution D^a (Haber and Mauris, 1988) and its asymptotic value D_{asy} (Aris, 1956) are also computed.

$$D_{asy} = \frac{4}{210}\frac{a^2v^2}{D_w} \tag{4.13}$$

$$D^a(t) = \frac{2}{105}v^2\tau_D - 18v^2\tau_D \sum_{n=1}^{\infty}(n\pi)^{-6} \times \exp\left(-(n\pi)^2\frac{t}{\tau_D}\right) \tag{4.14}$$

The results are plotted in Figure 4. 3b. Although the WP dispersion oscillates (owing to the unstructured character of the mesh) a satisfactory agreement is again observed. As in the dissipation rate, at least two different regimes of the solute distribution may be distinguished: (a) a linear increase in the variance is observed. This confirms the stretching phenomenon described above; (b) an asymptotic state is attained. The transition regime roughly coincides with the scalar dissipation rate, suggesting a link between both behaviors. Indeed, spreading enhances mixing in the earlier regime. In the later regime, solute plume extension is limited since sufficient mixing occurs.

4.4.2. Markovianity in space

Although solute only changes its velocity class because of the mixing process (which is Markovian in time), we can calculate the Transition Matrix in space $\boldsymbol{M}^{vs}$ (Le Borgne et al. 2008b) from the particle model. We believe that they are also Markovian in space, which is consistent with (Le Borgne et al., 2008a). We tested the Markovianity by comparing the transition probabilities with the ones obtained from a Markov chain model. The transition model must satisfy the Chapman-Kolmogorov equation (Risken, 1996), which reads for the transition matrices $\boldsymbol{M}(x)$ of a discrete Markov chain such as

$$\boldsymbol{M}(x + \Delta x) = \boldsymbol{M}(x)\boldsymbol{M}(\Delta x) \tag{4.15}$$

with $x, \Delta x > 0$. The latter implies

$$\boldsymbol{M}(nx) = \boldsymbol{M}^n(x) \tag{4.16}$$

Although the agreement is not exact (Figure 4. 4), the particles satisfactorily reproduce the Markov chain results. We can therefore conclude that mixing is Markovianity not only in time, but also in space.
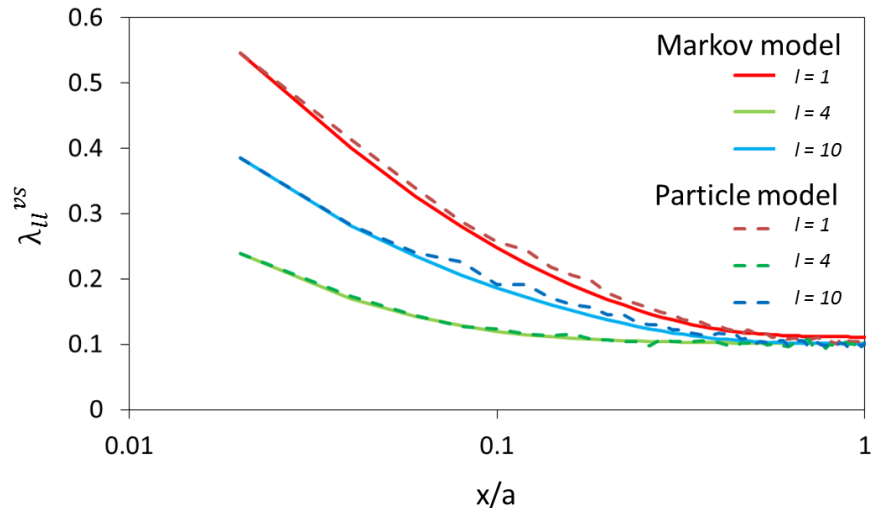
Figure 4. 4: Comparison of Particle Random Walk model and Markov model in distance for the return probability. The Markov model is defined for spatial increment of x = 0.02

4.5.   Conclusions

We present a new formulation for solute transport in heterogeneous cases, termed MAWMA. The formulation aims to reproduce diffusion and dispersion that could occur at pore scale applied to both continuum and Darcy scale. The formulation is an extension of WMA by making the transport state dependent on velocity as well as on time and space.

Water parcel models were employed to solve numerically the proposed equation. A centroid point was associated with each parcel, which defines its velocity and position at a given time. We tested the velocity transition produced by the mixing process

applying a water transition matrix in time $\boldsymbol{M}^{vt}$. This differs from the solute transition matrix in space $\boldsymbol{M}^{vs}$ used in the correlated CTRW model.

Taylor's stratified flow case was employed. MAWMA based method was compared with WMA based method and Random Walk particle models. A good agreement for diffusion and dispersion was observed. The results suggest that MAWMA will perform well for high heterogeneity cases.

Chapter 5

Testing Multi-Advective Water Mixing Approach in high heterogeneous media

5.1. Introduction

Although the Advection-dispersion equation (ADE) is the most widely used formulation to model solute transport through porous media, it does not adequately characterize transport in heterogeneous media (Le Borgne et al. 2008; Gjetvaj et al. 2015 and Willmann et al. 2008) where dispersion grows with scale (L.W. Gelhar et al., 1985; Neuman, 1990), non-equilibrium occurs (Alcolea et al., 2008 and Vogel et al., 2006), or breakthrough curves display tailing (Valocchi 1985; Carrera 1993). These features are not well represented by the ADE. Therefore, transport through heterogeneous media is called anomalous (i.e. non-Fickian transport). The problem becomes critical when chemical reactions are involved (Battiato et al. 2009; Sadhukhan et al. 2014; Scheibe et al. 2015; Soler-Sagarra et al. 2016 and Tartakovsky et al. 2009). Anomalous transport can be observed at different scales: from pore (Bijeljic et al. 2011; Kang et al. 2014; Seymour et al. 2004), column (Hatano et al. 1998; Heidari et al. 2014)

to field scale (Becker et al. 2000; Garabedian and LeBlanc 1991; Kang, Borgne, et al. 2015; Mckenna et al. 2001; Zech et al. 2015). Therefore, an alternative formulation for anomalous transport that takes advection, dispersion and mixing into consideration is therefore warranted (de Dreuzy et al. 2012; De Dreuzy et al. 2016).

Thus, below a certain scale, it is necessary to address the absence of structure definition. At this point, the velocity development shows Markovianity in space rather than time (Berkowitz et al. 2006; Klafter and Silbey 1980; Metzler and Klafter 2000; Montroll and Weiss 1965; Neuman and Tartakovsky 2009; Scher and Lax 1973; Scher and Montroll 1975). A number of alternatives to the ADE have been proposed to address anomalous transport. The most widely extended is the Continuous Time Random Walk, CTRW. It consists in random velocity transitions once the solute has travelled a certain space step. However, these transitions are not fully random processes, but correlated ones (Le Borgne et al. 2008a). Thus, a Transition Matrix M^{vs} is needed (De Anna et al. 2013; Benke and Painter 2003; Kang et al. 2011, 2014, 2015). M^{vs} stands for the matrix probability to change the velocity state v given a fixed space phase s step. In this context, velocity becomes a variable of concentration such as space and time. The solute dependency of velocity was expressed in a phase space formulation proposed by (P. K. Kang et al., 2017). However, this formulation does not take into account mixing.

Mixing is a consequence of diffusion among water bodies at a given time. Therefore, mixing is Markovian in time in contrast to dispersion. This observation suggests that solute transport should be localized not only in space and time, but also in velocity. The localization in time is of paramount importance since mixing has a direct impact on chemical reactions in fluids (Cirpka and Valocchi, 2007; De Simoni et al., 2005, 2007; Rezaei et al., 2005; Tartakovsky et al., 2008). The classic definition of mixing is proportional to the concentration gradient (Fick, 1855). In fast chemical reactions, the reaction rate may also be calculated with the concentration gradient (De Simoni et al., 2005). However, Einstein (1905) demonstrated that mixing is due to the Brownian movement of single particles. Although this is a downscaling formulation of Fick (1855) and leads to the same results, the comparison of these two expressions is inconsistent (as discussed in chapter 2). This inconsistency is evidenced by the fact that domains with constant concentration (where the concentration gradients are equal to

zero) are defined as immobile zones by Fick (1855) even though they are full of diffusing solute particles. As an alternative, the Water Mixing Approach (WMA) has been proposed in chapter 2. WMA defines the mixing flux as an exchange of waters that carries the mean concentrations of the cells. Thus, mixing is dependent on the concentrations (i.e. number of particles that cross the cell interface) instead of on their gradients.

Dispersion and mixing are different processes, but they are closely linked (Kitanidis, 1988, 1994). Spreading is essentially driven by advection variability and tends to enhance the concentration contrast, which in turn enhances mixing (Le Borgne et al. 2010; Chiogna et al. 2011; Rolle et al. 2009; Tartakovsky et al. 2008). The link is evidenced by the stretching and folding processes (De Anna et al. 2013; Jiménez-Martínez et al. 2015; Le Borgne et al. 2015). This link leads to a non-Fickian mixing at earlier times over a considerable period (Berkowitz et al. 2006; Le Borgne et al. 2008a; Le Borgne and Gouze 2008; Neuman and Tartakovsky 2009; Zhang et al. 2009). Fickian mixing at later times attributed to the spreading rate (Le Borgne et al., 2010a).

Several formulations have been put forward to overcome the problems of the ADE (Frippiat and Holeyman, 2008). At the continuum scale, alternative methods include CTRW (Berkowitz and Scher 1997; Bijeljic et al. 2011; Le Borgne et al. 2008a; Le Borgne et al. 2008b; Dentz et al. 2004; Dentz et al. 2015; Edery et al. 2014; Geiger et al. 2010; Kang et al. 2011; Wang and Cardenas 2014; Aquino and Dentz 2017), fADE (Benson et al., 2000; Cushman and Ginn, 2000), SCST (Becker and Shapiro, 2003) or MRMT (Babey et al., 2015; Jesús Carrera et al., 1998; J. R. De Dreuzy et al., 2013; Fernandez-Garcia and Sanchez-Vila, 2015; Haggerty and Gorelick, 1995; Soler-Sagarra et al., 2016). Given that chemical reaction occurs at pore scale (Steefel et al., 2005), some pore-scale methods such as Lattice Boltzmann equation (Acharya et al., 2007; Benzi et al., 1992; Chen and Doolen, 1998; Q. Kang et al., 2006; Willingham et al., 2008), Smoothed Particle Hydrodynamics (Liu and Liu, 2010; Tartakovsky et al., 2009, 2015; Tartakovsky et al., 2007), Pore Network models (Blunt, 2001; Blunt et al., 2002; Li, et al., 2006; Meile and Tuncay, 2006; Raoof et al., 2010; Raoof and Hassanizadeh, 2012; Varloteaux, 2013) or Density Kernel methods (Schmidt et al., 2017; Sole-Mari et al., 2019) have been studied. Hybrid continuum-pore scale methods have also been proposed (Ilenia Battiato et al., 2011; Leemput et al., 2007; Tartakovsky et al., 2008).

All these approaches partially meet the requirements listed by De Dreuzy and Carrera (2016).

Recently, the Multi-Advective Water Mixing Approach (MAWMA) was advanced in chapter 4 to simulate anomalous transport. MAWMA can be taken as a WMA extension. It is a phase space formulation (detailed in 5.2) where velocity is a new dimension of the state variable. The Water Parcel method (WP) can be derived by discretizing space, time and velocity (section 5.3.1). In this chapter we test the capacity of the WP model to reproduce transport through heterogeneous porous media.

5.2.   Governing equations

In chapter 4, we proposed a phase space formulation (MAWMA) to describe solute transport through porous media while meeting the requirements of De Dreuzy and Carrera (2016). As a phase space formulation, MAWMA considers that concentration depends not only on space and time, but also on velocity, i.e. *c=c(x,v,t) [M/L^3]*. Using velocity as a new dimension facilitates describing dispersion, because spreading results naturally from velocity variability, so that no explicit accounting is need for dispersion. Advection and mixing processes are defined by fluxes *f* in both the space, *s*, and velocity, *v*, domains. That is,

$$\phi \frac{\partial c(x,v,t)}{\partial t} = f_{adv,s} + f_{diff,s} + f_{adv,v} + f_{diff,v} + r \tag{5.1}$$

where *ϕ [L^3/L^3]* is porosity, *t [T]* is time and *r [M/L^3/T]* is a sink/source term, possibly reflecting chemical reactions. The first term on the right-hand side (rhs) represents advection within a velocity class, traditionally expressed in terms of Darcy flux, which we prefer to write here as a function of velocity as *q= ϕv [L^3/L^2/T]* (blue arrow in Figure 4. 1) as follows

$$f_{adv,s} = - \phi v \cdot \nabla c \tag{5.2}$$

The second term of the rhs represents diffusion within a velocity class, classically defined by Fick's law (orange arrow in Figure 4. 1). However, the Water Mixing Approach (WMA) was proposed as an alternative in chapter 7

$$f_{diff,s} = -\nabla \cdot (\overline{q_D c})$$

(5. 3)

Where the term $\overline{q_D c}$ is used to express solute exchanges associated to water mass exchanges, $q_D = \phi D_w / L_D \ [L^3/L^2/T]$ is the water diffusion flux exchanged, $D_w [L^2/T]$ is the water molecular diffusion coefficient and $L_D \ [L]$ is a characteristic diffusion scale. Eq. (5. 3) expresses diffusion as the exchange of water depending on the concentration instead of on its gradient.

The third term on the rhs of Eq. (5. 1) represents changes in $c(x,v,t)$ due to changes in velocity (green arrow in Figure 4. 1). Kang et al. (2017) expressed it in terms of solute mass probability p. We express it in terms of concentration considering that $p = \phi c/M$ (M being the total solute mass), which yields

$$f_{adv,v} = -\frac{v}{L_A} \phi c + \int_{v'} g^{vs}(v|v') \frac{v}{L_A} \phi c' dv' + r$$

(5. 4)

where $L_A \ [L]$ is the characteristic advection length, $g^{vs} \ [TL^{-1}]$ is probability density of a velocity transition after covering a step L_A in space and $c'=c(x,v',t)$. Note that the first term in the rhs of Eq. (5. 4) refers to transitions to velocity v. It does not involve any velocity integration because $\int_{v'} g^{vs}(v'|v)dv' = 1$.

Finally, we proposed expressing diffusive transitions in velocity in chapter 4 (purple arrow in Figure 4. 1) as

$$f_{diff,v} = \int_{v'} \phi f^{vt}(v|v')c' dv' - \int_{v'} \phi f^{vt}(v'|v)c dv'$$

(5. 5)

where $f^{vt} \ [L^{-1}]$ is the probability density, per unit time, of diffusive transitions between velocity states v. The expression ϕf^{vt} has units of water flux.

Note that, as in WMA, all fluxes are expressed in terms of water instead of solute concentrations, which become a mere attribute of water. This is why we termed the formulation of Eq. (5. 4) Multi-Advective Water Mixing Approach (MAWMA).

Eq. (5. 4) could also be expressed as a Lagrangian formulation. This requires revising the definition of material derivative. $d(\cdot)/dt$ reflects all changes in a flowing element of water and, thus. Therefore, it is expressed as the partial derivative minus the changes in c caused by advection. Since we are defining $f_{adv,v}$ to represent advective velocity transitions, we can write the material derivative as

$$\phi \frac{dc}{dt} = \phi \frac{\partial c}{\partial t} + \phi v \cdot \nabla c + \frac{v}{\bar{l}} \phi c - \int_{v\prime} g^{vs}(v|v\prime) \frac{v}{\bar{l}} \phi c\prime dv\prime \tag{5. 6}$$

This definition acknowledges that velocity transitions due to heterogeneity do not cause mixing, which helps us to focus on the impact of mixing, which depends exclusively on diffusive processes:

$$\phi \frac{dc}{dt} = -\nabla \cdot (\overline{q_D c}) + \int_{v\prime} \phi f^{vt}(v|v\prime) c\prime dv\prime - \int_{v\prime} \phi f^{vt}(v\prime|v) c dv\prime \tag{5. 7}$$

5.3.   Solution method

The equation presented in the previous section can be solved with any numerical methods. Here we present a modeling option (section 5.3.1), termed the Water Parcel (WP) method, which is an extension of the one proposed in in chapter 4. We present first this new extension, which require two transition probability matrices. We then describe the computation of these matrices and their properties.

5.3.1. Water Parcel method

Time, space and velocity must be discretized to solve Eq. (5. 7). For simplicity, the discretization procedure is the one used in chapter 4. We reduce the spatial dimensions to 1 by integrating the dimensions perpendicular to the mean flow. The velocity field of the entire domain is discretized in classes with the same flux (i.e., equally probable in the lagrangian velocity distribution). Since fast velocities concentrate most of the flux, they are less probable than slow velocities from an Eulerian point of view. Details of this velocity discretization are reported in Dentz et al. (2016).

The space and velocity domains are discretized in parcels with the same water volume. Each water parcel is associated to its centroid, which determines the position (inspace and velocity) at a given time. The length of a single parcel (i.e. its space extension along the x coordinate) is proportional to its velocity as reported in chapter 4. As a result, slow velocities have more parcels than fast velocities (see Figure 5. 1a), which is consistent with their higher eulerian probability (i.e. p_e in Dentz et al. 2016). The width is proportional to its probability (inversely proportional to its velocity). Eq. (5. 7) is integrated into the continuum space-velocity by using shape functions associated with each parcel. As in the Finite Volume method, the shape function equals 1 when (x,v) exists in the parcel domain. Otherwise it equals to 0. Therefore, all attributes of water parcels (e.g., concentration) will be regarded as homogeneous within each parcel.
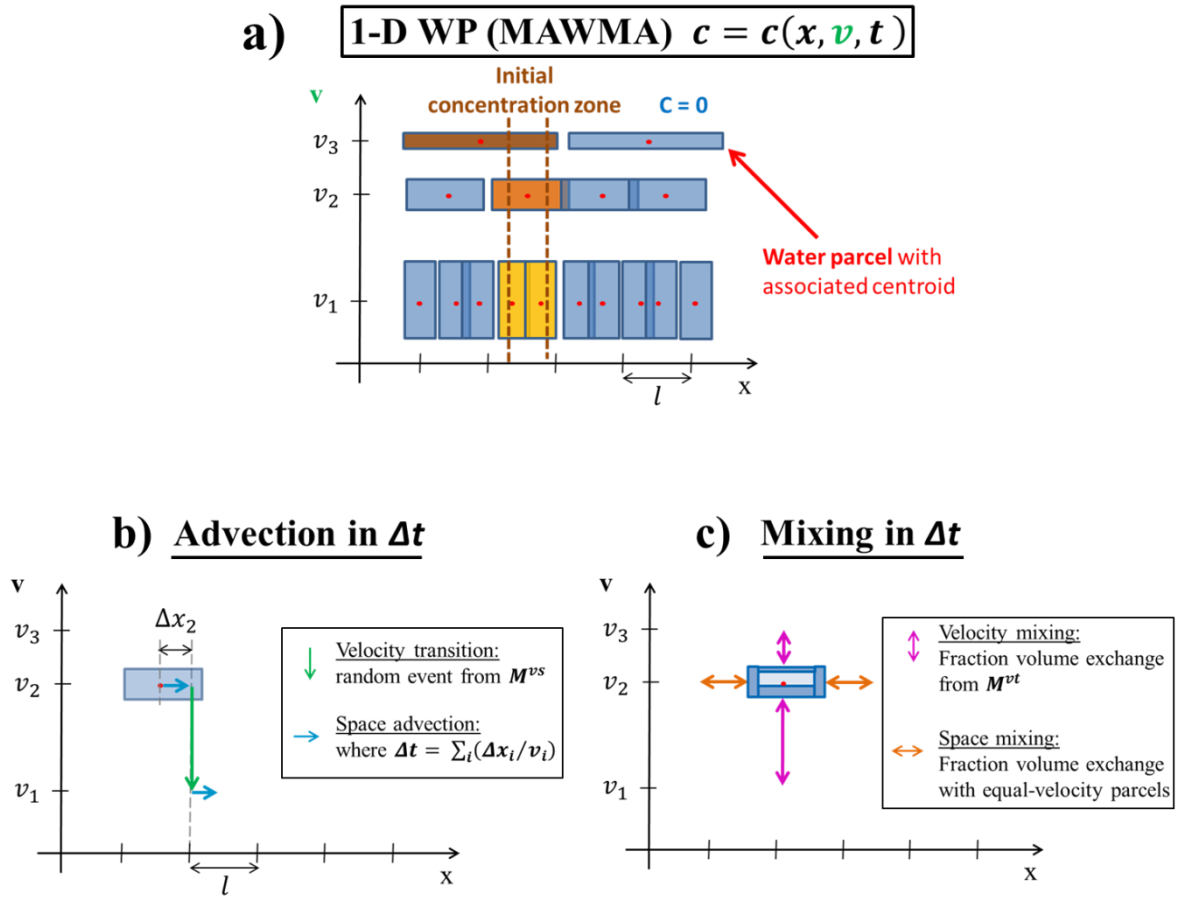
Figure 5. 1: Scheme of Water Parcels (WP) method using the Multi-Advective Water Mixing Approach formulation with three velocity classes: (a) initial distribution of parcels in the (x,v) domain and the initial concentration condition, (b) Advective process for a single water parcel and (c) Mixing process for a single water parcel

Parcels are injected and advected through the domain like solute particles. The injection velocity class is assigned randomly with equal probability for all classes.

Advection, Eqs. (5. 2) and (5. 4), is simulated by simply displacing the parcel centroid with its associated velocity until it has covered the distance L_A. Then, a random event is performed to assign a new velocity for the next space step L_A according to transition probabilities given by the transition matrix M_{adv}^{vs} (M_{ij} is the probability of jumping from velocity v_j to v_i). This transition matrix is similar to the classic solute transition matrix M^{vs} of Le Borgne et al. (2008b) (De Anna et al. 2013; Kang et al. 2011, 2014, 2015, 2017) except that it only accounts for advection transitions. Since the simulation takes place with fixed time steps, each parcel will take a different number of

steps to perform the next random event. However, the frequency of transitions is the same in all the velocity classes because they are equi-probable in flux. The advection scheme is plotted in Figure 5. 1b.

The discretized form of Eq. (5. 7) in a single parcel i of velocity class l is given by

$$V_w \frac{c_i^{k+1} - c_i^k}{\Delta t} = \sum_{y \neq i}^{N_{li}} F_{iy}(c_y - c_i) + \sum_{m \neq l}^{N_v} \sum_{j}^{N_{mi}} a_{ij} F_{lm}^{vt} c_j^k - \sum_{m \neq l}^{N_v} \sum_{j}^{N_{mi}} a_{ji} F_{ml}^{vt} c_i^k \quad i \in I_l \quad (5.8)$$

where V_w [L^3] is the water volume of each parcel, Δt [T] is the time step, N_{li} is the number of parcels y with velocity l spatially connected to i, F is the water volumetric flux diffused, N_v is the number of velocity classes, N_{mi} is the number of parcels of velocity class m connected with parcel i, and a_{ij} is the fraction of the diffusive flux assigned to velocity m, which will be exchanged with the j parcel. We interpret mixing as a water exchange process derived from water diffusion, which implies symmetry (i.e., $F_{iy} = F_{yi}$, $F_{lm}^{vt} = F_{ml}^{vt}$ and $a_{ij} = a_{ji}$)(the latter requires post processing).

We can rewrite Eq. (5. 8) using the concept of mixing ratio $\lambda = a \, \Delta t \, F/V_w$ (chapter 2), which leads to

$$c_i^{k+1} = \lambda_{ii} c_i^k + \sum_{y \neq i}^{N_{li}} \lambda_{iy} c_y^k + \sum_{m \neq l}^{N_v} \sum_{j}^{N_{mi}} \lambda_{ij} c_j^k \qquad (5.9)$$

The sum of all λ equals 1, because the coefficients multiplying c_j^k ($\forall j \neq i$) in the rhs of Eq. (5. 8) are always compensated by the same coefficient multiplying $-c_i^k$. Therefore $\lambda_{ii} = 1 - \sum_y^{N_{li}} \lambda_{iy} - \sum_m^{N_v} \sum_j^{N_{mi}} \lambda_{ij}$. A necessary and sufficient condition for stability is that $\lambda_{ii} > 0 \; \forall i$.

Eq. (5. 9) represents a mixing equation with mixing ratios that are independent of the species, which is consistent with the fact that it has been derived from the mixing of waters. Note that all transport processes described above involve water transfers. In chapter 2, we demonstrate the immediate extension from Eq. (5. 9) to reactive formulation.

5.3.2. Random Walk method

The WP method described in section 5.3.1 requires the velocity distribution, the diffusive transition matrix $\boldsymbol{M}^{vt}_{mix}$ for mixing and the advective transition matrix $\boldsymbol{M}^{vs}_{adv}$. Here, we compute these from random walk simulations of flow and transport, which we will also use to test the proposed approach. The model to simulate flow is essentially that of Hakoun et al. 2019. We summarize it for the sake of completeness. A 2-D multi-lognormal random permeability field $K(x)$ is generated with an isotropic Gaussian covariance function

$$\langle Y'(x)Y'(x')\rangle = \sigma_Y^2 exp\left(-\left(\frac{|x|}{\lambda}\right)^2\right)$$

(5. 10)

where $Y'(x) = Y(x) - \langle Y(x)\rangle$, $Y(x) = ln(K(x))$, σ_Y^2 is the log-permeability variance and λ is the correlation length. The random field $Y(x)$ with mean $\mu_Y = \langle Y(x)\rangle$ is generated using the Random Fields Package (Schlather et al., 2015) of the R software environment (R Core Team, 2015). Groundwater steady-state saturated flow is solved by imposing mass conservation and the Darcy equation:

$$v(x) = -\frac{K(x)\nabla h(x)}{\phi}$$

(5. 11)

where h is the hydraulic head. Fixed head boundary conditions are imposed to the upstream and downstream boundaries. No-flow conditions are imposed to the top and bottom boundaries. The flow model is solved by using the Finite Volume Method to first obtain heads and, then, using Eq. (5. 11) for the velocity field $v(x)$.

A Python code is employed to solve particle transport. Particle advection is calculated as in Pollock (1988). Diffusion displacement at a given time step is $L_D\xi$, where ξ $\sim N(0,1)$.

5.3.3. Algebra of Mixing Matrices

The water mixing ratio λ_{ij} defined in section 5.3.1 can be understood as the ij-th position of the water transition matrix $\boldsymbol{M}_{mix}^{vt}$ applied to time step. Here we describe how to compute the mixing matrix $\boldsymbol{M}_{mix}^{vt}$ from a RW simulation avobe the procedure is general, in the sense that it could be employed for transition matrices of advection (applied after space steps) or transition matrices of mixing to the space phase (e.g. chapter 2).

Transition matrices are obtained directly from their Markovian probability definition (i.e., M_{ij} is the probability of a particle to end in velocity class i, given that it started in class j, which implicitly carries the Markovian statement that the next state solely depends on the current state). Therefore, $M_{ij} = N_{ij}^{k+1}/N_j^k$, where N_{ij}^{k+1} is the number of particles that ended in velocity class i at time t^{k+1} after a diffusion step (to avoid advection transitions) having started in class j at time t^k and N_j^k. $\boldsymbol{M}_{adv}^{vs}$ is computed analogously, except that accounting is made not at every time step, but after the particle has covered the characteristic advection scale.

Two issues need to be addressed. First, the above definition refers to probabilities, while we need volumetric water exchanges. Second, markovianity needs to be tested. It was demonstrated by Leborgne et al (2018) for advection transitions, and it would be trivially true for mixing transitions in the absence of advection. However, it is not so clear when coupling advection and diffusion, especially when considering that low velocities occupy a much larger volume than high velocities. We will test markovianity as part of the example in section 5.4. However, we need first to clarify the relationship between transition probabilities and mixing matrices.

The relationship between the vector of solute probabilities p (p_t according to Dentz et al. (2016)) and velocity class concentration is expressed as

$$\boldsymbol{p} = m_T^{-1}\boldsymbol{S}\boldsymbol{c}$$

(5. 12)

where m_T is the total mass and $\boldsymbol{S}$ is the storage matrix containing the volume of each class. $\boldsymbol{S}$ is not expressed in Eularian processes (time steps) as in Lagrangian processes

(space steps). As explained above, we can obtain the probability transition matrix M_p by accounting particle transitions in RW simulations, which can be expressed as

$$p^{k+1} = M_p p^k$$

(5. 13)

Combining (5. 12) and (5. 13)

$$Sc^{k+1} = M_p Sc^k$$

(5. 14)

Then the concentrations for the next time step are as follows

$$c^{k+1} = S^{-1} M_p Sc^k$$

(5. 15)

Therefore, the transition matrix for transport simulations M_c can be obtained from the RW matrix M_p

$$M_c = S^{-1} M_p S$$

(5. 16)

A well-known property of Markov probability transition matrices is that the sum of the columns of M_p equals 1 (a particle in any velocity class must end in some class). However, the rows of the M_c must add up to 1, to express that concentrations do not change if equal in all velocity classes. In fact, component M_{Cij} can be viewed that as the volume of water received by class i from class j, expressed as a fraction of the volume in i (i.e., a mixing ratio), so that the rows must add up to 1 also to ensure that the class volume does not change. Therefore, the volume of water exchanged is expressed as

$$M_V = M_p S$$

(5. 17)

To satisfy mass conservation, water volume exchanged between velocity classes i and j must be equal (i.e., M_V must be symmetric). The computation procedure (starting with the probability transition matrix) does not ensure symmetry. In practice, it is nearly so. So, symmetry is imposed by setting

$$M_V = \frac{{M'_V}^t + M'_V}{2}$$

(5. 18)

where M'_V is the volume exchange matrix computed initially from Eq. (5. 17). Finally, the water transition matrix is expressed as

$$M_w = S^{-1} M_V \qquad (5. 19)$$

5.4. Applications

Although WP is a continuum scale method, its solute evolution must reproduce the particle based behaviour (Einstein, 1905). This is why it is tested with the classic RW presented in section 5.3.2. The model parameters are detailed in Table 5. 1. Three different Peclet number simulations are defined: ∞; 1000 and 50. The Peclet number is defined as follows

$$Pe = \lambda \langle v \rangle / D_w \qquad (5. 20)$$

Initial concentrations are defined in both methods. The WP method employs the initial flux weighted distribution of solute mass (Figure 5. 1a)

$$c_i(t = 0) = c_{ref} \frac{v_i}{\langle v \rangle} \qquad (5. 21)$$

where c_{ref} is the initial concentration reference, the angular bracket $\langle \cdot \rangle$ denotes the mean injection velocity (mean of the Lagrangian distribution) and v_i is the parcel velocity.

In order to simulate a water parcel distribution, each particle of the RW method has an initial time step with a random definition $\Delta t_0 = \Delta t \cdot \gamma$, being $\gamma \sim unif(0,1)$. This definition provides an innovative way to simulate transport since it differs from the classic Dirac delta. We believe it is a realistic situation, as it reproduces water injection. An initial number of particles N_p are placed along the domain width L_y at the fixed x_0 coordinate position. The particles have an initial Flux weighted distribution. This means that each cell in x_0 has N_c particles, which is a function of the cell velocity v_c expressed as follows

$$N_c = \frac{N_p}{L_y / \Delta y} \frac{v_c}{\langle v \rangle} \qquad (5. 22)$$

where Δy is the cell width. In order to simulate an injected concentration equal to 1, the mass of a single particle m_p is

$$m_p = \frac{c_{ref}\phi\langle v\rangle \Delta t L_y}{N_p} \tag{5.23}$$

The WP method should reproduce mean advection, dispersion, mixing and "be flexible enough to be applicable to real problems" (De Dreuzy and Carrera, 2016). This latter condition is somewhat subjective and will not be considered here, but we believe that WP may be applied to field cases because (i) it is defined at the continuum scale, so that it can benefit (ii) it localizes concentration in the (x,v,t) continuum domain and (iii) it is easily extended to reactive transport (chapter 2). Still, a number of developments are needed to address the real cases with a level of maturity comparable to stochastic methods (Neuman and Tartakovsky, 2009; Pool et al., 2015). Therefore, we restrict ourselves test advection, dispersion and mixing on the synthetic case for stationary conditions and mean uniform flow.

The mean advection is characterized by the mean position μ defined as

$$\mu(t) = m_x^{(1)}(t) - x_0 \tag{5.24}$$

where $m_x^{(k)}$ is the k-th order moment of the solute distribution in space

$$m_x^{(k)}(t) = \int_\Omega c\, x^k d\Omega \bigg/ \int_\Omega c\, d\Omega \tag{5.25}$$

where Ω is the flow domain. From the above definition, we can express dispersion by the standard deviation of spatial solute distribution σ_x^2, which is described as

$$\sigma_x^2(t) = m_x^{(2)}(t) - \mu(t)^2 \tag{5.26}$$

The Global mixing G (Pope, 2000) is defined as

$$G(t) = \int_\Omega c^2 d\Omega \tag{5.27}$$

Note that we can also define Global mixing G' in terms of the velocity domain such as

$$G'(t) = \int_v c'^2 dv \qquad (5.28)$$

where $c'=c(v,t)$ is the mean concentration of an velocity class.

Table 5. 1: Flow and transport problem parameters and simulation details

FLOW		TRANSPORT			
λ (m)	10	Num. time steps	100	c_{ref} (kg/m^3)	1
L_x	600λ	ϕ	0.3	Δt (s)	1
L_y	150λ	RW		Cases	
Δx, Δy	λ/10	$N_{Particles}$	2.25·10^6	D_w (m^2/s)	Peclet
μ_Y	0	WP		0	∞
σ_Y^2	1	N_v	30	10^{-2}	10^3
		$N_{parcels}$	1.44·10^5	0.2	50

5.4.1. Transition matrix validation with Markovian models

We defined three transition matrices in section 5.3.3: $\boldsymbol{M_p}$, $\boldsymbol{M_c}$, and $\boldsymbol{M_w}$. We test here the validity of their computation using a Markov chain model (Risken, 1996). We first compute the transition matrix $\boldsymbol{M_p}$ from RW (at $\sigma_Y^2 = 1$ and $Pe = 50$) simulations at three different times: $t = 1$, 5 and 250. The last time corresponds to the characteristic diffusive time ($\lambda^2/2/D_w$), so that we can assume that injected particles have sampled exhaustively the whole velocity space (recall that we are using flux averaged injection, so that the slow velocities volume is less exhaustively sampled than the fast velocities volume).

Matrices $\boldsymbol{M_c}$ and $\boldsymbol{M_w}$ are calculated as in section 5.3.3. Equation (5. 16) defines the step computation for the matrices $\boldsymbol{M_p}$. The Markovian models that employ M_c and M_w

use concentration c instead of p as the state variable. Concentration c is readily converted to p by using (5. 15). The initial solute probability distribution for any velocity class i is $p_i^0 = 1/N_v$.

The computed evolution of G' (Equation (5. 28)) in time is shown in Figure 5. 2. The first observation from Figure 5. 2 is that σ decreases in time, which reflects that a uniform flow averaged probability leads to a non-uniform concentration. That is, the same mass flux occurs in all velocity classes, but concentration is much longer in the high velocity classes. Mixing causes concentration to become uniform in all classes. Second, the M_p and M_c models evolve identically in time. Second, we observe that the M_w models always give identical results even though they are obtained from different M_p matrices. Mixing state deceases (higher G' in Figure 5. 2) in the M_p models from time $t = 1$ until reaching $t = 5$, when the poorest mixing state is attained. A state identical to M_w is reached at the characteristic time of diffusion ($t = 250$), confirming that the water transitions are always constant. This occurs despite the heterogeneity of solute distributions within the velocity class and is of major significance because mixing can be defined in a constant water transition matrix during the entire simulation, which is not the case with the solute matrices.
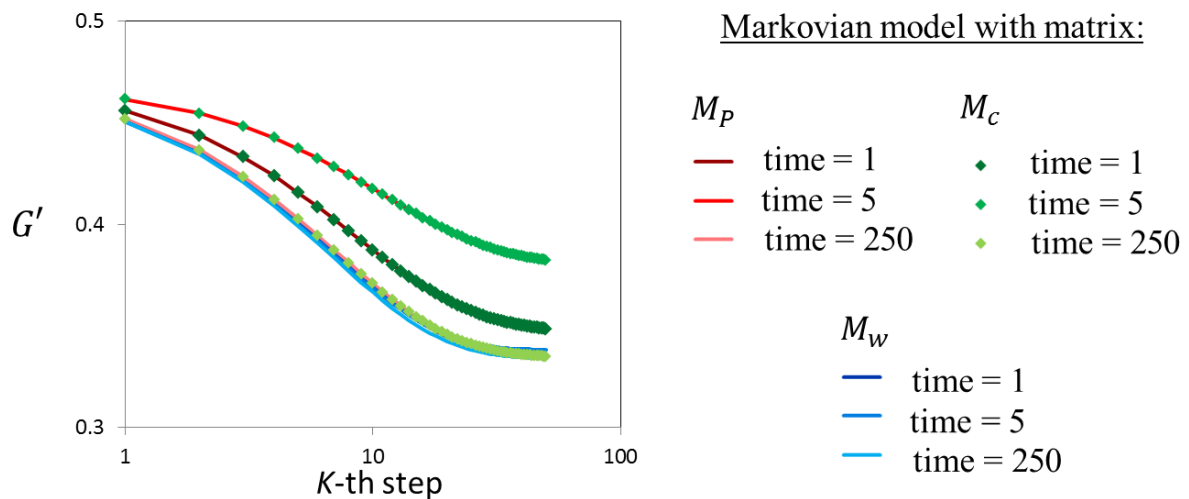
Figure 5. 2: Global mixing state evolution in v velocity phase of Markov models using the computed transition matrix of mixing in RW simulations at different time steps.

5.4.2. Statistical parameter comparison of transport through heterogeneous porous media

Mean position, spreading and mixing results for MAWMA and RW and $\sigma_Y^2 = 1$ are shown in Figure 5. 3. A perfect fit of mean position μ (Eq. (5. 24)) can be observed for all cases in Figure 5. 3a. Regarding spreading, the evolution of σ_x^2 (Eq. (5. 26)), using the RW, is consistent with those of Comolli et al. (2017) and Perez et al. (2019). Perez et al. 2019 also showed that at early times deviation is controlled by diffusion and is proportional to t^2. This explains differences in the WP and RW results in Figure 5. 3b. The WP grid is too coarse to reproduce early time diffusion of a Dirac pulse. The RW and WP results converge at late times because of advection variability resulting in the proportionality of t. Most of the simulations occur during an intermediate regime observed by Comolli et al. (2017). The RW results of the standard deviation deviate at early times and converge at late times, as expected. However, WP simulations converge at early times and deviate at late times for any Peclet number. This is because the initial concentration exceeds the initial zone (Figure 5. 1a). We suspect that an overmixing account for the deviation at late times.
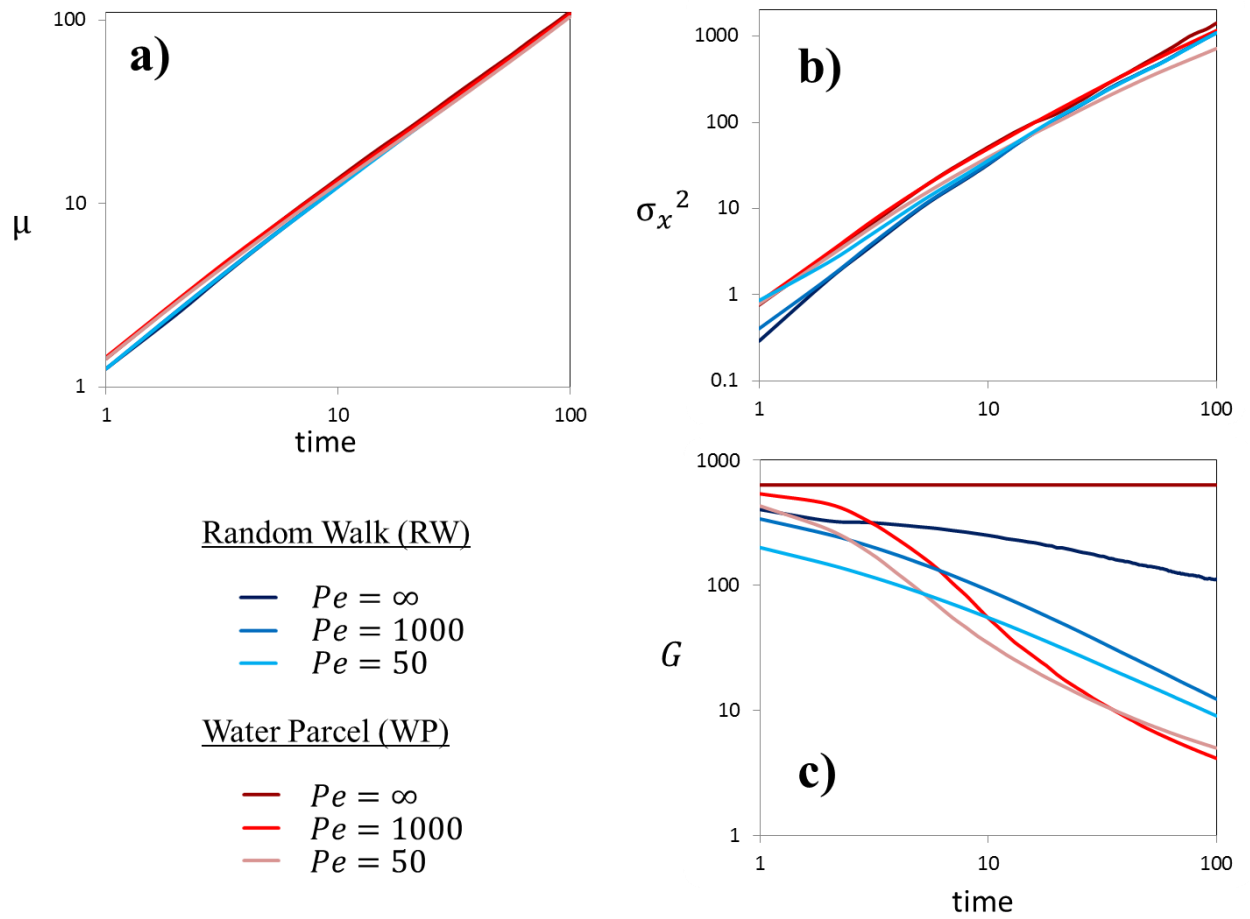
Figure 5. 3: Temporal evolution comparison of Statistic parameters between Random Walk and Water Parcel methods at $\sigma_Y^2 = 1$ heterogeneity level. (a) Mean x position (b) solute concentration variance in x and (c) Global mixing state

We now compare the results of global mix G plotted in Figure 5. 3c. We first evaluate the $Pe = \infty$ case. The mismatch observed is due to the mesh evaluation. WP displays the correct constant G because the entire solute remains in the initial parcel. In other words, no transition of solute occurs between parcels. By contrast, RW uses a structured mesh that is fixed for evaluation of concentration. The number of concentrated elements increases with time owing due to stretching (Le Borgne et al. 2014), which implies a reduction in the computed concentration, this is a common problem when comparing Eulerian (RW) and Lagrangian (WP) methods. For a more accurate comparison, RW should therefore be performed with a Lagrangian mesh (such as the one proposed in chapter 2).

In the other Pe cases, RW shows a monotonic decrease in G. However, WP underestimates mixing at early times. This mismatch is attributed to the mesh distinction given that similar discrepancies are again observed. In contrast, WP overestimates mixing with respect to RW at late times. This is consistent with the WP standard deviation behavior observed previously. We suspect this overestimation is related to incomplete mixing (Le Borgne et al. 2011; Gramlinget al. 2002). In other words, mixing occurs at scales lower than velocity discretization whereas WP changes the entire parcel concentration in the mixing process (i.e. homogenization), which confirms the mixing results observed in the above section. Some alternatives to incomplete mixing have been proposed (Perez et al., 2019). However, the mixing criterion of these authors is dependent on the solute state, whereas we seek to base it on the water volumes.

5.5. Conclusions

We present and test the MAWMA formulation for transport through heterogeneous porous media. The formulation is an extension of WMA, which considers transport of

water instead of solute concentration. Exchange of water volumes is used to reproduce mixing instead of individual species diffusion. Individual species concentrations are considered attributes of water. They may vary spatially, in which case the net solute mass exchange turns out to be proportionally to concentration gradient. But water and solutes exchanges occur independently of concentration gradients, which is why no concentration gradient is used to calculate the mixing process.

We use the WP method to reproduce MAWMA. WP requires a velocity discretization and two transition matrices: one to reproduce advection transitions, which is Markovian in space (i.e., transitions occur after fixed spatial steps, which is consistent with a fixed heterogeneity) and one to reproduce mixing which is Markovian in time (i.e., velocity transitions occur at a constant rate in time, which is consistent with Brownian motion). We have described how to compute these matrices from RW models. Our study shows that it is possible to obtain the water transition matrices from the classic solute transition matrices.

We use Markovian models with transition matices computed from different time steps of the RW simulations to compare transition matrices. We showed that, unlike M_c, M_w are invariant in time. Then, the adequate performance of WP of advection, dispersion and mixing are tested by comparing statistical parameters with the RW simulations. Although advective results show a suitable definition of velocity classes, mixing is poorly reproduced for two reasons: (a) mesh inequivalence and (b) incomplete mixing. The structured mesh of RW is Eulerian in contrast to the unstructured Lagrangian mesh used in WP. The WP method assumes a homogeneous concentration value within the parcel volume. However, in our study this is inappropriate because mixing is a process conducted at a lower scale than velocity definition.

In summary, the RW concentration evaluation requires a Lagrangian mesh (such as the isochronal one proposed by chapter 2). Moreover, WP needs a new evaluation of concentration in order to takes into account heterogeneity inside the parcels. This new evaluation should consider water volumes, which will ensure the independence of concentration states. This will facilitate coupling with chemical reaction calculations.

Chapter 6

Conclusions

This thesis proposes a new family of formulations for solute transport. The essence of the proposal lies in transporting water by advection (i.e., dragging of a water mass with its mean velocity), dispersion (i.e., spreading of a water mass caused by local fluctuations of velocity with respect to its mean), and mixing (i.e., blending different water masses by Brownian motion). Since water is the transported, solute concentration is reduced exclusively to a chemical attribute. An implication is that diffusive and dispersive processes are not written in terms of concentration gradients. Instead, Fick's Law emerges as a result of mixing water exchanges. That is, the proposed formulation is consistent with traditional formulations (e.g., Advection-Dispersion Equation, ADE) but leads naturally a new family of formulations where the entire transport phenomenon may be modeled as water processes. In homogeneous media, the formulation is termed Water Mixing Approach (WMA), which provides a clear decoupling of transport and chemistry. As a result, an easy algorithm was obtained to solve complex reactive transport simulations. The algorithm demonstrates that reactive problems can be solved immediately when transport is formulated as water exchange in any numerical method. We demonstrate the satisfactory accuracy and the computational cost (CPU) of WMA by using the Finite Volumes method in isochronal grids.

In order to confirm the usefulness of the WMA algorithm for reactive transport, it was extended to the Multi-Rate Mass Transfer (MRMT) formulation, which simulates mass transfer between a mobile and multiple immobile regions by diffusive or first-

order mass transfer terms. The resulting formulation, termed Multi-Rate Water Mixing (MRWM), was applied to four models inspired by dissolved CO_2 flow-through experiments to test the influence of geochemical localization (i.e., the localized spots occurrence of chemical reactions that could not take place with the mean concentrations). This application confirms the strong influence that coupling chemical and transport heterogeneity exerts on reactive transport phenomenon.

The WMA has also been extended to heterogeneous media by using a phase space formulation. Phase space formulations assume that the transport state depends not only on space and time but also on velocity. Adding a velocity complicates the problem, but solves elegantly the problem of dispersion. Spreading results naturally from transport variability among velocity classes, so that no explicit dispersion term is needed. Furthermore, they are well suited to incorporate the Markovianity of advection in space. Velocity transitions are Markovian in that they only depend on the current state after traveling a fixed spatial step. However, phase space formulations to date did not include mixing. In this thesis, mixing is treated also as a Markovian process, but in time (the next position after a time, not space, step only depends on the current one). The new formulation is termed Multi-Advective Water Mixing Approach (MAWMA). We have solved numerically using the of Water Parcel (WP) method, obtained by discretizing the space, time and velocity dimensions.

Two different velocity transition probability density functions (matrices, after discretizing velocities) are needed to compute advection and mixing in WP. These can be obtained from the original solute transition matrices computed by classical Random Walk (RW) simulations. We first test only the mixing transition matrix in a stratified flow case (Taylor dispersion problem), where no advection transtions occur. A satisfactory agreement is observed. We also confirm the Markovianity in space observed by other authors, although the mixing process is Markovian in time.

Afterwards the entire formulation is tested in heterogeneous porous media. We then include the matrix transition for advection in the WP models. Statistical measures of displacement, spreading and mixing were compared with RW simulations to test the method. The results show that WP overestimates mixing. We attribute this shortcoming to incomplete mixing, which is not acknowledged by the WP. Further research is therefore warranted to define a sub-WP scale mixing.

Appendix A

Example of streamline oriented isochronal mesh building procedure

The procedure to build the isochronal grid consists of the following steps (Figure A 1:):

1. Solve the flow equation using any available method to compute the flux field. Here we used the finite elements code TRACONF (Carrera et al. 1993).

2. Compute 2N+1 streamlines, N being the number of flowtubes. Again, any method may be appropriate. Here we used the method of Cordes and Kinzelbach (1992). The one of Pollock (1988) would have been appropriate for finite differences.

3. Define "isochronal" points (Figure A 1: b), starting at the inflow points of even streamlines and separated a distance $\Delta s = \Delta t \cdot q/\phi$ along stream lines.

4. Finally, build the cells by any of two options: (a) by joining points with the same travel time from the inflow, which is best for regular geometry boundaries; or (b) by joining points with the same head (Figure A 1: c and Figure A1d).

Note that, using the isochronal grid, advection is perfectly reproduced by the water parcels moving from cell to cell during each time step.
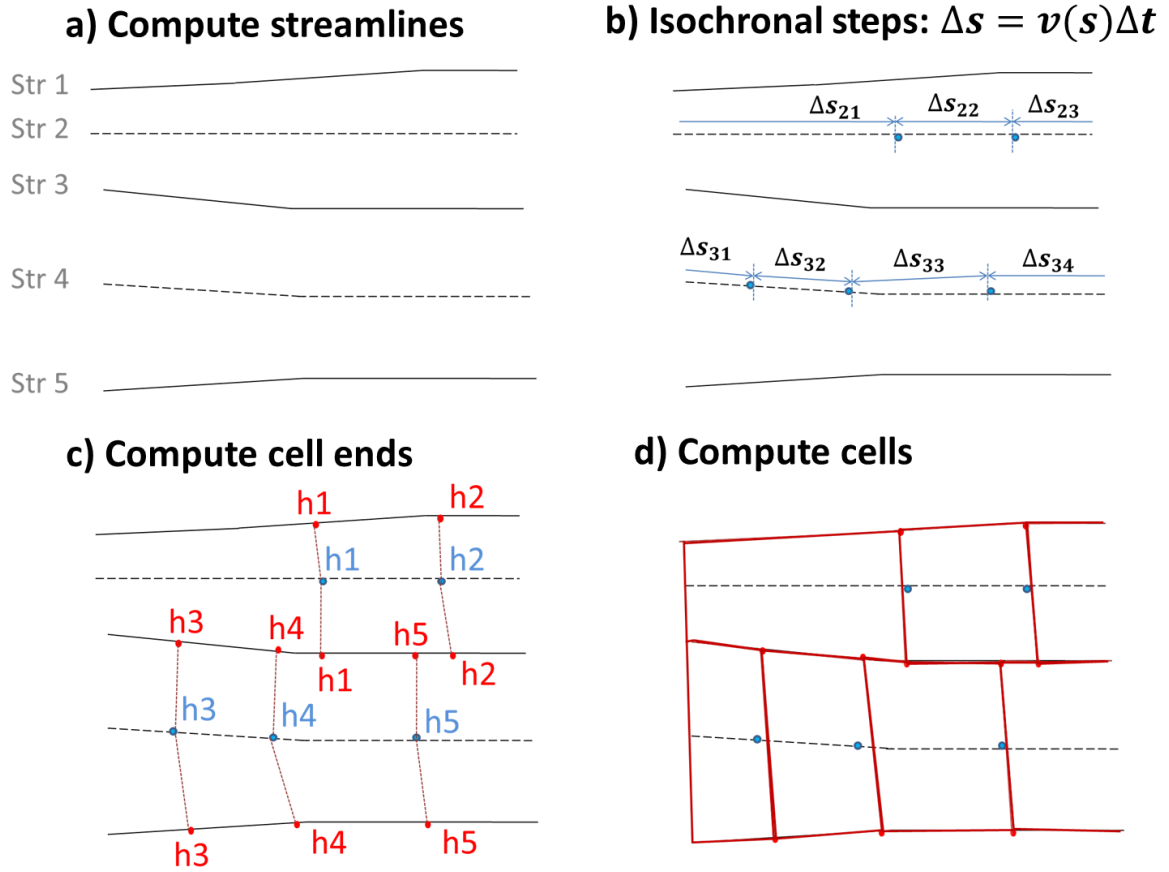
Figure A 1: Construction methodology of an isochronal grid

Appendix B

Dissipation rate in continuum injection

Although several works have contributed to the concept of the scalar dissipation rate (Le Borgne et al. 2010; Hidalgo et al. 2012; Jha et al. 2011; Nicolaides et al. 2015), we start with the classic vector expression (Pope, 2000; De Simoni et al, 2005)

$$\chi(t) = \int_{\Omega} \boldsymbol{\nabla} c \boldsymbol{D} \boldsymbol{\nabla} c \, d\Omega \qquad (\text{A 1})$$

We apply Green's first identity

$$\chi(t) = \int_{\Gamma} c \boldsymbol{D} \boldsymbol{\nabla} c \cdot \boldsymbol{n} \, d\Gamma - \int_{\Omega} c \boldsymbol{\nabla} \cdot (\boldsymbol{D} \boldsymbol{\nabla} c) \, d\Omega \qquad (\text{A 2})$$

where $\boldsymbol{n}$ is the unit vector perpendicular to boundary Γ. We now use the ADE, $\nabla \cdot (D\nabla c) = \phi(\partial c/\partial t) + q\nabla c$, and substitute it in the second term of the RHS of equation (A 2)

$$\chi(t) = \int_{\Gamma} c \boldsymbol{D} \boldsymbol{\nabla} c \cdot \boldsymbol{n} \, d\Gamma - \int_{\Omega} \phi \frac{1}{2} \frac{\partial c^2}{\partial t} d\Omega - \int_{\Omega} \frac{1}{2} \boldsymbol{q} \boldsymbol{\nabla} c^2 \, d\Omega \qquad (\text{A 3})$$

We use again Green's first identity in the third term of the RHS

$$\chi(t) = \int_{\Gamma} c \boldsymbol{D} \boldsymbol{\nabla} c \cdot \boldsymbol{n} \, d\Gamma - \int_{\Omega} \phi \frac{1}{2} \frac{\partial c^2}{\partial t} d\Omega - \int_{\Gamma} \frac{1}{2} \boldsymbol{q} c^2 \cdot \boldsymbol{n} \, d\Gamma + \int_{\Omega} \frac{1}{2} c^2 \boldsymbol{\nabla} \boldsymbol{q} \, d\Omega \quad (\text{A 4})$$

Appendix B: Dissipation rate in continuum injection

The last term is usually neglected, but its contribution can be acknowledged in transient flow problems. Therefore, we use the flow equation $\partial\phi/\partial t = -\nabla q$ in the fourth term of the RHS and regroup the equation

$$\chi(t) = \int_\Gamma c\left(\boldsymbol{D}\nabla c - \frac{1}{2}\boldsymbol{q}c\right)\cdot\boldsymbol{n}\,d\Gamma - \int_\Omega \frac{1}{2}\left(\phi\frac{\partial c^2}{\partial t} + c^2\frac{\partial\phi}{\partial t}\right)d\Omega \qquad (\text{A 5})$$

We now consider the inlet boundary condition $qc_{inj} = -(\boldsymbol{q}c - \boldsymbol{D}\nabla c)\cdot\boldsymbol{n}|_\Gamma$

$$\chi(t) = \int_\Gamma -c\boldsymbol{q}\left(c_{inj} - \frac{1}{2}c\right)\cdot\boldsymbol{n}\,d\Gamma - \int_\Omega \frac{1}{2}\left(\phi\frac{\partial c^2}{\partial t} + c^2\frac{\partial\phi}{\partial t}\right)d\Omega \qquad (\text{A 6})$$

Note that $\boldsymbol{n}$ has a sign opposite to that of the flux at inlet boundaries because $\boldsymbol{n}$ points outwards (i.e., $q = -\boldsymbol{q}\cdot\boldsymbol{n}|_\Gamma$) Given the latter and assuming that porosity is constant, we end up with

$$\chi(t) = \int_\Gamma cq\left(c_{inj} - \frac{1}{2}c\right)d\Gamma - \int_\Omega \frac{1}{2}\left(\phi\frac{\partial c^2}{\partial t}\right)d\Omega \qquad (\text{A 7})$$

Bibliography

Acharya, R. C., Valocchi, A. J., Werth, C. J., & Willingham, T. W. (2007). Pore-scale simulation of dispersion and reaction along a transverse mixing zone in two-dimensional porous media. *Water Resources Research*, *43*(October), 1–11. https://doi.org/10.1029/2007WR005969

Alcolea, A., Carrera, J., & Medina, A. (2008). Regularized pilot points method for reproducing the effect of small scale variability: Application to simulations of contaminant transport. *Journal of Hydrology*, *355*, 76–90. https://doi.org/10.1016/j.jhydrol.2008.03.004

Appelo, C. A. J., & Willemsen, A. (1987). Geochemical calculations and observations on salt water intrusions, I. A combined geochemical/mixing cell model. *Journal of Hydrology*, *94*, 313–330.

Aquino, T., & Dentz, M. (2017). Chemical Continuous Time Random Walks. *Physical Review Letters*, *119*(23), 1–5. https://doi.org/10.1103/PhysRevLett.119.230601

Aris, R. (1956). On the dispersion of a solute in a fluid flowing through a tube. *Proc. Roy. Soc. A*, *219*(186). https://doi.org/DOI: 10.1098/rspa.1956.0065

Ayora, C., Taberner, C., Saaltink, M. W., & Carrera, J. (1998). The genesis of dedolomites: A discusion based on reactive transport modeling. *Journal of Hydrology*, *209*, 346–365. https://doi.org/10.1016/S0022-1694(98)00095-X

Babey, T., de Dreuzy, J.-R., & Casenave, C. (2015). Multi-Rate Mass Transfer (MRMT) models for general diffusive porosity structures. *Advances in Water Resources*, *76*, 146–156. https://doi.org/10.1016/j.advwatres.2014.12.006

Barkai, E., & Cheng, Y.-C. (2003). Aging Continuous Time Random Walks. *The Journal of Chemical Physics*, *118*(6167). https://doi.org/10.1063/1.1559676

Batlle, F., Carrera, J., & Ayora, C. (2002). A comparison of lagrangian and eulerian formulations for reactive transport modelling. *XIV International Conference on Computational Methods in Water Resources. Delft, The Netherlands. 23-28 June.*

Bibliography

Battiato, I., Tartakovsky, D. M., Tartakovsky, a. M., & Scheibe, T. (2009). On breakdown of macroscopic models of mixing-controlled heterogeneous reactions in porous media. *Advances in Water Resources*, *32*(11), 1664–1673. https://doi.org/10.1016/j.advwatres.2009.08.008

Battiato, Ilenia, Tartakovsky, D. M., Tartakovsky, A. M., & Scheibe, T. D. (2011). Hybrid models of reactive transport in porous and fractured media. *Advances in Water Resources*, *34*(9), 1140–1150. https://doi.org/10.1016/j.advwatres.2011.01.012

Bea, S. A., Carrera, J., Ayora, C., Batlle, F., & Saaltink, M. W. (2009). CHEPROO: A Fortran 90 object-oriented module to solve chemical processes in Earth Science models. *Computers and Geosciences*, *35*(6), 1098–1112. https://doi.org/10.1016/j.cageo.2008.08.010

Bea, S., Carrera, J., Ayora, C., Batlle, F., & Saaltink, M. (2009). Cheproo: A Fortran 90 objectoriented module to solve chemical processes in Earth Science models. *Computers & Geosciences*, *35*, 1098–1112.

Bear, J. (1972). *Dynamics of fluids in porous media*. American Elsevier.

Becker, M. W., & Shapiro, A. M. (2000). Tracer transport in fractured crystalline rock: Evidence of nondiffusive breakthrough tailing. *Water Resources Research*, *36*(7), 1677. https://doi.org/10.1029/2000WR900080

Becker, M. W., & Shapiro, A. M. (2003). Interpreting tracer breakthrough tailing from different forced-gradient tracer experiment configurations in fractured bedrock. *Water Resources Research*, *39*(1), n/a-n/a. https://doi.org/10.1029/2001WR001190

Bell, L. S. J., & Binning, P. J. (2004). A split operator approach to reactive transport with the forward particle tracking Eulerian Lagrangian localized adjoint method. *Advances in Water Resources*, *27*, 323–334. https://doi.org/10.1016/j.advwatres.2004.02.004

Benke, R., & Painter, S. (2003). Modeling conservative tracer transport in fracture networks with a hybrid approach based on the Boltzmann transport equation. *Water Resources Research*, *39*(11), 1–11. https://doi.org/10.1029/2003WR001966

Benson, D. a., & Meerschaert, M. M. (2009). A simple and efficient random walk solution of multi-rate mobile/immobile mass transport equations. *Advances in Water Resources*, *32*(4), 532–539. https://doi.org/10.1016/j.advwatres.2009.01.002

Benson, D. a., Wheatcraft, S. W., & Meerschaert, M. M. (2000). Application of a fractional advection-dispersion equation. *Water Resources Research*, *36*(6), 1403–1412. https://doi.org/10.1029/2000WR900031

Benzi, R., Succi, S., & Vergassola, M. (1992). The lattice Boltzmann equation: theory and applications. *Physics Reports*, *222*, 145–197. https://doi.org/10.1016/0370-1573(92)90090-M

Berkowitz, B., Cortis, A., Dentz, M., & Scher, H. (2006). Modeling non-Fickian transport in geological formations as a continuous time random walk. *Reviews Geophysics*, *44*(RG2003), 1–49. https://doi.org/10.1029/2005RG000178.1.INTRODUCTION

Berkowitz, B., & Scher, H. (1997). Anomalous Transport in Random Fracture Networks. *Physical Review Letters*, *79*(20), 4038. https://doi.org/10.1103/PhysRevLett.79.4038

Berkowitz, B., & Scher, H. (1998). Theory of anomalous chemical transport in random fracture networks. *Physical Review E*, *57*(5), 5858–5869. https://doi.org/10.1103/PhysRevE.57.5858

Bethke, C. M. (1996). *Geochemical reaction modeling: concepts and applications* (Oxford Uni).

Bijeljic, B., & Blunt, M. J. (2006). Pore-scale modeling and continuous time random walk analysis of dispersion in porous media. *Water Resources Research*, *42*(W01202), 1–5. https://doi.org/10.1029/2005WR004578

Bijeljic, B., Mostaghimi, P., & Blunt, M. J. (2011). Signature of non-fickian solute transport in complex heterogeneous porous media. *Physical Review Letters*, *107*(20), 20–23. https://doi.org/10.1103/PhysRevLett.107.204502

Blunt, M. J. (2001). Flow in porous media—pore-network models and multiphase flow. *Current Opinion in Colloid & Interface Science*, *6*, 197–207.

https://doi.org/10.1016/S1359-0294(01)00084-X

Blunt, Martin J., Jackson, M. D., Piri, M., & Valvatne, P. H. (2002). Detailed physics, predictive capabilities and macroscopic consequences for pore-network models of multiphase flow. *Advances in Water Resources*, *25*, 1069–1089. https://doi.org/10.1016/S0309-1708(02)00049-0

Bolster, D., Valdés-Parada, F. J., Leborgne, T., Dentz, M., & Carrera, J. (2011). Mixing in confined stratified aquifers. *Journal of Contaminant Hydrology*, *120–121*(C), 198–212. https://doi.org/10.1016/j.jconhyd.2010.02.003

Campana, M. E. (1975). *Finite-state models of transport phenomena in hydrologic systems*. University of Arizona.

Carrera, J., Galarza, G., & Medina, A. (1993). TRACONF, Programa de elementos finitos para la solución de las ecuaciones de flujo y transporte en acuíferos confinados. *E.T.S.I. Caminos, Canales y Puertos, Universitat Politècnica de Catalunya, Barcelona, 53 Pp.*

Carrera, Jesús. (1993). An overview of uncertainties in modelling groundwater solute transport. *Journal of Contaminant Hydrology*, *13*, 23–48. https://doi.org/10.1016/0169-7722(93)90049-X

Carrera, Jesús, Sànchez-Vila, X., Benet, I., Medina, A., Galarza, G., & Guimerà;, J. (1998). On matrix diffusion: formulations, solution methods and qualitative effects. *Hydrogeology Journal*, *6*(1), 178–190.

Carroll, S., McNab, W., Dai, Z., & Torres, S. (2013). Reactivity of Mt. Simon sandstone and the Eau Claire shale under CO2 storage conditions. *Environmental Science and Technology*, *47*(1), 252–261.

Chen, S., & Doolen, G. D. (1998). Lattice Boltzmann Method for fluids flows. *Annual Reviews Fluid Mechanics*, *30*, 329–364. https://doi.org/10.1007/978-3-540-27982-2

Cheng, H., Cvetkovic, V., & Selroos, J. O. (2003). Hydrodynamic control of tracer retention in heterogeneous rock fractures. *Water Resources Research*, *39*(5). https://doi.org/10.1029/2002WR001354

Chiogna, G., Cirpka, O. A., Grathwohl, P., & Rolle, M. (2011). Transverse mixing of conservative and reactive tracers in porous media: Quantification through the concepts of flux-related and critical dilution indices. *Water Resources Research*, *47*(2), 1–15. https://doi.org/10.1029/2010WR009608

Chiogna, G., Eberhardt, C., Grathwohl, P., Cirpka, O. A., & Rolle, M. (2010). Evidence of compound-dependent hydrodynamic and mechanical transverse dispersion by multitracer laboratory experiments. *Environmental Science and Technology*, *44*(2), 688–693. https://doi.org/10.1021/es9023964

Cirpka, O. A., Frind, E. O., & Helmig, R. (1999a). Numerical methods for reactive transport on rectangular and streamline-oriented grids. *Advances in Water Resources*, *22*(7), 711–728. https://doi.org/10.1016/S0309-1708(98)00051-7

Cirpka, O. A., Frind, E. O., & Helmig, R. (1999b). Streamline-oriented grid generation for transport modelling in two-dimensional domains including wells. *Advances in Water Resources*, *22*(7), 697–710. https://doi.org/10.1016/S0309-1708(98)00050-5

Cirpka, O. A., & Valocchi, A. J. (2007). Two-dimensional concentration distribution for mixing-controlled bioreactive transport in steady state. *Advances in Water Resources*, *30*, 1668–1679. https://doi.org/10.1016/j.advwatres.2008.10.018

Comolli, A., & Dentz, M. (2017). Anomalous dispersion in correlated porous media: a coupled continuous time random walk approach. *European Physical Journal B*, *90*(9), 35–40. https://doi.org/10.1140/epjb/e2017-80370-6

Cordes, C., & Kinzelbach, W. (1992). Continuous groundwater velocity fields and path lines in linear, bilinear, and trilinear finite elements. *Water Resour. Res.*, *28*(11), 2903–2911. https://doi.org/10.1029/92WR01686

Cortis, A. (2004). Numerical simulation of non-Fickian transport in geological formations with multiple-scale heterogeneities. *Water Resources Research*, *40*, 1–16. https://doi.org/10.1029/2003WR002750

Crane, M. J., & Blunt, M. J. (1999). Streamline-based simulation of solute transport. *Water Resources Research*, *35*(10), 3061–3078. https://doi.org/10.1029/1999WR900145

Bibliography

Cushman, J. H., & Ginn, T. R. (2000). Fractional advection-dispersion equation: A classical mass balance with convolution-Fickian flux. *Water Resources Research*, *36*(12), 3763–3766.

Cvetkovic, V., & Gotovac, H. (2014). On the upscaling of chemical transport in fractured rock. *Water Resources Research*, *50*(7), 5797–5816. https://doi.org/10.1002/2013WR014956.Received

Cvetkovic, V., Selroos, J. O., & Cheng, H. (1999). Transport of reactive tracers in rock fractures. *Journal of Fluid Mechanics*, *378*, 335–356. https://doi.org/10.1017/S0022112098003450

Dadvand, P., Rossi, R., & Oñate, E. (2010). An object-oriented environment for developing finite element codes for multi-disciplinary applications. In *Archives of Computational Methods in Engineering* (Vol. 17, Issue 3). https://doi.org/10.1007/s11831-010-9045-2

De Anna, P., Jimenez-martinez, J., Tabuteau, H., Turuban, R., Le Borgne, T., Derrien, M., & Meheust, Y. (2013). Mixing and Reaction Kinetics in Porous Media : An Experimental Pore Scale Quanti fi cation. *Environmental Science & Technology*. https://doi.org/10.1021/es403105b

De Anna, P., Le Borgne, T., Dentz, M., Tartakovsky, A. M., Bolster, D., & Davy, P. (2013). Flow intermittency, dispersion, and correlated continuous time random walks in porous media. *Physical Review Letters*, *110*(18), 1–5. https://doi.org/10.1103/PhysRevLett.110.184502

de Dreuzy, J.-R., Carrera, J., Dentz, M., & Le Borgne, T. (2012). Time evolution of mixing in heterogeneous porous media. *Water Resources Research*, *48*(6), W06511. https://doi.org/10.1029/2011WR011360

De Dreuzy, J. R., Rapaport, a., Babey, T., & Harmand, J. (2013). Influence of porosity structures on mixing-induced reactivity at chemical equilibrium in mobile/immobile Multi-Rate Mass Transfer (MRMT) and Multiple INteracting Continua (MINC) models. *Water Resources Research*, *49*, 8511–8530. https://doi.org/10.1002/2013WR013808

De Dreuzy, Jean Raynald, & Carrera, J. (2016). On the validity of effective

formulations for transport through heterogeneous porous media. *Hydrology and Earth System Sciences*, *20*(4), 1319–1330. https://doi.org/10.5194/hess-20-1319-2016

De Simoni, M., Carrera, J., Sánchez-Vila, X., & Guadagnini, A. (2005). A procedure for the solution of multicomponent reactive transport problems. *Water Resources Research*, *41*(11). https://doi.org/10.1029/2005WR004056

De Simoni, M., Sanchez-Vila, X., Carrera, J., & Saaltink, M. W. (2007). A mixing ratios-based formulation for multicomponent reactive transport. *Water Resources Research*, *43*(W07419). https://doi.org/10.1029/2006WR005256

Delay, F., Ackerer, P., & Danquigny, C. (2005). Simulating Solute Transport in Porous or Fractured Formations Using Random Walk Particle Tracking. *Vadose Zone Journal*, *4*(2), 360. https://doi.org/10.2136/vzj2004.0125

Dentz, M., & Berkowitz, B. (2003). Transport behavior of a passive solute in continuous time random walks and multirate mass transfer. *Water Resources Research*, *39*(5), 1–20. https://doi.org/10.1029/2001WR001163

Dentz, M., & Carrera, J. (2007). Mixing and spreading in stratified flow. *Physics of Fluids*, *19*(1), 017107. https://doi.org/10.1063/1.2427089

Dentz, M., Cortis, A., Scher, H., & Berkowitz, B. (2004). Time behavior of solute transport in heterogeneous media: transition from anomalous to normal transport. *Advances in Water Resources*, *27*, 155–173. https://doi.org/10.1016/j.advwatres.2003.11.002

Dentz, M., Kang, P. K., Comolli, A., Borgne, T. Le, & Lester, D. R. (2016). Continuous Time Random Walks for the Evolution of Lagrangian Velocities. *Physical Review Fluids*, *1*, 074004. https://doi.org/10.1103/PhysRevFluids.1.074004

Dentz, M., Kang, P. K., & Le Borgne, T. (2015). Continuous time random walks for non-local radial solute transport. *Advances in Water Resources*, *82*, 16–26. https://doi.org/10.1016/j.advwatres.2015.04.005

Dentz, M., Le Borgne, T., Englert, A., & Bijeljic, B. (2011). Mixing, spreading and reaction in heterogeneous media: A brief review. *Journal of Contaminant*

Hydrology, *120–121*, 1–17. https://doi.org/10.1016/j.jconhyd.2010.05.002

Di Donato, G., Obi, E. O., & Blunt, M. J. (2003). Anomalous transport in heterogeneous media demonstrated by streamline-based simulation. *Geophysical Research Letters*, *30*(12), 1–4. https://doi.org/10.1029/2003GL017196

Donado, L. D., Sanchez-Vila, X., Dentz, M., Carrera, J., & Bolster, D. (2009a). Multicomponent reactive transport in multicontinuum media. *Water Resources Research*, *45*, 1–11. https://doi.org/10.1029/2008WR006823

Donado, L. D., Sanchez-Vila, X., Dentz, M., Carrera, J., & Bolster, D. (2009b). Multicomponent reactive transport in multicontinuum media. *Water Resources Research*, *45*(11). https://doi.org/10.1029/2008WR006823

Edery, Y., Guadagnini, A., Scher, H., & Berkowitz, B. (2014). Origins of anomalous transport in heterogeneous media: Structural and dynamic controls. *Water Resources Research*, *50*, 1490–1505. https://doi.org/10.1002/2013WR015111

Einstein, A. (1905). On the Motion of Small Particles Suspended in a Stationary Liquid, as Required by the Molecular Kinetic Theory of Heat. *Annalen Der Physik*, *322*(8), 549–560. https://doi.org/10.1002/andp.19053220806

Fang, Y., Yeh, G.-T., & Burgos, W. D. (2003). A general paradigm to model reaction-based biogeochemical processes in batch systems. *Water Resources Research*, *39*(4), 1–25. https://doi.org/10.1029/2002WR001694

Fernandez-Garcia, D., & Sanchez-Vila, X. (2015). Mathematical equivalence between time-dependent single-rate and multiratemass transfer models. *Water Resources Research*, *51*, 3166–3180. https://doi.org/10.1016/0022-1694(68)90080-2

Fernàndez-Garcia, D., & Sanchez-Vila, X. (2011). Optimal reconstruction of concentrations, gradients and reaction rates from particle distributions. *Journal of Contaminant Hydrology*, *120–121*(C), 99–114. https://doi.org/10.1016/j.jconhyd.2010.05.001

Fick, A. (1855). On liquid diffusion. *Poggendorffs Annalen*, *94*(59).

Frampton, A., & Cvetkovic, V. (2007). Upscaling particle transport in discrete fracture networks: 2. Reactive tracers. *Water Resources Research*, *43*(10), 1–10.

https://doi.org/10.1029/2006WR005336

Friedly, J. C., & Rubin, J. (1992). Solute transport with multiple equilibrium controlled or kinetically controlled chemical reactions. *Water Resources Research*, *28*(6), 1935–1953.

Frind, E. O. (1982). The principal direction technique: A new approach to groundwater contaminant transport modelling. In K. Holz, U. Meissner, W. Zielke, C. Brebia, G. Pinder and W. Gray (Eds.),. *Proceedings of the Fourth International Conference on Finite Elements in Water Resources.*, 13–25.

Frippiat, C. C., & Holeyman, A. E. (2008). A comparative review of upscaling methods for solute transport in heterogeneous porous media. *Journal of Hydrology*, *362*(1–2), 150–176. https://doi.org/10.1016/j.jhydrol.2008.08.015

Fu, Q., Lu, P., Konishi, H., Dilmore, R., Xu, H., Seyfried, W., & Zhu, C. (2009). Coupled alkali-feldspar dissolution and secondary mineral precipitation in batch systems: 1. New experiments at 200 C and 300 bars. *Chemical Geology*, *258*(3–4), 125–135.

Garabedian, S. P., & LeBlanc, D. R. (1991). Large-Scale natural gradient tracer test in sand and gravel, Cape Cod, Massachusetts 2. Analysis of spatial moments for a nonreactive tracer. *Water Resources Research*, *27*(5), 911–924.

Geiger, S., Cortis, A., & Birkholzer, J. T. (2010). Upscaling solute transport in naturally fractured porous media with the continuous time random walk method. *Water Resources Research*, *46*(12), 1–13. https://doi.org/10.1029/2010WR009133

Geiger, Sebastian, Dentz, M., & Neuweiler, I. (2013). A Novel Multi-Rate Dual-Porosity Model for Improved Simulation of Fractured and Multiporosity Reservoirs. *Society of Petroleum Engineers*, *18*(04), 670–684.

Gelhar, L.W., Mantoglou, A., Welty, C., & Rehfeldt, K. R. (1985). *A Review of Field-Scale Physical Solute Transport Processes In Saturated and Unsaturated Porous Media, EPRI Report EA-4190*.

Gelhar, Lynn W., & Axness, C. L. (1983). Three-dimensional stochastic analysis of macrodispersion in aquifers. *Water Resources Research*, *19*(1), 161–180.

https://doi.org/10.1029/WR019i001p00161

Gerke, H. H., & van Genuchten, M. T. (1996). Macroscopic representation of structural geometry for simulating water and solute movement in dual-porosity media. *Advances in Water Resources*, *19*(6), 343–357. https://doi.org/10.1016/0309-1708(96)00012-7

Ginn, T. R., Schreyer, L. G., Sanchez-Vila, X., Nassar, M. K., Ali, A. A., & Kräutle, S. (2017). Revisiting the Analytical Solution Approach to Mixing-Limited Equilibrium Multicomponent Reactive Transport Using Mixing Ratios: Identification of Basis, Fixing an Error, and Dealing With Multiple Minerals. *Water Resources Research*, *53*(11), 9941–9959. https://doi.org/10.1002/2017WR020759

Ginn, T. R., Simmons, C. S., & Wood, B. D. (1995a). Stochastic-convective transport with nonlinear reaction: biodegradation with microbial growth. *Water Resources Research*, *31*(11), 2689–2700.

Ginn, T. R., Simmons, C. S., & Wood, B. D. (1995b). Stochastic-convective transport with nonlinear reaction: Biodegradation with microbial growth. *Water Resources Research*, *31*(11), 2689–2700.

Gjetvaj, F., Russian, A., Gouze, P., & Dentz, M. (2015). Dual control of flow field heterogeneity and immobile porosity on non-Fickian transport in Berea sandstone. *Water Resources Research*, *51*, 8273–8293. https://doi.org/10.1002/2014WR015432.Received

Gotovac, H., Cvetkovic, V., & Andricevic, R. (2009). Flow and travel time statistics in highly heterogeneous porous media. *Water Resources Research*, *45*(7), 1–24. https://doi.org/10.1029/2008WR007168

Gouze, P., Melean, Y., Le Borgne, T., Dentz, M., & Carrera, J. (2008). Non-Fickian dispersion in porous media explained by heterogeneous microscale matrix diffusion. *Water Resources Research*, *44*(11), 1–19. https://doi.org/10.1029/2007WR006690

Gramling, C. M., Harvey, C. F., & Meigs, L. C. (2002). Reactive transport in porous media: A comparison of model prediction with laboratory visualization.

Environmental Science and Technology, *36*(11), 2508–2514.
https://doi.org/10.1021/es0157144

Grisak, G., & Pickens, J. (1980). Solute transport through fractured media: 1. The effect
of matrix diffusion. *Water Resources Research*, *16*(4), 719–730.
http://onlinelibrary.wiley.com/doi/10.1029/WR016i004p00719/full

Haber, S., & Mauris, R. (1988). Lagrangian approach to time-dependent laminar
dispersion in rectangular conduits. Part 1. Two-dimensional flows. *Journal of
Fluid Mechanics*, *190*, 201–215.

Haberman, R. (1998). *Elementary applied partial differential equations* (E. Cliffs (ed.);
third). Prentice Hall.

Haggerty, R., & Gorelick, S. M. (1995). Multiple-Rate Mass Transfer for Modeling
Diffusion and Surface Reactions in Media with Pore-Scale Heterogeneity. *Water
Resources Research*, *31*(10), 2383–2400.

Haggerty, R., McKenna, S. a., & Meigs, L. C. (2000). On the late-time behavior of
tracer test breakthrough curves. *Water Resources Research*, *36*(12), 3467–3479.

Hakoun, V., Comolli, A., & Dentz, M. (2019). Upscaling and Prediction of Lagrangian
Velocity Dynamics in Heterogeneous Porous Media. *Water Resources Research*,
55(5), 3976–3996. https://doi.org/10.1029/2018WR023810

Harris, K. R., & Woolf, L. A. (1980). Pressure and Temperature Dependence of the Self
Diffusion Coefficient of Water and Oxygen-18 Water. *Journal of the Chemical
Society, Faraday Trans. 1*, *76*, 377–385.

Harvey, C. F., & Gorelick, S. M. (1995). Temporal moment-generating equations:
Modeling transport and mass transfer in heterogeneous aquifers. *Water Resources
Research*, *31*(8), 1895–1911.

Hatano, Y., & Hatano, N. (1998). Dispersive transport of ions in column experiments:
An explanation of long-tailed profiles. *Water Resources Research*, *34*(5), 1027–
1033.

Heidari, P., & Li, L. (2014). Solute transport in low-heterogeneity sandboxes: The role
of correlation length and permeability variance. *Water Resources Research*, *50*,

Bibliography

8240–8264. https://doi.org/10.1002/2015WR017273.Received

Herrera, P. A., Valocchi, A. J., & Beckie, R. D. (2010). A multidimensional streamline-based method to simulate reactive solute transport in heterogeneous porous media. *Advances in Water Resources*, *33*(7), 711–727. https://doi.org/10.1016/j.advwatres.2010.03.001

Hidalgo, J. J., Fe, J., Cueto-Felgueroso, L., & Juanes, R. (2012). Scaling of convective mixing in porous media. *Physical Review Letters*, *109*(26), 1–5. https://doi.org/10.1103/PhysRevLett.109.264503

Holzner, M., Morales, V. L., Willmann, M., & Dentz, M. (2015). Intermittent Lagrangian velocities and accelerations in three-dimensional porous medium flow. *Physical Review E - Statistical, Nonlinear, and Soft Matter Physics*, *92*(1). https://doi.org/10.1103/PhysRevE.92.013015

Huyakorn, P. S. (1983). Computational Methods in Subsurface Flow. *ACADEMIC PRESS*.

Jha, B., Cueto-Felgueroso, L., & Juanes, R. (2011). Fluid mixing from viscous fingering. *Physical Review Letters*, *106*(19), 1–4. https://doi.org/10.1103/PhysRevLett.106.194502

Jiménez-Martínez, J., Anna, P. De, Tabuteau, H., Turuban, R., Borgne, T. Le, & Méheust, Y. (2015). Pore-scale mechanisms for the enhancement of mixing in unsaturated porous media and implications for chemical reactions. *Geophysical Research Letters*, *42*(13), 5316–5324. https://doi.org/10.1002/2015GL064513

Jurado, A., Gago-Ferrero, P., Vàzquez-Suñé, E., Carrera, J., Pujades, E., Díaz-Cruz, M. S., & Barceló, D. (2014). Urban groundwater contamination by residues of UV filters. *Journal of Hazardous Materials*, *271*, 141–149. https://doi.org/10.1016/j.jhazmat.2014.01.036

Kang, P. K., Anna, P. De, Nunes, J. P., Bijeljic, B., Blunt, M. J., & Juanes, R. (2014). Pore-scale intermittent velocity structure underpinning anomalous transport through 3-D porous media. *Geophysical Research Letters*, *41*, 6184–6190. https://doi.org/10.1002/2014GL061475.1.

Kang, P. K., Borgne, T. Le, Dentz, M., Bour, O., Juanes, R., Kang, P., Borgne, T. Le, Dentz, M., Bour, O., & Juanes, R. (2015). Impact of velocity correlation and distribution on transport in fractured media: Field evidence and theoreticalmodel. *Water Resources Research RESEARCH*, 940–959. https://doi.org/10.1002/2014WR015799.Received

Kang, P. K., Dentz, M., Le Borgne, T., & Juanes, R. (2011). Spatial Markov model of anomalous transport through random lattice networks. *Physical Review Letters*, *107*(18), 1–5. https://doi.org/10.1103/PhysRevLett.107.180602

Kang, P. K., Dentz, M., Le Borgne, T., & Juanes, R. (2015). Anomalous transport on regular fracture networks: Impact of conductivity heterogeneity and mixing at fracture intersections. *Physical Review E - Statistical, Nonlinear, and Soft Matter Physics*, *92*(2), 1–15. https://doi.org/10.1103/PhysRevE.92.022148

Kang, P. K., Dentz, M., Le Borgne, T., Lee, S., & Juanes, R. (2017). Anomalous transport in disordered fracture networks: Spatial Markov model for dispersion with variable injection modes. *Advances in Water Resources*, *0*, 1–15. https://doi.org/10.1016/j.advwatres.2017.03.024

Kang, Q., Lichtner, P. C., & Zhang, D. (2006). Lattice Boltzmann pore-scale model for multicomponent reactive transport in porous media. *Journal of Geophysical Research*, *111*, 1–12. https://doi.org/10.1029/2005JB003951

Kapoor, V., & Kitanidis, P. K. (1998). Concentration fluctuations and dilution in aquifers. *Water Resour. Res.*, *34*(5), 1181–1193.

Kerner, B. S. (1998). Experimental features of self-organization in traffic flow. *Physical Review Letters*, *81*(17), 3797–3800. https://doi.org/10.1103/PhysRevLett.81.3797

Kinzelbach, W. (1986). Groundwater modeling - an introduction with sample programs in BASIC. *ELSEVIER*. https://doi.org/10.1016/S0167-5648(08)70743-3

Kitanidis, P. K. (1988). Prediction by the method of moments of transport in a heterogeneous formation. *Journal of Hydrology*, *102*(1), 453–473. https://doi.org/10.1016/0022-1694(88)90111-4

Kitanidis, Peter K. (1988). Prediction by the method of moments of transport in a

Bibliography

heterogeneous formation. *Journal of Hydrology*, *102*(1), 453–464.

Kitanidis, Peter K. (1994). The concept of the dilution index. *Water Resour. Res.*, *30*(7), 2011–2026.

Klafter, J., & Silbey, R. (1980). Derivation of the continuous-time random-walk eEquation. *Physical Review Letters*, *44*(2), 55–58. https://doi.org/10.1103/PhysRevLett.44.55

Kleinfelter, N., Moroni, M., & Cushman, J. H. (2005). Application of the finite-size Lyapunov exponent to particle tracking velocimetry in fluid mechanics experiments. *Physical Review E - Statistical, Nonlinear, and Soft Matter Physics*, *72*(5), 1–12. https://doi.org/10.1103/PhysRevE.72.056306

Konikow, L. F. (2010). Applying Dispersive Changes to Lagrangian Particles in Groundwater Transport Models. *Transport in Porous Media*, *85*(2), 437–449. https://doi.org/10.1007/s11242-010-9571-2

Kräutle, S., & Knabner, P. (2005). A new numerical reduction scheme for fully coupled multicomponent transport-reaction problems in porous media. *Water Resources Research*, *41*, 1–17. https://doi.org/10.1029/2004WR003624

Kräutle, S., & Knabner, P. (2007). A reduction scheme for coupled multicomponent transport-reaction problems in porous media: Generalization to problems with heterogeneous equilibrium reactions. *Water Resources Research*, *43*, 1–15. https://doi.org/10.1029/2005WR004465

Le Borgne, T., Dentz, M., & Villermaux, E. (2015). The lamellar description of mixing in porous media. *Journal of Fluid Mechanics*, *770*, 458–498. https://doi.org/10.1017/jfm.2015.117

Le Borgne, T., Dentz, M., & Villermaux, E. (2015). The lamellar description of mixing in porous media. *Journal of Fluid Mechanics*, *770*, 458–498. https://doi.org/10.1017/jfm.2015.117

Le Borgne, T., & Gouze, P. (2008). Non-Fickian dispersion in porous media: 2. Model validation from measurements at different scales. *Water Resources Research*, *44*(6), 1–10. https://doi.org/10.1029/2007WR006279

Le Borgne, Tanguy, Dentz, M., Bolster, D., Carrera, J., de Dreuzy, J. R., & Davy, P. (2010a). Non-Fickian mixing: Temporal evolution of the scalar dissipation rate in heterogeneous porous media. *Advances in Water Resources*, *33*(12), 1468–1475. https://doi.org/10.1016/j.advwatres.2010.08.006

Le Borgne, Tanguy, Dentz, M., Bolster, D., Carrera, J., de Dreuzy, J. R., & Davy, P. (2010b). Non-Fickian mixing: Temporal evolution of the scalar dissipation rate in heterogeneous porous media. *Advances in Water Resources*, *33*(12), 1468–1475. https://doi.org/10.1016/j.advwatres.2010.08.006

Le Borgne, Tanguy, Dentz, M., & Carrera, J. (2008a). Spatial Markov processes for modeling Lagrangian particle dynamics in heterogeneous porous media. *Physical Review E - Statistical, Nonlinear, and Soft Matter Physics*, *78*(2), 1–9. https://doi.org/10.1103/PhysRevE.78.026308

Le Borgne, Tanguy, Dentz, M., & Carrera, J. (2008b). Lagrangian statistical model for transport in highly heterogeneous velocity fields. *Physical Review Letters*, *101*(9), 090601. https://doi.org/10.1103/PhysRevLett.101.090601

Le Borgne, Tanguy, Dentz, M., Davy, P., Bolster, D., Carrera, J., De Dreuzy, J. R., & Bour, O. (2011). Persistence of incomplete mixing: A key to anomalous transport. *Physical Review E - Statistical, Nonlinear, and Soft Matter Physics*, *84*(1), 1–4. https://doi.org/10.1103/PhysRevE.84.015301

Le Borgne, Tanguy, Dentz, M., & Villermaux, E. (2013). Stretching, coalescence, and mixing in porous media. *Physical Review Letters*, *110*(20), 1–5. https://doi.org/10.1103/PhysRevLett.110.204501

Le Borgne, Tanguy, Ginn, T. R., & Dentz, M. (2014). Impact of fluid deformation on mixing-induced chemical reactions in heterogeneous flows. *Geophysical Research Letters*, *41*(22), 7898–7906. https://doi.org/10.1002/2014GL062038

Leemput, P. Van, Vandekerckhove, C., Vanroose, W., & Roose, D. (2007). Accuracy of hybrid Lattice Boltzmann/Finite differences schemes for reaction-diffusion systems. *Multiscale Model. Simul*, *6*(3), 838–857.

Leptos, K. C., Guasto, J. S., Gollub, J. P., Pesci, A. I., & Goldstein, R. E. (2009). Dynamics of Enhanced Tracer Diffusion in Suspensions of Swimming Eukaryotic

Microorganisms. *Physical Review Letters*, *103*(19), 1–4.
https://doi.org/10.1103/PhysRevLett.103.198103

Lester, D. R., Metcalfe, G., & Trefry, M. G. (2014). Anomalous transport and chaotic
advection in homogeneous porous media. *Physical Review E - Statistical,
Nonlinear, and Soft Matter Physics*, *90*(6), 1–5.
https://doi.org/10.1103/PhysRevE.90.063012

Li, L., Peters, C. A., & Celia, M. A. (2006). Upscaling geochemical reaction rates using
pore-scale network modeling. *Advances in Water Resources*, *29*, 1351–1370.
https://doi.org/10.1016/j.advwatres.2005.10.011

Lichtner, P. C. (1985). Continuum model for simultaneous chemical reactions and mass
transport in hydrothermal systems. *Geochimica et Cosmochimica Acta*, *49*(3), 779–
800. https://doi.org/10.1016/0016-7037(85)90172-3

Liu, M. B., & Liu, G. R. (2010). Smoothed particle hydrodynamics (SPH): An overview
and recent developments. *Archives of Computational Methods in Engineering*, *17*,
25–76. https://doi.org/10.1007/s11831-010-9040-7

Luquot, L., Andreani, M., Gouze, P., & Camps, P. (2012). CO2 percolation experiment
through chlorite/zeolite-rich sandstone (Pretty Hill Formation – Otway Basin–
Australia). *Chemical Geology*, *294–295*, 75–88.

Luquot, L., Gouze, P., Niemi, A., Bensabat, J., & Carrera, J. (2016). Laboratory CO2-
rich brine percolation experiments through Heletz samples (Israel): Role of the
flow rate and brine composition. *International Journal of Greenhouse Gas
Control*, *this issue*. https://doi.org/10.1016/j.ijggc.2015.10.023

MacQuarrie, K. T. B., & Sudicky, E. A. (1990). Simulation of biodegradable organic
contaminants in groundwater: 2. Plume behavior in uniform and random flow
fields. *Water Resources Research*, *26*(2), 223–239.

Małoszewski, P., & Zuber, A. (1985). On the theory of tracer experiments in fissured
rocks with a porous matrix. *Journal of Hydrology*, *79*, 333–358.
https://doi.org/10.1016/0022-1694(85)90064-2

Mayer, K. U., Benner, S. G., Blowes, D. W., & Frind, E. O. (1999). The reactive

transport model MIN3P: application to acid mine drainage generation and treatment-nickel rim mine site, Sudbury, Ontario. *Conference on Mining and the Environment*, *99*, 145–154.

Mckenna, S. A., Meigs, L. C., & Haggerty, R. (2001). Tracer tests in a fractured dolomite 3. Double-porosity, multiple-rate mass transfer processes in convergent flow tracer tests. *Water Resources Research*, *37*(5), 1143–1154.

Meile, C., & Tuncay, K. (2006). Scale dependence of reaction rates in porous media. *Advances in Water Resources*, *29*, 62–71. https://doi.org/10.1016/j.advwatres.2005.05.007

Metzler, R., & Klafter, J. (2000). The random walk's guide to anomalous diffusion: a fractional dynamics approach. *Physics Reports*, *339*, 1–77.

Mills, R. T., Lichtner, P. C., & Lu, C. (2005). PFLOTRAN: A massively parallel simulator for reactive flows in geologic media. *SC2005,(Poster), Seattle, WA*.

Mills, R. T., Lu, C., Lichtner, P. C., & Hammond, G. E. (2007). Simulating subsurface flow and transport on ultrascale computers using PFLOTRAN. *Journal of Physics: Conference Series*, *78*(1), 12051.

Molins, S., Carrera, J., Ayora, C., & Saaltink, M. W. (2004). A formulation for decoupling components in reactive transport problems. *Water Resources Research*, *40*(10), W103011–W1030113.

Molz, F. J., & Widdowson, M. A. (1988). Internal inconsistencies in dispersiondominated models that incorporate chemical and microbial kinetics. *Water Resources Research*, *24*(4), 615–619.

Montroll, E. W., & Weiss, G. H. (1965). Random Walks on Lattices. II. *Journal of Mathematical Physics*, *6*, 167. https://doi.org/10.1063/1.1704269

Moreno, L., & Neretnieks, I. (1993). Fluid flow and solute transport in a network of channels. *Journal of Contaminant Hydrology*, *14*, 163–192. https://doi.org/10.1016/0169-7722(93)90023-L

Nardi, A., Idiart, A., Trinchero, P., de Vries, L. M., & Molinero, J. (2014). Interface COMSOL-PHREEQC (iCP), an efficient numerical framework for the solution of

coupled multiphysics and geochemistry. *Computers & Geosciences*, *69*, 10–21. https://doi.org/10.1016/j.cageo.2014.04.011

Neuman, S. P. (1990). Universal Scaling of Hydraulic Conductivities and Dispersivities in Geologic Media c is a constant , a fractal dimension where E is the topological depends only on the constants cr • and L s ,. Yet when one. *Water Resources Research*, *26*(8), 1749–1758. https://doi.org/10.1029/WR026i008p01749

Neuman, S. P., & Tartakovsky, D. M. (2009). Perspective on theories of non-Fickian transport in heterogeneous media. *Advances in Water Resources*, *32*, 670–680. https://doi.org/10.1016/j.advwatres.2008.08.005

Nicolaides, C., Jha, B., Cueto-Felgueroso, L., & Juanes, R. (2015). Impact of viscous fingering and permeability heterogeneity on fluid mixing in porous media. *Water Resources Research*, *51*, 2634–2647. https://doi.org/10.1002/2014WR016259

Nicolaides, Christos, Cueto-Felgueroso, L., & Juanes, R. (2010). Anomalous physical transport in complex networks. *Physical Review E - Statistical, Nonlinear, and Soft Matter Physics*, *82*(5), 1–4. https://doi.org/10.1103/PhysRevE.82.055101

Niemi, A., Bensabat, J., Fagerlund, F., Sauter, M., Ghergut, J., Licha, T., Fierz, T., Wiegand, G., Rasmusson, M., Rasmusson, K., Shtivelman, V., Gendler, M., & Partners, M. (2012). Small-scale injection into a deep geological formation at Heletz, Israel. *Energy Procedia*, *23*, 504–511.

Niemi, Auli, Bensabatb, J., Shtivelmanc, V., Edlmannd, K., Gouzee, P., Luquote, L., Hingerlg, F., Bensong, S. M., Pezarde, P. A., Rasmussona, K., Lianga, T., Fagerlunda, F., Gendlerc, M., Goldbergc, I., Tatomirh, A., Langeh, T., Sauterh, M., & Freifeld, B. (2016). Heletz experimental site overview, characterization and data analysis for CO2 injection and geological storage. *International Journal of Greenhouse Gas Control*, *48*, 3–23.

Painter, S., & Cvetkovic, V. (2005). Upscaling discrete fracture network simulations: An alternative to continuum transport models. *Water Resources Research*, *41*(2), 1–10. https://doi.org/10.1029/2004WR003682

Palandri, J. L., & Kharaka, Y. K. (2004). A compilation of rate parameters of water-mineral interaction kinetics for application to geochemical modeling. In *U.S.*

Geological Survey Open file Report (Vols. 2004–1068).
https://doi.org/10.1098/rspb.2004.2754

Parkhurst, D. L., & Appelo, C. A. J. (1999). User's guide to PHREEQC (version 2)--A computer program for speciation, batch-reaction, one-dimensional transport, and inverse geochemical calculations. *U.S. Geological Survey Water-Resources Investigations*, *Report 99-*, 312 p.

Parkhurst, D. L., Kipp, K. L., & Charlton, S. R. (2010). PHAST Version 2—A program for simulating groundwater flow, solute transport, and multicomponent geochemical reactions. *U.S. Geological Survey Techniques and Methods*, *6–A35*, 235 p.

Pelizardi, F., Bea, S. A., Carrera, J., & Vives, L. (2017). Identifying geochemical processes using End Member Mixing Analysis to decouple chemical components for mixing ratio calculations. *Journal of Hydrology*, *550*, 144–156. https://doi.org/10.1016/j.jhydrol.2017.04.010

Perez, L. J., Hidalgo, J. J., & Dentz, M. (2019). Upscaling of Mixing-Limited Bimolecular Chemical Reactions in Poiseuille Flow. *Water Resources Research*, *55*(1), 249–269. https://doi.org/10.1029/2018WR022730

Pollock, D. W. (1988). Semianalytical Computation of Path Lines for Finite-Difference Models. In *Ground Water* (Vol. 26, Issue 6, pp. 743–750). https://doi.org/10.1111/j.1745-6584.1988.tb00425.x

Pool, M., Carrera, J., Alcolea, A., & Bocanegra, E. M. (2015). A comparison of deterministic and stochastic approaches for regional scale inverse modeling on the Mar del Plata aquifer. *Journal of Hydrology*, *531*, 214–229. https://doi.org/10.1016/j.jhydrol.2015.09.064

Pope, S. B. (2000). Flows Turbulent. In *Cambridge University Press* (p. 771). https://doi.org/10.1139/apnm-2013-0536

Pruess, K. (2005). ECO2N: A TOUGH2 fluid property module for mixtures of water, NaCl, and CO2. *Lawrence Berkeley National Laboratory Report LBNL-57592, Berkeley, CA.*

Bibliography

R Core Team. (2015). *R: A language and environment for statistical computing.* R Foundation for Statistical Computing.

Ramasomanana, F., Younes, A., & Fahs, M. (2012). Modeling 2D multispecies reactive transport in saturated/unsaturated porous media with the eulerian-lagrangian localized adjoint method. *Water, Air, and Soil Pollution*, *223*(4), 1801–1813. https://doi.org/10.1007/s11270-011-0985-4

Raoof, A., & Hassanizadeh, S. M. (2012). A new formulation for pore-network modeling of two-phase flow. *Water Resources Research*, *48*, W01514. https://doi.org/10.1029/2010WR010180

Raoof, Amir, Hassanizadeh, S. M., & Leijnse, A. (2010). Upscaling Transport of Adsorbing Solutes in Porous Media: Pore-Network Modeling. *Vadose Zone Journal*, *9*(3), 624–636.

Ray, C., Ellsworth, T. R., Valocchi, A. J., & Boast, C. W. (1997). An improved dual porosity model for chemical transport in macroporous soils. *Journal of Hydrology*, *193*, 270–292. https://doi.org/10.1016/S0022-1694(96)03141-1

Rezaei, M., Sanz, E., Raeisi, E., Ayora, C., Vázquez-Suñé, E., & Carrera, J. (2005). Reactive transport modeling of calcite dissolution in the fresh-salt water mixing zone. *Journal of Hydrology*, *311*(1–4), 282–298. https://doi.org/10.1016/j.jhydrol.2004.12.017

Rinaldo, A., Bertuzzo, E., Mari, L., Righetto, L., Blokesch, M., Gatto, M., Casagrandi, R., Murray, M., Vesenbeckh, S. M., & Rodriguez-Iturbe, I. (2012). Reassessment of the 2010-2011 Haiti cholera outbreak and rainfall-driven multiseason projections. *Proceedings of the National Academy of Sciences of the United States of America*, *109*(17), 6602–6607. https://doi.org/10.1073/pnas.1203333109

Risken, H. (1996). *The Fokker-Planck Equation* (Springer).

Rolle, M., Eberhardt, C., Chiogna, G., Cirpka, O. A., & Grathwohl, P. (2009). Enhancement of dilution and transverse reactive mixing in porous media: Experiments and model-based interpretation. *Journal of Contaminant Hydrology*, *110*(3–4), 130–142. https://doi.org/10.1016/j.jconhyd.2009.10.003

Roth, K., & Jury, W. A. (1993). Linear transport models for adsorbing solutes. *Water Resources Research*, *29*(4), 1195–1203. https://doi.org/10.1029/92WR02537

Rubin, J. (1983). Transport of reacting solutes in porous media: Relation between mathematical nature of problem formulation and chemical nature of reactions. *Water Resources Research*, *19*(5), 1231–1252. https://doi.org/10.1029/WR019i005p01231

Russian, A., Dentz, M., & Gouze, P. (2016). Time domain random walks for hydrodynamic transport in heterogeneous media. *Water Resources Research*, *52*(51), 5974–5997. https://doi.org/10.1002/2016WR018977.Received

Saaltink, M. W., Batlle, F., Ayora, C., Carrera, J., & Olivella, S. (2004). RETRASO, a code for modeling reactive transport in saturated and unsaturated porous media. *Geologica Acta*, *2*(3), 235–251.

Saaltink, M. W., Carrera, J., & Ayora, C. (2001). On the behavior of approaches to simulate reactive transport. *Journal of Contaminant Hydrology*, *48*(3), 213–235. http://www.ncbi.nlm.nih.gov/pubmed/11285932

Saaltink, Maarten W, Ayora, C., & Carrera, J. (1998). A mathematical formulation for reactive transport that eliminates mineral concentrations. *Water Resour. Res.*, *34*(7), 1649–1656. https://doi.org/10.1029/98WR00552

Sadhukhan, S., Gouze, P., & Dutta, T. (2014). A simulation study of reactive flow in 2-D involving dissolution and precipitation in sedimentary rocks. *Journal of Hydrology*, *519*(PB), 2101–2110. https://doi.org/10.1016/j.jhydrol.2014.10.019

Salamon, P., Fernàndez-Garcia, D., & Gómez-Hernández, J. J. (2006). Modeling mass transfer processes using random walk particle tracking. *Water Resources Research*, *42*, 1–14. https://doi.org/10.1029/2006WR004927

Samper, J., Yang, C., & Montenegro, L. (2003). CORE 2D version 4: A code for non-isothermal water flow and reactive solute transport. *Users Manual. University of La Coruña, Spain*, 131.

Sanchez-Vila, X., Dentz, M., & Donado, L. D. (2007). Transport-controlled reaction rates under local non-equilibrium conditions. *Geophysical Research Letters*,

Bibliography

34(10), 1–5. https://doi.org/10.1029/2007GL029410

Scheibe, T. D., Schuchardt, K., Agarwal, K., Chase, J., Yang, X., Palmer, B. J.,
Tartakovsky, A. M., Elsethagen, T., & Redden, G. (2015). Hybrid multiscale
simulation of a mixing-controlled reaction. *Advances in Water Resources*, *83*, 228–
239. https://doi.org/10.1016/j.advwatres.2015.06.006

Scher, H., & Lax, M. (1973). Stochastic transport in a disordered solid. I. Theory.
Physical Review B, *7*(10), 4491–4502. https://doi.org/10.1103/PhysRevB.7.4491

Scher, Harvey, & Montroll, E. W. (1975). Anomalous transit-time dispersion in
amorphous solids. *Physical Review B*, *12*(6), 2455–2477.
https://doi.org/10.1103/PhysRevB.12.2455

Schlather, M., Malinowski, A., Menck, P. J., Oesting, M., & Strokorb, K. (2015).
Analysis, Simulation and Prediction of Multivariate Random Fields with Package
RandomFields. *Journal of Statistical Software*, *63*(8), 1–25.
https://doi.org/10.1002/wics.10

Schmidt, M. J., Pankavich, S., & Benson, D. A. (2017). A Kernel-based Lagrangian
method for imperfectly-mixed chemical reactions. *Journal of Computational
Physics*, *336*, 288–307. https://doi.org/10.1016/j.jcp.2017.02.012

Seymour, J. D., Gage, J. P., Codd, S. L., & Gerlach, R. (2004). Anomalous fluid
transport in porous media induced by biofilm growth. *Physical Review Letters*,
93(19), 5–8. https://doi.org/10.1103/PhysRevLett.93.198103

Shapiro, A. M. (2001). Effective matrix diffusion in kilometer-scale transport in
fractured crystalline rock. *Water Resources Research*, *37*(3), 507–522.
https://doi.org/10.1029/2000wr900301

Silva, O., Carrera, J., Kumar, S., Dentz, M., Alcolea, A., & Willmann, M. (2009). A
general real-time formulation for multi-rate mass transfer problems. *Hydrology
and Earth System Sciences*, *13*(8), 1399–1411.

Šimůnek, J., Šejna, M., Saito, H., Sakai, M., & van Genuchten, M. T. (2008). *The
HYDRUS-1D Software Package for Simulating the One-Dimensional Movement of
Water, Heat, and Multiple Solutes in Variably-Saturated Media* (4.08; Issue April).

University of California, Riverside, Dept. of Environmental Sciences HYDRUS Software Series, 3, 330.

Sole-Mari, G., Bolster, D., Fernàndez-Garcia, D., & Sanchez-Vila, X. (2019). Particle density estimation with grid-projected and boundary-corrected adaptive kernels. *Advances in Water Resources*, *131*(May), 103382. https://doi.org/10.1016/j.advwatres.2019.103382

Soler-Sagarra, J., Luquot, L., Martínez-Pérez, L., Saaltink, M. W., De Gaspari, F., & Carrera, J. (2016). Simulation of chemical reaction localization using a multi-porosity reactive transport approach. *International Journal of Greenhouse Gas Control*, *48*, 59–68. https://doi.org/10.1016/j.ijggc.2016.01.026

Soler-Sagarra, J., Saaltink, M. W., Nardi, A., De gaspari, F., & Carrera, J. (2018). Water Mixing Approach (WMA) for reactive transport modeling applied in advection dominated problems. *(Submitted)*.

Spyrou, M. (2009). *The Diffusion Coefficient of Water: A Neutron Scattering Study using Molecular Dynamics Simulations*. Physics Department of the University of Surrey.

Steefel, C. I., Appelo, C. A. J., Arora, B., Jacques, D., Kalbacher, T., Kolditz, O., Lagneau, V., Lichtner, P. C., Mayer, K. U., Meeussen, J. C. L., Molins, S., Moulton, D., Shao, H., Simunek, J., Spycher, N., Yabusaki, S. B., & Yeh, G. T. (2015). Reactive transport codes for subsurface environmental simulation. In *Computational Geosciences* (Vol. 19, Issue 3). https://doi.org/10.1007/s10596-014-9443-x

Steefel, C. I., & Lichtner, P. C. (1998). Multicomponent reactive transport in discrete fractures II: Infiltration of hyperalkaline groundwater at Maqarin, Jordan, a natural analogue site. *Journal of Hydrology*, *209*(1–4), 200–224. https://doi.org/10.1016/S0022-1694(98)00173-5

Steefel, C.I., & Yabusaki, S. B. (1996). *os3D / GIMRT Software for Modeling multicomponent-multidimensional reactive transport*. (No. PNNL-11166; 39KP00000). Pacific Northwest National Lab., Richland, WA (US).

Steefel, C I, DePaolo, D. J., & Lichtner, P. C. (2005). Reactive transport modeling: An

essential tool and a new research approach for the Earth sciences. *Earth and Planetary Science Letters*, *240*, 539–558.

Steefel, C I, & MacQuarrie, K. T. B. (1996). Approaches to modeling reactive transport in porous media. *Reviews in Mineralogy and Geochemistry*, *34*(1), 83-125.

Steefel, Carl I. (2009). *CrunchFlow: User's manual*. http://www.csteefel.com/CrunchFlowIntroduction.html

Sudicky, E. a. (1989). The Laplace Transform Galerkin Technique: A time-continuous finite element theory and application to mass transport in groundwater. *Water Resources Research*, *25*, 1833–1846. https://doi.org/10.1029/WR025i008p01833

Suresh Kumar, G. (2008). Effect of sorption intensities on dispersivity and macro-dispersion coefficient in a single fracture with matrix diffusion. *Hydrogeology Journal*, *16*, 235–249. https://doi.org/10.1007/s10040-007-0234-5

Tartakovsky, a. M., Tartakovsky, G. D., & Scheibe, T. D. (2009). Effects of incomplete mixing on multicomponent reactive transport. *Advances in Water Resources*, *32*, 1674–1679. https://doi.org/10.1016/j.advwatres.2009.08.012

Tartakovsky, a. M., Trask, N., Pan, K., Jones, B., Pan, W., & Williams, J. R. (2015). Smoothed particle hydrodynamics and its applications for multiphase flow and reactive transport in porous media. *Computational Geosciences*, 28. https://doi.org/10.1007/s10596-015-9468-9

Tartakovsky, A. M., Redden, G., Lichtner, P. C., Scheibe, T. D., & Meakin, P. (2008). Mixing-induced precipitation: Experimental study and multiscale numerical analysis. *Water Resources Research*, *44*(6), 1–19. https://doi.org/10.1029/2006WR005725

Tartakovsky, A. M., Tartakovsky, D. M., Scheibe, T. D., & Meakin, P. (2008). Hybrid simulations of reaction-diffusion systems in porous media. *SIAM J. Sci. Comput.*, *30*(6), 2799–2816. https://doi.org/10.1137/090745854

Tartakovsky, Alexandre M., Meakin, P., Scheibe, T. D., & Eichler West, R. M. (2007). Simulations of reactive transport and precipitation with smoothed particle hydrodynamics. *Journal of Computational Physics*, *222*, 654–672.

https://doi.org/10.1016/j.jcp.2006.08.013

Tartakovsky, Alexandre M., Tartakovsky, D. M., & Meakin, P. (2008). Stochastic langevin model for flow and transport in porous media. *Physical Review Letters*, *101*(4), 1–4. https://doi.org/10.1103/PhysRevLett.101.044502

Taylor, G. (1953). Dispersion of Soluble Matter in Solvent Flowing Slowly through a Tube. *Proceedings of the Royal Society A: Mathematical, Physical and Engineering Sciences*, *219*(1137), 186–203. https://doi.org/10.1098/rspa.1953.0139

Thiele, M. R., Batycky, R. P., & Blunt, M. J. (1997). A streamline-based 3d field-scale compositional reservoir simulator. *Society of Petroleum Engineers Annual Technical Conference and Exhibition*.

Toride, N., Leij, F. J., & Van Genuchten, M. T. (1993). A Comprehensive Set of Analytical Solutions for Nonequilibrium Solute Transport With First-Order Decay and Zero-Order Production. *Water Resources Research*, *29*(7), 2167–2182.

Tsang, Y. W. (1995). Study of alternative tracer tests in characterizing transport in fractured rocks. *Geophysical Research Letters*, *22*(11), 1421–1424.

Tutolo, B., Luhmann, A., Kong, X. Z., Saar, M., & Seyfried Jr, W. E. (2015). CO2 sequestration in feldspar-rich sandstone: Coupled evolution of fluid chemistry, mineral reaction rates, and hydrogeochemical properties. *Geochim. Cosmochim. Acta, 160*, 132–154.

Valhondo, C., Carrera, J., Ayora, C., Tubau, I., Martinez-Landa, L., Nödler, K., & Licha, T. (2015). Characterizing redox conditions and monitoring attenuation of selected pharmaceuticals during artificial recharge through a reactive layer. *Science of the Total Environment*, *512–513*(C), 240–250. https://doi.org/10.1016/j.scitotenv.2015.01.030

Valocchi, A. J. (1985). Validity of the Local Equilibrium Assumption for Modeling Sorbing Solute Transport Through Homogeneous Soils. *Water Resources Research*, *21*(6), 808–820.

Varloteaux, C. (2013). *modélisation multi-échelles des mécanismes de transport réactif. Implact sur les propriétés pétrophysiques des roches lors du stockage de CO2*.

Bibliography

Université Pierre et Marie Curie.

Viswanathan, G., Afanasyev, V., Buldyrev, S. V., Murphy, E. J., Prince, P. A., & Stanley, H. E. (1996). Lévy flight search patterns of wandering albatrosses. *Nature*, *381*, 413–415. https://doi.org/10.1038/381413a0

Vogel, H.-J., Cousin, I., Ippisch, O., & Bastian, P. (2006). The dominant role of structure for solute transport in soil: Experimental evidence and modelling of structure and transport in a field experiment. *Hydrology and Earth System Sciences*, *10*(4), 495–506. https://doi.org/10.5194/hessd-2-2153-2005

Wang, L., & Cardenas, M. B. (2014). Non-Fickian transport through two-dimensional rough fractures: Assessment and prediction. *Water Resources Research*, *50*, 5375–5377. https://doi.org/10.1002/2013WR014979.Reply

Wang, P. P., Zheng, C., & Gorelick, S. M. (2005). A general approach to advective–dispersive transport with multirate mass transfer. *Advances in Water Resources*, *28*(1), 33–42. https://doi.org/10.1016/j.advwatres.2004.10.003

Werth, C. J., Cirpka, O. A., & Grathwohl, P. (2006). Enhanced mixing and reaction through flow focusing in heterogeneous porous media. *Water Resources Research*, *42*(12), 1–10. https://doi.org/10.1029/2005WR004511

Whitesides, G. M. (2006). The origins and the future of microfluidics. *Nature*, *442*(7101), 368–373. https://doi.org/10.1038/nature05058

Willingham, T. W., Werth, C. J., & Valocchi, A. J. (2008). Evaluation of the effects of porous media structure on mixing-controlled reactions using pore-scale modeling and micromodel experiments. *Environmental Science and Technology*, *42*(9), 3185–3193. https://doi.org/10.1021/es7022835

Willmann, M., Carrera, J., & Sánchez-Vila, X. (2008a). Transport upscaling in heterogeneous aquifers: What physical parameters control memory functions? *Water Resources Research*, *44*(12), 1–13. https://doi.org/10.1029/2007WR006531

Willmann, M., Carrera, J., & Sánchez-Vila, X. (2008b). Transport upscaling in heterogeneous aquifers: What physical parameters control memory functions? *Water Resources Research*, *44*, 1–13. https://doi.org/10.1029/2007WR006531

Willmann, M., Carrera, J., Sanchez-Vila, X., Silva, O., & Dentz, M. (2010). Coupling of mass transfer and reactive transport for nonlinear reactions in heterogeneous media. *Water Resources Research*, *46*(7), W07512. https://doi.org/10.1029/2009WR007739

Winston, R. B., Konikow, L. F., & Hornberger, G. Z. (2018). Volume-Weighted Particle-Tracking Method for Solute-Transport Modeling: Implementation in MODFLOW-GWT. In *Book 6, Modeling Techniques*. https://doi.org/10.3133/tm6A58

Wolery, T. J. (1992). EQ3NR, a computer program for geochemical aqueous speciation-solubility calculation : user's guide and documentation. In *URCL-MA-110662 PTIII* (Lawrence L).

Wolery, T. J., Jackson, K. J., Bourcier, W. L., Bruton, C. J., Viani, B. E., Knauss, K. G., & Delany, J. M. (1990). Current status of the EQ3/6 software package for geochemical modeling, in: Melchior, C. *Bassett, R.L. (Eds.), Chemical Modeling of Aqueous Systems II. Am. Chem. Soc. Symp. Ser.*, *416*, 104–116.

Xu, T., Spycher, N., Sonnenthal, E., Zhang, G., Zheng, L., & Pruess, K. (2011). TOUGHREACT Version 2.0: A Simulator for Subsurface Reactive Transport under Non-Isothermal Multiphase Flow Conditions. *Computers & Geosciences*, *37*(6), 763–774.

Yabusaki, S. ., Steefel, C. ., & Wood, B. . (1998). Multidimensional, multicomponent, subsurface reactive transport in nonuniform velocity fields: code verification using an advective reactive streamtube approach. *Journal of Contaminant Hydrology*, *30*(3–4), 299–331. https://doi.org/10.1016/S0169-7722(97)00050-8

Yeh, G. T., Sun, J., Jardine, P. M., Burgos, W. D., Fang, Y., Li, M. H., & Siegel, M. D. (2004). *HYDROGEOCHEM 5.0: A Coupled Model of Fluid Flow, Thermal Transport, and HYDROGEO-CHEMical Transport through Saturated-Unsaturated Media: Version 5.0* (Issue May). ORNL/TM-2004/103, 37831.

Yeh, G. T., & Tripathi, V. S. (1989). A critical evaluation of recent developments in hydrogeochemical transport models of reactive multichemical components. *Water Resources Research*, *25*(1), 93–108.

Bibliography

Yu, S. R., Burkhardt, M., Nowak, M., Ries, J., Petráek, Z., Scholpp, S., Schwille, P., & Brand, M. (2009). Fgf8 morphogen gradient forms by a source-sink mechanism with freely diffusing molecules. *Nature*, *461*(7263), 533–536. https://doi.org/10.1038/nature08391

Zech, A., Attinger, S., Cvetković, V. D., Dagan, G., Dietrich, P., Fiori, A., Rubin, Y. N., & Teutsch, G. (2015). Is unique scaling of aquifer macrodispersivity supported by field data? *Water Resources Research*, *51*(9), 7662–7679. https://doi.org/10.1002/2015WR017200.A

Zhang, F., Yeh, G. T., Parker, J. C., Brooks, S. C., Pace, M. N., Kim, Y. J., Jardine, P. M., & Watson, D. B. (2007). A reaction-based paradigm to model reactive chemical transport in groundwater with general kinetic and equilibrium reactions. *Journal of Contaminant Hydrology*, *92*(1), 10–32. https://doi.org/10.1016/j.jconhyd.2006.11.007

Zhang, Y., Benson, D. A., & Baeumer, B. (2007). Predicting the tails of breakthrough curves in regional-scale alluvial systems. *Ground Water*, *45*(4), 473–484. https://doi.org/10.1111/j.1745-6584.2007.00320.x

Zhang, Yingqi, Liu, H. H., Zhou, Q., & Finsterle, S. (2006). Effects of diffusive property heterogeneity on effective matrix diffusion coefficient for fractured rock. *Water Resources Research*, *42*(December 2005), 1–8. https://doi.org/10.1029/2005WR004513

Zhang, Yong, Benson, D. A., & Reeves, D. M. (2009). Time and space nonlocalities underlying fractional-derivative models: Distinction and literature review of field applications. *Advances in Water Resources*, *32*(4), 561–581. https://doi.org/10.1016/j.advwatres.2009.01.008